

**PYROMETALLURGICAL PROCESSING OF POST-
CONSUMER ELECTRONICS FOR RECOVERY
OF METAL VALUES**

by
Scott A. Shuey

ProQuest Number: 10797124

All rights reserved

INFORMATION TO ALL USERS

The quality of this reproduction is dependent upon the quality of the copy submitted.

In the unlikely event that the author did not send a complete manuscript and there are missing pages, these will be noted. Also, if material had to be removed, a note will indicate the deletion.



ProQuest 10797124

Published by ProQuest LLC (2019). Copyright of the Dissertation is held by the Author.

All rights reserved.


This work is protected against unauthorized copying under Title 17, United States Code
Microform Edition © ProQuest LLC.

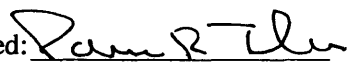
ProQuest LLC.
789 East Eisenhower Parkway
P.O. Box 1346
Ann Arbor, MI 48106 – 1346

A thesis submitted to the Faculty and Board of Trustees of the Colorado School of Mines in partial fulfillment of the requirements for the degree of Doctor of Philosophy (Metallurgical and Materials Engineering)

Golden, Colorado

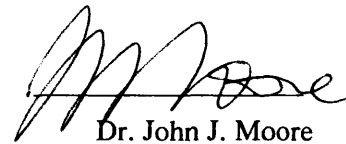
Date: April 10, 2006

Signed: 
Scott A. Shuey

Approved: 
Dr. Patrick R. Taylor
Thesis Adviser

Golden, Colorado

Date: 4/10/06



Dr. John J. Moore
Professor and Head
Metallurgical and Materials Engineering Department

ABSTRACT

The recycling of electronic waste (e-waste) tends to be a complex undertaking when considering the intimate bonding of materials in the average printed circuit board. The development of a recycling process is further complicated when considering the wide variety of products being generated under the heading of “electronics” as well as the constant change in materials of construction coupled with the speed at which electronics are changing. Research conducted at CSM focuses on developing an understanding of the behavior of individual polymer constituents in the presence of alkali and alkali-earth carbonates as well as the behavior of mixed polymer materials. This understanding leads to a process designed to entrap halides in-situ during pyrometallurgical pre-processing resulting in a reduction in the propensity of the formation of dioxins and furans or volatile metal halides. The resulting gas phase may then be combusted to reclaim thermal values. Carbon and metal rich solids may then be processed for metal recovery.

TABLE OF CONTENTS

ABSTRACTiii

TABLE OF CONTENTS iv

LIST OF FIGURES vii

LIST OF TABLES xxiii

ACKNOWLEDGEMENTS..... xxiv

Chapter 1 Introduction 1

 1.1 Defining Electronic Waste..... 1

 1.2 Annual Waste Generation and Growth..... 2

 1.3 Material Composition..... 5

 1.4 Material Value 8

 1.5 Government Legislation 10

 1.5.1 US State Government Legislation..... 10

 1.5.2 US Federal Government Legislation..... 11

Chapter 2 RECYCLING OPTIONS 12

 2.1 Reuse..... 12

 2.2 Reprocess..... 12

 2.2.1 Adherent Technologies Inc..... 13

 2.2.2 Boliden Mineral 14

 2.2.2.1 Zinc Fuming Furnace 15

 2.2.2.2 Kaldo Furnace 15

 2.2.2.3 Plant Operation..... 16

 2.2.3 Teck Cominco Ltd. 16

 2.2.4 Noranda Recycling, Inc. 17

 2.2.5 Union Mineria..... 18

 2.2.6 Sabin, Pashelinsky and Engelhard 19

 2.3 Processing Summary 20

Chapter 3 EXPERIMENTAL TECHNIQUES 21

 3.1 Research Parameters 21

3.2 Research Program	22
Chapter 4 THERMODYNAMIC MODELING.....	23
4.1 Direct Smelting: Metal/Metal Oxide.....	32
4.2 Thermal Processing: Metal-Halide Systems.....	37
4.3 Thermal Processing: Halide Sequestering Agents	31
4.4 Thermodynamic Modeling Results.....	35
Chapter 5 ORGANIC BEHAVIOR AT TEMPERATURE	36
5.1 Organic Behavior—Rotary Kiln Equipment and Procedure	36
5.2 Phase 1: High Flow System with Various Solid Carbonate Sources	41
5.3 Phase 2: Closed System with Various Solid Carbonate Sources	48
5.4 Organic Behavior Study Results.....	56
Chapter 6 SEQUESTERING AGENTS.....	57
6.1 Sequestering Agents—Tube Furnace Equipment and Procedure	57
6.2 Sequestering Agents—Experimental Matrix	59
6.2.1 PVC behavior and Chloride entrapment	59
6.2.2 PTFE behavior and Fluoride entrapment from mixed PVC, PTFE and PE	61
6.2.3 Mixed polymer (PVC, PTFE and PE) behavior and Halide entrapment.....	65
6.2.4 Decomposition Temperature Depression in Polymer Mixtures.....	67
6.2.5 Halide Sequestering Efficiency	69
6.3 Atmosphere Effects.....	70
6.4 Sequestering Agents Study Results.....	72
Chapter 7 DTA-MS EVALUATION.....	73
Chapter 8 PROPOSED PROCESS	76
8.1 E-Waste Processing.....	76
8.1.1 Tube Furnace E-Waste Experiments.....	77
8.1.2 Rotary Kiln E-Waste Experiments.....	83
8.1.2.1 Rotary Kiln E-Waste.....	83
8.1.2.2 Rotary Kiln E-Waste + NaHCO ₃	85
8.1.2.3 Measured Dioxin/Furan Reduction in Rotary Kiln Experiments.....	88
8.2 E-Waste Processing Summary.....	89
8.3 Flowsheet-Heat and Material Balance	89

8.4 Process Summary	100
Chapter 9 CONCLUSIONS.....	101
Chapter 10 SUGGESTIONS FOR FURTHER WORK.....	103
REFERENCES	105
APPENDICIED ON ACCOMPANYING CD IN BACK POCKET	
APPENDIX A Organic Behavior at Temperature—Data	109
APPENDIX B Organic Behavior in the Presence of Sequestering Agents—Data.....	158
APPENDIX C X-Ray Diffraction Data.....	247
APPENDIX D DTA-MS Data.....	290

LIST OF FIGURES

Figure 1.1 New and Obsolete Computers.....	3
Figure 1.2 Cumulative Computer Resource	4
Figure 1.3 Element Distribution in a Desktop PC with Monitor	5
Figure 1.4 Element Distribution in a Desktop PC without Monitor.....	6
Figure 4.1 Oxide Stability vs Oxidation Potential: Slag and Metal Elements.....	24
Figure 4.2 Oxide Stability vs Oxidation Potential: Volatiles Elements	25
Figure 4.3 Vapor Pressures.....	26
Figure 4.4 HSC 5.1 equilibrium composition of 1 tonne of e-waste, <50 kg/mt E-Waste.....	28
Figure 4.5 HSC 5.1 equilibrium composition of 1 tonne of e-waste, <15 kg/mt E-Waste.....	29
Figure 4.6 HSC 5.1 alternate equilibrium composition of 1 tonne of e-waste.....	30
Figure 4.7 HSC 5.1 equilibrium composition of 1 tonne of e-waste and excess O _{2(g)}	31
Figure 4.8 HSC 5.1 equilibrium composition of 1 tonne of e-waste and 1.8X MgCO ₃	32
Figure 4.9 HSC 5.1 equilibrium composition of 1 tonne of e-waste and 1.8X CaCO ₃	33
Figure 4.10 HSC 5.1 equilibrium composition of 1 tonne of e-waste and 1.8X NaHCO ₃	34
Figure 5.1 Experimental System-Schematic.....	37
Figure 5.2 Data Acquisition and Control.....	39
Figure 5.3 Condenser, Filter and Scrubber.....	41
Figure 5.4 Experimental System.....	42
Figure 5.5 Exp 2: 1 g PE, 2 slpm CO _{2(g)}	45
Figure 5.6 Exp 9: 10 g PE, 5.22 g CaCO ₃ , 2 slpm CO _{2(g)}	46
Figure 5.7 Exp 10: 10 g PE, 5.22 g CaCO ₃ , 2 slpm N _{2(g)}	47
Figure 5.8 Exp 36: 5 g PE, 10 g C, 2 slpm CO _{2(g)}	49
Figure 5.9 Exp 37: 5 g PE, 15 g C, 15 g MgCO ₃ Mg(OH) ₂ ·3H ₂ O, 2 slpm CO _{2(g)}	50
Figure 5.10 Exp 38: 5 g PE, 15 g MgCO ₃ Mg(OH) ₂ ·3H ₂ O, 2 slpm CO _{2(g)}	51
Figure 5.11 Exp 39: 5 g PE, 15 g MgCO ₃ Mg(OH) ₂ ·3H ₂ O, 2 slpm CO _{2(g)}	52
Figure 5.12 Exp 41: 5 g PE, 15 g MgCO ₃ , 2 slpm CO _{2(g)}	53
Figure 5.13 Acid Digestion Residue Recovery.....	54

Figure 5.14 Carbon Grade of Residue.....	55
Figure 6.1 Tube Furnace System-Schematic.....	57
Figure 6.2 Sample Heat Curve of PVC + NaHCO ₃	60
Figure 6.3 Teflon 1: 1.00 g PTFE, 3.36 g (1X) NaHCO ₃ , 1.0 slpm CO _{2(g)} , 550°C.....	62
Figure 6.4 Teflon 1 XRD: 1.00 g PTFE, 3.36 g (1X) NaHCO ₃ , 1.0 slpm CO _{2(g)} , 545°C.....	63
Figure 6.5 Teflon 2 XRD: 1.00 g PTFE, 3.36 g (1X) NaHCO ₃ , 1.0 slpm CO _{2(g)} , 555°C.....	64
Figure 6.6 Teflon 17 Redo II: 0.5 g (PVC, PTFE, PE), 1.0 slpm CO _{2(g)}	66
Figure 6.7 Teflon 21: 0.50 g (PVC, PTFE, PE), 3.50 g (1.5X) NaHCO ₃ , 1.0 slpm CO _{2(g)}	67
Figure 6.8 Halide Polymer Reaction Temperatures.....	68
Figure 8.1 E-Waste Sample.....	77
Figure 8.2 E-Waste Temperature Data.....	78
Figure 8.3 Gas Analysis, 6.30 g E-Waste.....	79
Figure 8.4 6.30 g E-Waste, 1.26 g NaHCO ₃	80
Figure 8.5 Gas Analysis, 6.30 g E-Waste, 1.26 g NaHCO ₃	81
Figure 8.6 XRD Analysis of E-Waste with and without NaHCO ₃	82
Figure 8.7 Continuous Feed Rotary Kiln: E-Waste (Final 4 Part 1).....	84
Figure 8.8 Continuous Feed Rotary Kiln: E-Waste (Final 4 Part 2).....	85
Figure 8.9 Continuous Feed Rotary Kiln: E-Waste with NaHCO ₃ (Final 5).....	86
Figure 8.10 Processed E-Waste Sample.....	87
Figure 8.11 Proposed Unit Operation.....	90
Figure 8.12 Heat and Mass Balance—Flowchart.....	96
Figure 8.13 Sodium Slag Ternary Phase Diagram.....	98
Figure 8.14 Cu-Ni-Sn Ternary Phase Diagram.....	99
Figure A1 Exp 1: 200 g PE, 2.0 slpm CO _{2(g)} , 600°C.....	CD 110
Figure A2 Exp 1: 200 g PE, 2.0 slpm CO _{2(g)} , 600°C.....	CD 111
Figure A3 Exp 2: 1 g PE, 2.0 slpm CO _{2(g)} , 600°C.....	CD 112
Figure A4 Exp 3: 1 g PE, 10 g MgO, 2.0 slpm CO _{2(g)} , 600°C.....	CD 113
Figure A5 Exp 3: 1 g PE, 10 g MgO, 2.0 slpm CO _{2(g)} , 600°C.....	CD 114
Figure A6 Exp 9: 10 g PE, 5.22 g CaCO ₃ , 2.0 slpm CO _{2(g)}	CD 115
Figure A7 Exp 9: 10 g PE, 5.22 g CaCO ₃ , 2.0 slpm CO _{2(g)}	CD 116

Figure A8 Exp 10: 10 g PE, 5.22 g CaCO ₃ , 2.0 slpm N _{2(g)}	CD 117
Figure A9 Exp 10: 10 g PE, 5.22 g CaCO ₃ , 2.0 slpm N _{2(g)}	CD 118
Figure A10 Exp 11: 10 g PE, 5.22 g MgCO ₃ Mg(OH) ₂ ·3H ₂ O, 2.0 slpm CO _{2(g)}	CD 119
Figure A11 Exp 11: 10 g PE, 5.22 g MgCO ₃ Mg(OH) ₂ ·3H ₂ O, 2.0 slpm CO _{2(g)}	CD 120
Figure A12 Exp 12: 10 g PE, 4.4 g MgCO ₃ Mg(OH) ₂ ·3H ₂ O, 2.0 slpm N _{2(g)}	CD 121
Figure A13 Exp 12: 10 g PE, 4.4 g MgCO ₃ Mg(OH) ₂ ·3H ₂ O, 2.0 slpm N _{2(g)}	CD 122
Figure A14 Exp 13: 10 g PE, 4.4 g MgCO ₃ Mg(OH) ₂ ·3H ₂ O, 2.2 g CaCO ₃ , 2.0 slpm CO _{2(g)}	CD 123
Figure A15 Exp 13: 10 g PE, 4.4 g MgCO ₃ Mg(OH) ₂ ·3H ₂ O, 2.2 g CaCO ₃ , 2.0 slpm CO _{2(g)}	CD 124
Figure A16 Exp 14: 10 g PE, 4.4 g MgCO ₃ Mg(OH) ₂ ·3H ₂ O, 2.2 g CaCO ₃ , 2.0 slpm N _{2(g)}	CD 125
Figure A17 Exp 15: 10 g PE, 4.4 g MgCO ₃ Mg(OH) ₂ ·3H ₂ O, 2.0 slpm CO.....	CD 126
Figure A18 Exp 18: 5 g PE, 15 g MgCO ₃ Mg(OH) ₂ ·3H ₂ O, Purge with CO _{2(g)} , 400°C.....	CD 127
Figure A19 Exp 18: 5 g PE, 15 g MgCO ₃ Mg(OH) ₂ ·3H ₂ O, Purge with CO _{2(g)} , 400°C.....	CD 128
Figure A20 Exp 19: 5 g PE, 15 g MgCO ₃ Mg(OH) ₂ ·3H ₂ O, Purge with CO _{2(g)} , 450°C.....	CD 129
Figure A21 Exp 20: 5 g PE, 15 g MgCO ₃ Mg(OH) ₂ ·3H ₂ O, Purge with CO _{2(g)} , 350°C.....	CD 130
Figure A22 Exp 21: 5 g PE, 15 g MgCO ₃ Mg(OH) ₂ ·3H ₂ O, Purge with CO _{2(g)} , 300°C.....	CD 131
Figure A23 Exp 22: 0 g PE, 0 g MgCO ₃ Mg(OH) ₂ ·3H ₂ O, Purge with CO _{2(g)} , 350°C.....	CD 132
Figure A24 Exp 23: 0 g PE, 15 g MgCO ₃ Mg(OH) ₂ ·3H ₂ O, Purge with CO _{2(g)} , 350°C.....	CD 133
Figure A25 Exp 24: 5 g PE, 6.2 g MgO (from Exp 23), Purge with CO _{2(g)} , 350°C.....	CD 134
Figure A26 Exp 25: 10 g PE, 15 g MgCO ₃ Mg(OH) ₂ ·3H ₂ O, Purge with CO _{2(g)} , 350°C.....	CD 135
Figure A27 Exp 26: 10 g PE, 15 g MgCO ₃ Mg(OH) ₂ ·3H ₂ O, Purge with CO _{2(g)} , 400°C.....	CD 136
Figure A28 Exp 27: 10 g PE, 15 g MgCO ₃ Mg(OH) ₂ ·3H ₂ O, Purge with CO _{2(g)} , 450°C.....	CD 137
Figure A29 Exp 28: 5 g PE, 15 g MgCO ₃ Mg(OH) ₂ ·3H ₂ O, Purge with CO _{2(g)} , 450°C.....	CD 138
Figure A30 Exp 29: 5 g PE, 15 g MgCO ₃ Mg(OH) ₂ ·3H ₂ O, Purge with CO _{2(g)} , 400°C.....	CD 139
Figure A31 Exp 30: 5 g PE, 6.2 g MgO.....	CD 140
Figure A32 Exp 31: 5 g PE, 6.2 g MgO.....	CD 141
Figure A33 Exp 32: 5 g PE, 15 g MgCO ₃ Mg(OH) ₂ ·3H ₂ O.....	CD 142
Figure A34 Exp 33: 5 g PE, 15 g MgCO ₃ Mg(OH) ₂ ·3H ₂ O.....	CD 143
Figure A35 Exp 34: 5 g PE, 15 g MgCO ₃ Mg(OH) ₂ ·3H ₂ O.....	CD 144
Figure A36 Exp 35: 5 g PE, 15 g MgCO ₃ Mg(OH) ₂ ·3H ₂ O.....	CD 145
Figure A37 Exp 36: 5 g PE, 15 g Carbon.....	CD 146

Figure A38 Exp 37: 5 g PE, 15 g $\text{MgCO}_3\text{Mg}(\text{OH})_2 \cdot 3\text{H}_2\text{O}$	CD 147
Figure A49 Exp 38: 5 g PE, 15 g $\text{MgCO}_3\text{Mg}(\text{OH})_2 \cdot 3\text{H}_2\text{O}$	CD 148
Figure A40 Exp 39: 5 g PE, 15 g $\text{MgCO}_3\text{Mg}(\text{OH})_2 \cdot 3\text{H}_2\text{O}$	CD 149
Figure A41 Exp 40: 5 g PE, 15 g $\text{MgCO}_3\text{Mg}(\text{OH})_2 \cdot 3\text{H}_2\text{O}$	CD 150
Figure A42 Exp 41: 5 g PE, 15 g MgCO_3 , Purge with $\text{CO}_{2(g)}$	CD 151
Figure A43 Exp 42: 5 g PE, 15 g MgCO_3 , Purge with $\text{CO}_{2(g)}$	CD 152
Figure A44 Exp 43: 5 g PE, 15 g MgCO_3 , Purge with $\text{CO}_{2(g)}$	CD 153
Figure A45 Exp 44: 50 g PE, 50 g $\text{MgCO}_3\text{Mg}(\text{OH})_2 \cdot 3\text{H}_2\text{O}$, 0.61 slpm $\text{CO}_{2(g)}$, 450°C	CD 154
Figure A46 Exp 44: 50 g PE, 50 g $\text{MgCO}_3\text{Mg}(\text{OH})_2 \cdot 3\text{H}_2\text{O}$, 0.61 slpm $\text{CO}_{2(g)}$, 450°C	CD 155
Figure A47 Exp 45: 50 g PE, 50 g $\text{MgCO}_3\text{Mg}(\text{OH})_2 \cdot 3\text{H}_2\text{O}$, 0.61 slpm $\text{CO}_{2(g)}$, 425°C	CD 156
Figure A48 Exp 46: 50 g PE, 10 g $\text{MgCO}_3\text{Mg}(\text{OH})_2 \cdot 3\text{H}_2\text{O}$, 50 g CaCO_3 , 0.61 slpm $\text{CO}_{2(g)}$, 425°C	CD 158
Figure B1 Baseline Temp curves for Tube Furnace Experiments	CD 159
Figure B2 Sodium Compound Baseline Temp Curves	CD 160
Figure B3 Temp Curve Empty Boat, 400°C, 1.0 slpm $\text{CO}_{2(g)}$	CD 161
Figure B4 Temp Curve 0.80 g CaCO_3 Ref 400°C, 1.0 slpm $\text{CO}_{2(g)}$	CD 162
Figure B5 Temp Curve 0.68 g MgCO_3 Ref 400°C, 1.0 slpm $\text{CO}_{2(g)}$	CD 163
Figure B6 Temp Curve 0.85 g Na_2CO_3 Ref 400°C, 1.0 slpm $\text{CO}_{2(g)}$	CD 164
Figure B7 Temp Curve 0.64 g NaOH Ref 400°C, 1.0 slpm $\text{CO}_{2(g)}$	CD 165
Figure B8 Temp Curve 1.35 g NaHCO_3 Ref 400°C, 1.0 slpm $\text{CO}_{2(g)}$	CD 166
Figure B9 Temp Curve 1.00 g PVC Ref 400°C, 1.0 slpm $\text{CO}_{2(g)}$	CD 167
Figure B10 Temp Curve Exp 2: 1.00 g PVC, 1.35 g (1X) NaHCO_3 , 1.0 slpm $\text{CO}_{2(g)}$ 400°C	CD 168
Figure B11 Temp Curve Exp 3: 1.00 g PVC, 0.80 g (1X) CaCO_3 400°C, 1.0 slpm $\text{CO}_{2(g)}$	CD 169
Figure B12 Temp Curve Exp 4: 1.00 g PVC, 0.85 g Na_2CO_3 , 450°C, 1.0 slpm $\text{CO}_{2(g)}$	CD 170
Figure B13 Temp Curve Exp 5: 1.00 g PVC, 0.68 g MgCO_3 , 450°C, 1.0 slpm $\text{CO}_{2(g)}$	CD 171
Figure B14 Temp Curve Exp 6: 1.00 g PVC, 1.34 g (1X) NaHCO_3 , 450°C, 1.0 slpm $\text{CO}_{2(g)}$	CD 172
Figure B15 Temp Curve Exp 7: 1.00 g PVC, 0.64 g (1X) NaOH 400°C, 1.0 slpm $\text{CO}_{2(g)}$	CD 173

Figure B16 Temp Curve Exp 8: 1.00 g PVC, 0.85 g (1X) Na ₂ CO ₃ , 400°C, 1.0 slpm	
CO _{2(g)}	CD 174
Figure B17 Temp Curve Exp 9: 1.00 g PVC, 0.68 g (1X) MgCO ₃ , 400°C, 1.0 slpm	
CO _{2(g)}	CD 175
Figure B18 Temp Curve Exp 10: 1.00 g PVC, 0.80 g CaCO ₃ , 450°C, 1.0 slpm CO _{2(g)}	CD 176
Figure B19 Temp Curve Exp 11: 1.00 g PVC, 0.85 g (1X) Na ₂ CO ₃ , 500°C, 1.0 slpm	
CO _{2(g)}	CD 177
Figure B20 Temp Curve Exp 12: 1.00 g PVC, 0.80 g (1X) CaCO ₃ , 500°C, 1.0 slpm	
CO _{2(g)}	CD 178
Figure B21 Temp Curve Exp 13: 1.00 g PVC, 0.64 g (1X) NaOH, 450°C, 1.0 slpm	
CO _{2(g)}	CD 179
Figure B22 Temp Curve Exp 14: 1.00 g PVC, 1.34 g (1X) NaHCO ₃ , 500°C, 1.0 slpm	
CO _{2(g)}	CD 180
Figure B23 Temp Curve Exp 15: 1.00 g PVC, 0.68 g (1X) MgCO ₃ , 500°C, 1.0 slpm	
CO _{2(g)}	CD 181
Figure B24 Temp Curve 1.00 g PVC Ref 600°C, 1.0 slpm CO _{2(g)}	CD 182
Figure B25 Temp Curve 1.00 g PTFE Ref 545°C, 1.0 slpm CO _{2(g)}	CD 183
Figure B26 Temp Curve 1.00 g PTFE Ref 600°C, 1.0 slpm CO _{2(g)}	CD 184
Figure B27 Temp Curve Teflon 1: 1.00 g PTFE, 3.36 g (1X) NaHCO ₃ , 1.0 slpm CO _{2(g)} ...	CD 185
Figure B28 Temp Curve Teflon 2: 1.00 g PTFE, 3.34 g (1X) Na ₂ CO ₃ , 555°C, 1.0 slpm	
CO _{2(g)}	CD 186
Figure B29 Temp Curve Teflon 3: 1.00 g PTFE, 3.36 g (1X) NaHCO ₃ , 550°C, 1.0 slpm	
CO _{2(g)}	CD 187
Figure B30 Temp Curve Teflon 4: 1.00 g PTFE, 1.60 g (1X) NaOH, 1.0 slpm CO _{2(g)}	CD 188
Figure B31 Temp Curve Teflon 5: 1.00 g PTFE, 3.36 g (1X) NaHCO ₃ , 1.0 slpm CO _{2(g)} ,	
600°C	CD 189
Figure B32 Temp Curve Teflon 6: 1.00 g PTFE, 1.60 g (1X) NaOH, 1.0 slpm CO _{2(g)}	CD 190
Figure B33 Temp Curve Teflon 7: 1.00 g PTFE, 2.11 g Na ₂ CO ₃ , 1.0 slpm CO _{2(g)}	CD 191
Figure B34 Temp Curve Teflon 8: 1.00 g PTFE, 1.00 g PVC, 7.06 g NaHCO ₃ , 1.0 slpm	
CO _{2(g)}	CD 192

Figure B35 Temp Curve Teflon 9: 0.5 g (PVC, PTFE, PE), 2.30 g NaHCO ₃ , 1.0 slpm.....	
CO _{2(g)}	CD 193
Figure B36 Temp Curve Teflon 10: 0.5 g (PVC, PTFE, PE), 1.0 slpm CO _{2(g)}	CD 194
Figure B37 Temp Curve Teflon 11: 1.00 g PE, 1.0 slpm CO _{2(g)}	CD 195
Figure B38 Temp Curve Teflon 12: 0.5 g PVC, 0.5 g PE, 0.67 g NaOH, 1.0 slpm CO _{2(g)}	CD 196
Figure B39 Temp Curve Teflon 13: 0.5 g PTFE, 2.52 g NaHCO ₃ (1.5X) 1.0 slpm CO _{2(g)}	CD 197
Figure B40 Temp Curve Teflon 14: 0.5 g PVC, 1.00 g NaHCO ₃ , 1.0 slpm CO _{2(g)}	CD 198
Figure B41 Temp Curve Teflon 15: 0.5 g PVC, 0.5 g PE, 1.0 slpm CO _{2(g)}	CD 199
Figure B42 Temp Curve Teflon 16: 0.5 g PTFE, 0.5 g PE, 1.0 slpm CO _{2(g)}	CD 200
Figure B43 Temp Curve Teflon 16 Redo II: 0.5 g PTFE, 0.5 g PE, 1.0 slpm CO _{2(g)}	CD 201
Figure B44 Temp Curve Teflon 17 Redo II: 0.5 g PVC, 0.5 g PTFE, 0.5 g PE, 1.0 slpm.....	
CO _{2(g)}	CD 202
Figure B45 Temp Curve Teflon 18 redo: 0.5 g PTFE, 0.5 g PVC, 1.0 slpm CO _{2(g)}	CD 203
Figure B46 Temp Curve Teflon 19: 0.5 g PVC, 0.5 g PE, 1.00 g (1.5X) NaHCO ₃ , 1.0 slpm	
CO _{2(g)}	CD 204
Figure B47 Temp Curve Teflon 19 Redo II: 0.5 g PVC, 0.5 g PE, 1.00 g NaHCO ₃ , 1.0 slpm	
CO _{2(g)}	CD 205
Figure B48 Temp Curve Teflon 20: 0.5 g PTFE, 0.5 g PE, 2.52 g (1.5X) NaHCO ₃ , 1.0 slpm	
CO _{2(g)}	CD 206
Figure B49 Temp Curve Teflon 21: 0.5 g (PTFE, PVC, PE), 3.5 g (1.5X) NaHCO ₃ , 1.0 slpm	
CO _{2(g)}	CD 207
Figure B50 Temp Curve Teflon 22: 0.5 g PVC, 0.5 g PTFE, 3.5 g (1.5X) NaHCO ₃ , 1.0 slpm	
CO _{2(g)}	CD 208
Figure B51 Temp Curve Teflon 23 Redo II: .25 g PVC, 1.00 g PE, 1.0 slpm CO _{2(g)}	CD 209
Figure B52 Temp Curve Teflon 24: 0.25 g PTFE, 1.00 g PE, 1.0 slpm CO _{2(g)}	CD 210
Figure B53 Temp Curve Teflon 24 Redo: 0.25 g PTFE, 1.00 g PE, 1.0 slpm CO _{2(g)}	CD 211
Figure B54 Temp Curve Teflon 25: 0.25 g PVC, 0.25 g PTFE, 1.00 g PE, 1.0 slpm CO _{2(g)}	CD 212
Figure B55 Temp Curve Teflon 25 Redo: .25 g PVC, .25 g PTFE, 1.00 g PE, 1.0 slpm CO _{2(g)}	
.....	CD 213

Figure B56 Temp Curve Teflon 26: 0.25 g PVC, 1.00 g PE, 0.5 g (1.5X) NaHCO ₃ , 1.0 slpm CO _{2(g)}	CD 214
Figure B57 Temp Curve Teflon 27: 0.25 g PTFE, 1.00 g PE, 1.25 g (1.5X) NaHCO ₃ , 1.0 slpm CO _{2(g)}	CD 215
Figure B58 Temp Curve Teflon 28: 0.25 g PVC, 0.25 g PTFE, 1.00 g PE, 1.76 g (1.5X) NaHCO ₃ , 1.0 slpm CO _{2(g)} , 600°C (5 min).....	CD 216
Figure B59 Temp Curve Teflon 29: 0.25 g PVC, 0.25 g PTFE, 1.00 g PE, 1.76 g (1.5X) NaHCO ₃ , 1.0 slpm CO _{2(g)} , 500°C (5 min).....	CD 217
Figure B60 Temp Curve Teflon 30: 0.25 g PVC, 0.25 g PTFE, 1.00 g PE, 1.76 g (1.5X) NaHCO ₃ , 1.0 slpm CO _{2(g)} , 550°C (5 min).....	CD 218
Figure B61 Temp Curve Teflon 31: 0.25 g PVC, 0.25 g PTFE, 1.00 g PE, 1.76 g (1.5X) NaHCO ₃ , 500°C (20 min).....	CD 219
Figure B62 Temp Curve NOVA 1: 0.5 g (PVC, PTFE, PE), 3.5 g (1.5X) NaHCO ₃ , 0.5 slpm N _{2(g)} , 0.5 slpm CO _{2(g)}	CD 220
Figure B63 Temp Curve NOVA 1: 0.5 g (PVC, PTFE, PE), 3.5 g (1.5X) NaHCO ₃ , 0.5 slpm N _{2(g)} , 0.5 slpm CO _{2(g)}	CD 221
Figure B64 Temp Curve Comp 2: 0.5 g (PTFE, PVC, PE), 3.5 g (1.5X) NaHCO ₃ , 0.5 slpm N _{2(g)} , 0.5 slpm CO _{2(g)}	CD 222
Figure B65 Temp Curve NOVA 2: 0.5 g (PVC, PTFE, PE), 3.5 g (1.5X) NaHCO ₃ , 1 slpm CO _{2(g)}	CD 223
Figure B66 Gas Production NOVA 2: 0.5 g (PVC, PTFE, PE), 3.5 g (1.5X) NaHCO ₃ , 1 slpm CO _{2(g)}	CD 224
Figure B67 Temp Curve NOVA 3: 0.5 g (PVC, PTFE, PE), 3.5 g (1.5X) NaHCO ₃ , 1.0 slpm N _{2(g)}	CD 225
Figure B68 Gas Production NOVA 3: 0.5 g (PVC, PTFE, PE), 3.5 g (1.5X) NaHCO ₃ , 1.0 slpm N _{2(g)}	CD 226
Figure B69 Temp Curve Comp 1: 0.5 g (PTFE, PVC, PE), 3.5 g (1.5X) NaHCO ₃ , 1 slpm N _{2(g)}	CD 227
Figure B70 Temp Curve NOVA 4: 0.5 g (PVC, PTFE, PE), 3.5 g (1.5X) NaHCO ₃ , 0.5 slpm CO _(g) , 0.5 slpm CO _{2(g)}	CD 228

Figure B71 Gas Production NOVA 4: 0.5 g (PVC, PTFE, PE), 3.5 g (1.5X) NaHCO ₃ , 0.5 slpm CO _(g) , 0.5 slpm CO _{2(g)}	CD 229
Figure B72 Temp Curve Comp 3: 0.5 g (PTFE, PVC, PE), 3.5 g (1.5X) NaHCO ₃ , 0.5 slpm CO _(g) , 0.5 slpm CO _{2(g)}	CD 230
Figure B73 Temp Curve NOVA 5: 0.5 g (PTFE, PVC, PE), 3.5 g (1.5X) NaHCO ₃ , 1.0 slpm CO _(g)	CD 231
Figure B74 Gas Production NOVA 5: 0.5 g (PTFE, PVC, PE), 3.5 g (1.5X) NaHCO ₃ , 1.0 slpm CO _(g)	CD 232
Figure B75 Temp Curve Comp 4: 0.5 g (PVC, PTFE, PE), 3.5 g (1.5X) NaHCO ₃ , 1 slpm CO _(g)	CD 233
Figure B76 Temp Curve E-Waste 1: 6.3 g -1/4" Computer Board Sample	CD 234
Figure B77 Gas Production E-Waste 1: 6.3 g -1/4" Computer Board Sample	CD 235
Figure B78 Temp Curve E-Waste 1: 6.3 g -1/4" Computer Board + 1.30 g NaHCO ₃	CD 236
Figure B79 Gas Production E-Waste 1: 6.3 g -1/4" Computer Board + 1.30 g NaHCO ₃ ...	CD 237
Figure B80 Temp and Gas Data Final 4a: 150 g E-Waste Screw Feed	CD 238
Figure B81 Gas Data Final 4a: 150 g E-Waste Screw Feed	CD 239
Figure B82 Volumetric Gas Production Final 4a: 150 g E-Waste Screw Feed	CD 240
Figure B83 Temp and Gas Data Final 4b: 150 g E-Waste Screw Feed	CD 241
Figure B84 Gas Data Final 4b: 150 g E-Waste Screw Feed	CD 242
Figure B85 Volumetric Gas Production Final 4b: 150 g E-Waste Screw Feed	CD 243
Figure B86 Temp and Gas Data Final 5: 150 g E-Waste, 30 g NaHCO ₃ Screw Feed	CD 244
Figure B87 Gas Data Final 5: 150 g E-Waste, 30 g NaHCO ₃ Screw Feed	CD 245
Figure B88 Volumetric Gas Production Final 5: 150 g E-Waste, 30 g NaHCO ₃ Screw Feed	CD 247
Figure C1 XRD PE Reference Pattern	CD 248
Figure C2 XRD PVC Reference Pattern	CD 249
Figure C3 XRD PTFE Reference Pattern	CD 250
Figure C4 XRD Na ₂ CO ₃ from NaHCO ₃ Reference Pattern 400°C	CD 251
Figure C5 XRD Exp.2: 1.00 g PVC, 1.35 g (1X) NaHCO ₃ , 1.0 slpm CO _{2(g)} , 400°C	CD 252
Figure C6 XRD Exp.3: 1.00 g PVC, 0.80 g (1X) CaCO ₃ 400°C, 1.0 slpm CO _{2(g)}	CD 253

Figure C7 XRD Exp.4: 1.00 g PVC, 0.85 g Na ₂ CO ₃ , 450°C, 1.0 slpm CO _{2(g)}	CD 254
Figure C8 XRD Exp.5: 1.00 g PVC, 0.68 g MgCO ₃ , 450°C, 1.0 slpm CO _{2(g)}	CD 255
Figure C9 XRD Exp.6: 1.00 g PVC, 1.34 g (1X) NaHCO ₃ , 450°C, 1.0 slpm CO _{2(g)}	CD 256
Figure C10 XRD Exp.7: 1.00 g PVC, 0.64 g (1X) NaOH 400°C, 1.0 slpm CO _{2(g)}	CD 257
Figure C11 XRD Exp.8: 1.00 g PVC, 0.85 g (1X) Na ₂ CO ₃ 400°C, 1.0 slpm CO _{2(g)}	CD 258
Figure C12 XRD Exp.9: 1.00 g PVC, 0.68 g (1X) MgCO ₃ 400°C, 1.0 slpm CO _{2(g)}	CD 259
Figure C13 XRD Exp.10: 1.00 g PVC, 0.80 g CaCO ₃ , 450°C, 1.0 slpm CO _{2(g)}	CD 260
Figure C14 XRD Exp.11: 1.00 g PVC, 0.85 g (1X) Na ₂ CO ₃ , 500°C, 1.0 slpm CO _{2(g)}	CD 261
Figure C15 XRD Exp.12: 1.00 g PVC, 0.80 g (1X) CaCO ₃ , 500°C, 1.0 slpm CO _{2(g)}	CD 262
Figure C16 XRD Exp.13: 1.00 g PVC, 0.64 g (1X) NaOH, 450°C, 1.0 slpm CO _{2(g)}	CD 263
Figure C17 XRD Exp.14: 1.00 g PVC, 1.34 g (1X) NaHCO ₃ , 500°C, 1.0 slpm CO _{2(g)}	CD 264
Figure C18 XRD Exp.15: 1.00 g PVC, 0.68 g (1X) MgCO ₃ , 500°C, 1.0 slpm CO _{2(g)}	CD 265
Figure C19 XRD Teflon 1: 1.00 g PTFE, 3.36 g (1X) NaHCO ₃ , 1.0 slpm CO _{2(g)} , 545°C ...	CD 266
Figure C20 XRD Teflon 2: 1.00 g PTFE, 3.34 g (1X) Na ₂ CO ₃ , 1.0 slpm CO _{2(g)} , 555°C.....	CD 267
Figure C21 XRD Teflon 3: 1.00 g PTFE, 3.36 g (1X) NaHCO ₃ , 550°C, 1.0 slpm CO _{2(g)} ,	
600°C	CD 268
Figure C22 XRD Teflon 4: 1.00 g PTFE, 1.60 g (1X) NaOH, 1.0 slpm CO _{2(g)} , 600°C.....	CD 269
Figure C23 XRD Teflon 5: 1.00 g PTFE, 3.36 g (1X) NaHCO ₃ , 1.0 slpm CO _{2(g)} , 600°C ...	CD 270
Figure C24 XRD Teflon 6: 1.00 g PTFE, 1.60 g (1X) NaOH, 1.0 slpm CO _{2(g)} , 600°C.....	CD 271
Figure C25 XRD Teflon 7: 1.00 g PTFE, 2.11 g Na ₂ CO ₃ , 1.0 slpm CO _{2(g)} , 600°C.....	CD 272
Figure C26 XRD Teflon 9: 0.5 g (PVC, PTFE, PE), 2.30 g NaHCO ₃ , 1.0 slpm CO _{2(g)} ,	
600°C	CD 273
Figure C27 XRD Teflon 13: 0.5 g PTFE, 2.52 g NaHCO ₃ (1.5X) 1.0 slpm CO _{2(g)} , 600°C .	CD 274
Figure C28 XRD Teflon 14: 0.5 g PVC, 1.00 g NaHCO ₃ , 1.0 slpm CO _{2(g)} , 600°C.....	CD 275
Figure C29 XRD Teflon 19: 0.5 g PVC, 0.5 g PE, 1.00 g (1.5X) NaHCO ₃ , 1.0 slpm CO _{2(g)} ,	
600°C	CD 276
Figure C30 XRD Teflon 20: 0.5 g PTFE, 0.5 g PE, 2.52 g (1.5X) NaHCO ₃ , 1.0 slpm CO _{2(g)} ,	
600°C	CD 277
Figure C31 XRD Teflon 21: 0.5 g PVC, 0.5 g PTFE, 0.5 g PE, 3.5 g (1.5X) NaHCO ₃ , 1.0 slpm	
CO _{2(g)} , 600°C	CD 278

Figure C32 XRD Teflon 22: 0.5 g PVC, 0.5 g PTFE, 3.5 g (1.5X) NaHCO ₃ , 1.0 slpm CO _{2(g)} , 600°C	CD 279
Figure C33 XRD Teflon 26: 0.25 g PVC, 1.00 g PE, 0.5 g (1.5X) NaHCO ₃ , 1.0 slpm CO _{2(g)} , 600°C	CD 280
Figure C34 XRD Teflon 27: 0.25 g PTFE, 1.00 g PE, 1.25 g (1.5X) NaHCO ₃ , 1.0 slpm CO _{2(g)} , 600°C	CD 281
Figure C35 XRD Teflon 28: 0.25 g PVC, 0.25 g PTFE, 1.00 g PE, 1.76 g (1.5X) NaHCO ₃ , 1.0 slpm CO _{2(g)} , 600°C (5 min).....	CD 282
Figure C36 XRD Teflon 29: 0.25 g PVC, 0.25 g PTFE, 1.00 g PE, 1.76 g (1.5X) NaHCO ₃ , 1.0 slpm CO _{2(g)} , 500°C (5 min).....	CD 283
Figure C37 XRD Teflon 30: 0.25 g PVC, 0.25 g PTFE, 1.00 g PE, 1.76 g (1.5X) NaHCO ₃ , 1.0 slpm CO _{2(g)} , 550°C (5 min).....	CD 284
Figure C38 XRD Teflon 31: 0.25 g PVC, 0.25 g PTFE, 1.00 g PE, 1.76 g (1.5X) NaHCO ₃ , 500°C (20 min)	CD 285
Figure C39 XRD Comp 2: 0.5 g (PTFE, PVC, PE), 3.5 g (1.5X) NaHCO ₃ , 0.5 slpm N _{2(g)} , 0.5 slpm CO _{2(g)} (1-14-06)	CD 286
Figure C40 XRD Comp 1: 0.5 g (PTFE, PVC, PE), 3.5 g (1.5X) NaHCO ₃ , 1 slpm N _{2(g)}	CD 287
Figure C41 XRD Final 1: 6.3 g E-Waste.....	CD 288
Figure C42 XRD Final 5: 6.3 g E-Waste, 1.2 g NaHCO ₃	CD 289
Figure D1a PTFE: TG and DTG Data.....	CD 291
Figure D1b PTFE: DTG and DTA Data.....	CD 291
Figure D1c PTFE: DTG and CH ₄ MS Data.....	CD 291
Figure D1d PTFE: DTG and H ₂ O MS Data	CD 291
Figure D1e PTFE: DTG and HF MS Data	CD 292
Figure D1f PTFE: DTG and C ₂ H ₄ MS Data.....	CD 292
Figure D1g PTFE: DTG and HCl MS Data.....	CD 292
Figure D1h PTFE: DTG and 68 Furan/Dioxin MS Data.....	CD 292
Figure D1i PTFE: DTG and C ₆ H ₆ MS Data	CD 293
Figure D1j PTFE: DTG and TFE MS Data	CD 293
Figure D2a NaHCO ₃ : TG and DTG Data.....	CD 294

Figure D2b NaHCO ₃ : DTG and DTA Data.....	CD 294
Figure D2c NaHCO ₃ : DTG and CH ₄ MS Data.....	CD 294
Figure D2d NaHCO ₃ : DTG and H ₂ O MS Data	CD 294
Figure D2e NaHCO ₃ : DTG and C ₂ H ₄ MS Data.....	CD 295
Figure D2f NaHCO ₃ : DTG and HCl MS Data	CD 295
Figure D2g NaHCO ₃ : DTG and 68 Furan/Dioxin MS Data.....	CD 295
Figure D2h NaHCO ₃ : DTG and C ₆ H ₆ MS Data	CD 295
Figure D2i NaHCO ₃ : DTG and TFE MS Data	CD 296
Figure D3a Na ₂ CO ₃ : TG and DTG Data	CD 297
Figure D3b Na ₂ CO ₃ : DTG and DTA Data	CD 297
Figure D3c Na ₂ CO ₃ : DTG and CH ₄ MS Data	CD 297
Figure D3d Na ₂ CO ₃ : DTG and H ₂ O MS Data.....	CD 297
Figure D3e Na ₂ CO ₃ : DTG and C ₂ H ₄ MS Data	CD 298
Figure D3f Na ₂ CO ₃ : DTG and HCl MS Data.....	CD 298
Figure D3g Na ₂ CO ₃ : DTG and 68 Furan/Dioxin MS Data	CD 298
Figure D3h Na ₂ CO ₃ : DTG and C ₆ H ₆ MS Data.....	CD 298
Figure D3i Na ₂ CO ₃ : DTG and TFE MS Data.....	CD 299
Figure D4a NaHCO ₃ + PVC: TG and DTG Data	CD 300
Figure D4b NaHCO ₃ + PVC: DTG and DTA Data	CD 300
Figure D4c NaHCO ₃ + PVC: DTG and CH ₄ MS Data	CD 300
Figure D4d NaHCO ₃ + PVC: DTG and H ₂ O MS Data.....	CD 300
Figure D4e NaHCO ₃ + PVC: DTG and C ₂ H ₄ MS Data	CD 301
Figure D4f NaHCO ₃ + PVC: DTG and HCl MS Data.....	CD 301
Figure D4g NaHCO ₃ + PVC: DTG and 68 Furan/Dioxin MS Data	CD 301
Figure D4h NaHCO ₃ + PVC: DTG and C ₆ H ₆ MS Data.....	CD 301
Figure D4i NaHCO ₃ + PVC: DTG and TFE MS Data.....	CD 302
Figure D5a Na ₂ CO ₃ + PVC: TG and DTG Data.....	CD 303
Figure D5b Na ₂ CO ₃ + PVC: DTG and DTA Data.....	CD 303
Figure D5c Na ₂ CO ₃ + PVC: DTG and CH ₄ MS Data.....	CD 303
Figure D5d Na ₂ CO ₃ + PVC: DTG and H ₂ O MS Data	CD 303

Figure D5e Na ₂ CO ₃ + PVC: DTG and C ₂ H ₄ MS Data.....	CD 304
Figure D5f Na ₂ CO ₃ + PVC: DTG and HCl MS Data	CD 304
Figure D5g Na ₂ CO ₃ + PVC: DTG and 68 Furan/Dioxin MS Data.....	CD 304
Figure D5h Na ₂ CO ₃ + PVC: DTG and C ₆ H ₆ MS Data	CD 304
Figure D5i Na ₂ CO ₃ + PVC: DTG and TFE MS Data	CD 305
Figure D6a NaHCO ₃ + PTFE: TG and DTG Data.....	CD 306
Figure D6b NaHCO ₃ + PTFE: DTG and DTA Data.....	CD 306
Figure D6c NaHCO ₃ + PTFE: DTG and CH ₄ MS Data.....	CD 306
Figure D6d NaHCO ₃ + PTFE: DTG and H ₂ O MS Data	CD 306
Figure D6e NaHCO ₃ + PTFE: DTG and C ₂ H ₄ MS Data.....	CD 307
Figure D6f NaHCO ₃ + PTFE: DTG and HCl MS Data	CD 307
Figure D6g NaHCO ₃ + PTFE: DTG and 68 Furan/Dioxin MS Data.....	CD 307
Figure D6h NaHCO ₃ + PTFE: DTG and C ₆ H ₆ MS Data	CD 307
Figure D6i NaHCO ₃ + PTFE: DTG and TFE MS Data	CD 308
Figure D7a Na ₂ CO ₃ + PTFE: TG and DTG Data	CD 309
Figure D7b Na ₂ CO ₃ + PTFE: DTG and DTA Data	CD 309
Figure D7c Na ₂ CO ₃ + PTFE: DTG and CH ₄ MS Data	CD 309
Figure D7d Na ₂ CO ₃ + PTFE: DTG and H ₂ O MS Data.....	CD 309
Figure D7e Na ₂ CO ₃ + PTFE: DTG and C ₂ H ₄ MS Data	CD 310
Figure D7f Na ₂ CO ₃ + PTFE: DTG and HCl MS Data.....	CD 310
Figure D7g Na ₂ CO ₃ + PTFE: DTG and 68 Furan/Dioxin MS Data	CD 310
Figure D7h Na ₂ CO ₃ + PTFE: DTG and C ₆ H ₆ MS Data.....	CD 310
Figure D7i Na ₂ CO ₃ + PTFE: DTG and TFE MS Data.....	CD 311
Figure D8a NaHCO ₃ + PVC + PE: TG and DTG Data.....	CD 312
Figure D8b NaHCO ₃ + PVC + PE: DTG and DTA Data.....	CD 312
Figure D8c NaHCO ₃ + PVC + PE: DTG and CH ₄ MS Data.....	CD 312
Figure D8d NaHCO ₃ + PVC + PE: DTG and H ₂ O MS Data	CD 312
Figure D8e NaHCO ₃ + PVC + PE: DTG and C ₂ H ₄ MS Data.....	CD 313
Figure D8f NaHCO ₃ + PVC + PE: DTG and HCl MS Data	CD 313
Figure D8g NaHCO ₃ + PVC + PE: DTG and 68 Furan/Dioxin MS Data.....	CD 313

Figure D8h NaHCO ₃ + PVC + PE: DTG and C ₆ H ₆ MS Data	CD 313
Figure D8i NaHCO ₃ + PVC + PE: DTG and TFE MS Data	CD 314
Figure D9a Na ₂ CO ₃ + PVC + PE: TG and DTG Data	CD 315
Figure D9b Na ₂ CO ₃ + PVC + PE: DTG and DTA Data	CD 315
Figure D9c Na ₂ CO ₃ + PVC + PE: DTG and CH ₄ MS Data	CD 315
Figure D9d Na ₂ CO ₃ + PVC + PE: DTG and H ₂ O MS Data.....	CD 315
Figure D9e Na ₂ CO ₃ + PVC + PE: DTG and C ₂ H ₄ MS Data	CD 316
Figure D9f Na ₂ CO ₃ + PVC + PE: DTG and HCl MS Data.....	CD 316
Figure D9g Na ₂ CO ₃ + PVC + PE: DTG and 68 Furan/Dioxin MS Data	CD 316
Figure D9h Na ₂ CO ₃ + PVC + PE: DTG and C ₆ H ₆ MS Data.....	CD 316
Figure D9i Na ₂ CO ₃ + PVC + PE: DTG and TFE MS Data.....	CD 317
Figure D10a NaHCO ₃ + PTFE + PE: TG and DTG Data	CD 318
Figure D10b NaHCO ₃ + PTFE + PE: DTG and DTA Data	CD 318
Figure D10c NaHCO ₃ + PTFE + PE: DTG and CH ₄ MS Data	CD 318
Figure D10d NaHCO ₃ + PTFE + PE: DTG and H ₂ O MS Data.....	CD 318
Figure D10e NaHCO ₃ + PTFE + PE: DTG and C ₂ H ₄ MS Data	CD 319
Figure D10f NaHCO ₃ + PTFE + PE: DTG and HCl MS Data.....	CD 319
Figure D10g NaHCO ₃ + PTFE + PE: DTG and 68 Furan/Dioxin MS Data	CD 319
Figure D10h NaHCO ₃ + PTFE + PE: DTG and C ₆ H ₆ MS Data.....	CD 319
Figure D10i NaHCO ₃ + PTFE + PE: DTG and TFE MS Data.....	CD 320
Figure D11a Na ₂ CO ₃ + PTFE + PE: TG and DTG Data.....	CD 321
Figure D11b Na ₂ CO ₃ + PTFE + PE: DTG and DTA Data.....	CD 321
Figure D11c Na ₂ CO ₃ + PTFE + PE: DTG and CH ₄ MS Data.....	CD 321
Figure D11d Na ₂ CO ₃ + PTFE + PE: DTG and H ₂ O MS Data.....	CD 321
Figure D11e Na ₂ CO ₃ + PTFE + PE: DTG and C ₂ H ₄ MS Data.....	CD 322
Figure D11f Na ₂ CO ₃ + PTFE + PE: DTG and HCl MS Data.....	CD 322
Figure D11g Na ₂ CO ₃ + PTFE + PE: DTG and 68 Furan/Dioxin MS Data.....	CD 322
Figure D11h Na ₂ CO ₃ + PTFE + PE: DTG and C ₆ H ₆ MS Data.....	CD 322
Figure D11i Na ₂ CO ₃ + PTFE + PE: DTG and TFE MS Data	CD 323
Figure D12a NaHCO ₃ + PVC + PTFE: TG and DTG Data	CD 324

Figure D12b NaHCO ₃ + PVC + PTFE: DTG and DTA Data	CD 324
Figure D12c NaHCO ₃ + PVC + PTFE: DTG and CH ₄ MS Data	CD 324
Figure D12d NaHCO ₃ + PVC + PTFE: DTG and H ₂ O MS Data	CD 324
Figure D12e NaHCO ₃ + PVC + PTFE: DTG and C ₂ H ₄ MS Data	CD 325
Figure D12f NaHCO ₃ + PVC + PTFE: DTG and HCl MS Data	CD 325
Figure D12g NaHCO ₃ + PVC + PTFE: DTG and 68 Furan/Dioxin MS Data	CD 325
Figure D12h NaHCO ₃ + PVC + PTFE: DTG and C ₆ H ₆ MS Data	CD 325
Figure D12i NaHCO ₃ + PVC + PTFE: DTG and TFE MS Data	CD 326
Figure D13a Na ₂ CO ₃ + PVC + PTFE: TG and DTG Data	CD 327
Figure D13b Na ₂ CO ₃ + PVC + PTFE: DTG and DTA Data	CD 327
Figure D13c Na ₂ CO ₃ + PVC + PTFE: DTG and CH ₄ MS Data	CD 327
Figure D13d Na ₂ CO ₃ + PVC + PTFE: DTG and H ₂ O MS Data	CD 327
Figure D13e Na ₂ CO ₃ + PVC + PTFE: DTG and C ₂ H ₄ MS Data	CD 328
Figure D13f Na ₂ CO ₃ + PVC + PTFE: DTG and HCl MS Data	CD 328
Figure D13g Na ₂ CO ₃ + PVC + PTFE: DTG and 68 Furan/Dioxin MS Data	CD 328
Figure D13h Na ₂ CO ₃ + PVC + PTFE: DTG and C ₆ H ₆ MS Data	CD 328
Figure D13i Na ₂ CO ₃ + PVC + PTFE: DTG and TFE MS Data	CD 329
Figure D14a PVC: TG and DTG Data	CD 330
Figure D14b PVC: DTG and DTA Data	CD 330
Figure D14c PVC: DTG and CH ₄ MS Data	CD 330
Figure D14d PVC: DTG and H ₂ O MS Data	CD 330
Figure D14e PVC: DTG and C ₂ H ₄ MS Data	CD 331
Figure D14f PVC: DTG and HCl MS Data	CD 331
Figure D14g PVC: DTG and 68 Furan/Dioxin MS Data	CD 331
Figure D14h PVC: DTG and C ₆ H ₆ MS Data	CD 331
Figure D14i PVC: DTG and TFE MS Data	CD 332
Figure D15a PVC + PTFE: TG and DTG Data	CD 333
Figure D15b PVC + PTFE: DTG and DTA Data	CD 333
Figure D15c PVC + PTFE: DTG and CH ₄ MS Data	CD 333
Figure D15d PVC + PTFE: DTG and H ₂ O H ₂ O MS Data	CD 333

Figure D15e PVC + PTFE: DTG and HF MS Data.....	CD 334
Figure D15f PVC + PTFE: DTG and C ₂ H ₄ MS Data	CD 334
Figure D15g PVC + PTFE: DTG and HCl MS Data	CD 334
Figure D15h PVC + PTFE: DTG and 68 Furan/Dioxin MS Data	CD 334
Figure D15i PVC + PTFE: DTG and C ₆ H ₆ MS Data.....	CD 335
Figure D15j PVC + PTFE: DTG and TFE MS Data.....	CD 335
Figure D16a PVC + PE: TG and DTG Data.....	CD 336
Figure D16b PVC + PE: DTG and DTA Data.....	CD 336
Figure D16c PVC + PE: DTG and CH ₄ MS Data.....	CD 336
Figure D16d PVC + PE: DTG and H ₂ O MS Data	CD 336
Figure D16e PVC + PE: DTG and HF MS Data	CD 337
Figure D16f PVC + PE: DTG and C ₂ H ₄ MS Data.....	CD 337
Figure D16g PVC + PE: DTG and HCl MS Data.....	CD 337
Figure D16h PVC + PE: DTG and 68 Furan/Dioxin MS Data.....	CD 337
Figure D16i PVC + PE: DTG and C ₆ H ₆ MS Data	CD 338
Figure D16j PVC + PE: DTG and TFE MS Data	CD 338
Figure D17a PTFE + PE: TG and DTG Data	CD 339
Figure D17b PTFE + PE: DTG and DTA Data	CD 339
Figure D17c PTFE + PE: DTG and CH ₄ MS Data	CD 339
Figure D17d PTFE + PE: DTG and H ₂ O MS Data.....	CD 339
Figure D17e PTFE + PE: DTG and HF MS Data.....	CD 340
Figure D17f PTFE + PE: DTG and C ₂ H ₄ MS Data	CD 340
Figure D17g PTFE + PE: DTG and HCl MS Data	CD 340
Figure D17h PTFE + PE: DTG and 68 Furan/Dioxin MS Data	CD 340
Figure D17i PTFE + PE: DTG and C ₆ H ₆ MS Data.....	CD 341
Figure D17j PTFE + PE: DTG and TFE MS Data.....	CD 341
Figure D18a PVC + PTFE + PE: TG and DTG Data.....	CD 342
Figure D18b PVC + PTFE + PE: DTG and DTA Data.....	CD 342
Figure D18c PVC + PTFE + PE: DTG and CH ₄ MS Data.....	CD 342
Figure D18d PVC + PTFE + PE: DTG and H ₂ O MS Data	CD 342

Figure D18e PVC + PTFE + PE: DTG and HF MS Data	CD 343
Figure D18f PVC + PTFE + PE: DTG and C ₂ H ₄ MS Data.....	CD 343
Figure D18g PVC + PTFE + PE: DTG and HCl MS Data.....	CD 343
Figure D18h PVC + PTFE + PE: DTG and 68 Furan/Dioxin MS Data.....	CD 343
Figure D18i PVC + PTFE + PE: DTG and C ₆ H ₆ MS Data	CD 344
Figure D18j PVC + PTFE + PE: DTG and TFE MS Data	CD 344
Figure D19a PE: TG and DTG Data	CD 345
Figure D19b PE: DTG and DTA Data	CD 345
Figure D19c PE: DTG and CH ₄ MS Data	CD 345
Figure D19d PE: DTG and H ₂ O MS Data.....	CD 345
Figure D19e PE: DTG and HF MS Data.....	CD 346
Figure D19f PE: DTG and C ₂ H ₄ MS Data	CD 346
Figure D19g PE: DTG and HCl MS Data	CD 346
Figure D19h PE: DTG and 68 Furan/Dioxin MS Data.....	CD 346
Figure D19i PE: DTG and C ₆ H ₆ MS Data.....	CD 347
Figure D19j PE: DTG and TFE MS Data.....	CD 347

LIST OF TABLES

Table 2.1 General Printed Circuit Board Composition	7
Table 2.2 Metal Assay of E-Waste—Literature Review	8
Table 2.3 Average Valuation—Literature Review	9
Table 2.4 Thermal Value.....	9
Table 4.1 Idealized Metal and Slag Composition	27
Table 5.1 Rotary Kiln Data Acquired	38
Table 5.2 Polymer Reference Data, in N _{2(g)}	43
Table 6.1 Tube Furnace Data Acquired	58
Table 6.2 % Cl- Retained in Ash +/- 3.41%.....	60
Table 6.3 Mixed Polymer Matrix.....	65
Table 6.4 Mixed Polymer Halide Sequestering	69
Table 6.5 Atmospheres Investigated	70
Table 6.6 Gas Production vs, Atmosphere	71
Table 7.1 Mixed Polymer/Carbonate Samples - TG/DTA–MS.....	74
Table 8.1 Comparable Gas Products-E-Waste Tube Furnace.....	81
Table 8.2 Comparable Gas Products: E-Waste Rotary Kiln.....	84
Table 8.3 Comparable Gas Products: E-Waste + NaHCO ₃ Rotary Kiln.....	87
Table 8.4 Dioxin/Furan Results for Kiln Experiments.....	88
Table 8.5 Heat and Mass Balance: Initial Kiln operation.....	90
Table 8.6 Operational Parameters and 1st Order Kiln Design Specifications	91
Table 8.7 Solids Combustion Inputs, Energy Recovery.....	92
Table 8.8 Solids Combustion Outputs, Gas and Fume.....	93
Table 8.9 Solids Combustion Outputs, Slag and Metal.....	94
Table 8.10 Gas Combustion Inputs, Energy Recovery	95
Table 8.11 Gas Combustion Outputs, Energy Recovery	96
Table 8.12 Primary Slag Constituents.....	98
Table 8.13 Sodium Slag Composition.....	98

ACKNOWLEDGEMENTS

Appreciation is given to Phelps Dodge for financial supporting in the area of extractive metallurgy, facilitating my higher education I would also extend my appreciation to the members of my committee for their support and for setting a high standard

Appreciation is given to Copper Consulting Industries and Paul Kruesi for financial and intellectual support concerning equipment and PE research in support of patent work by Mr. Kruesi.

The assistance of Anne Kvithyld and Sean Geal of Norwegian University of Science and Technology (NTNU) in Trondheim Norway to perform in the DTA-MS evaluation is greatly appreciated.

The assistance of Josh Montenegro, who worked with me for the last year on this research as my technician, was integral in the timely completion of the work His more than competent involvement in the research is greatly appreciated.

My greatest appreciation goes to Wife Margaret for her support over the past for years, helping to make for a stable and encouraging base from which to peruse my Ph.D.

CHAPTER 1

INTRODUCTION

Industrial sponsors have expressed an interest in the evaluation of processing options for electronic waste with the primary goal of defining operational parameters aimed at reducing and/or eliminating the formation of dioxins and furans during the pyrometallurgical processing of e-waste. A secondary issue of the possible creation of problematic metal halide compounds was also identified during preliminary investigations. The reduction and/or elimination of both the problematic organic and metal halide compounds is the primary goal of this research.

1.1 Defining Electronic Waste

With the wide variety of products produced under the heading of “electronics,” constant change in materials of construction, and the speed at which electronics are changing, there exists a wide variety of e-waste material generated. While the segment of interest to this research may be defined as “populated printed circuit boards and associated wiring,” all circuit boards are not created equal. Aside from the time dependent nature of chemical content, circuit boards from computer systems (computer motherboards, expansion cards, etc.) will have a different make-up than boards from cellular phones. Further affecting the non-uniform nature of e-waste is the less than uniform system of collection for e-waste as well as the fact that these collection systems are in the early stages of development in the United States. Some local municipalities conduct day- or week-long collection projects to deal with the issue of e-waste in the local landfills. Some manufacturers; e.g. IBM, Intel, HP; provide selective programs for the return of old computer systems. The European Union (EU) and Pacific Rim are further along in the development and operation of a viable collection network. This is due to governmental regulation rather than a sense of an individual’s social responsibility.

The recycling of electronic waste has been looked at for both resource recovery and waste minimization for many years. Various industries look at processing options from differing points of view and with differing in-house technologies available for application. As post-consumer electronic material has a complex and varying make-up, it lends itself to a number of processing options aimed at primary recovery for any number of elements.

Depending on the background of the engineers involved in the process development, research can be focused on different aspects of the complex waste material. Chemical engineers may focus on the recovery of the organic fraction as low molecular weight compounds or monomers. These organics could then be destined for reprocessing to provide fresh polycarbonate material. The remaining metal/ceramic material may be disposed of as mixed-metal scrap secondary product or residue. The economics of this process would be based primarily on the recovery of organic monomers. Metallurgists would tend to focus on the metal recovery with the organic seen as entrained energy value or a troublesome source of halogens complicating the recovery of the metals and possibly creating a dioxin/furan problem during metal recovery.

1.2 Annual Waste Generation and Growth

The label "E-Waste" can apply to many long-term (capital) items: televisions, VCR/DVD players, Stereos, etc., and short-term (consumable) items: computers, cellular telephones, portable music/information systems, etc. The short term, high turnover items tend to dominate the e-waste pool based on sheer volume. The near-term exception may be CRTs in the US due to the conversion from analog broadcasting to digital, mandated by Federal Law initially by the end of 2006, encouraging the replacement of TV's and creating a spike in the volume of discarded units.

It is estimated that 50% of the homes in the US and Canada have a working computer. With a 2004 estimate of 109 million households in the US and 12.8 million in Canada, this adds up to 60.9 million operating computers in the home. Applying a conservative estimate of one computer in the workplace for each computer in the home takes this number to 136 million operating units.

Taking into consideration what may be seen as planned obsolescence, between the rapid advancement in computer technology and the need for higher performance to operate the latest operating system and software, a lifespan averaging three years is not out of line (2-3 years for business use, 3-5 years for home). Using these conservative numbers as a baseline, incorporating an average population growth of 0.6% and a projected increase in computer sales of 10%, one can project a volume upwards of 134 million computers that will be made obsolete and replaced with new units in 2006 (Figure 1.1). As large a number as this estimation may seem, the Computer Industry Almanac (C.I.A. 2006), estimates the number of PCs in use in 2004 for the US and Canada to be 246.2 million—1.8 times larger than the number provided here.

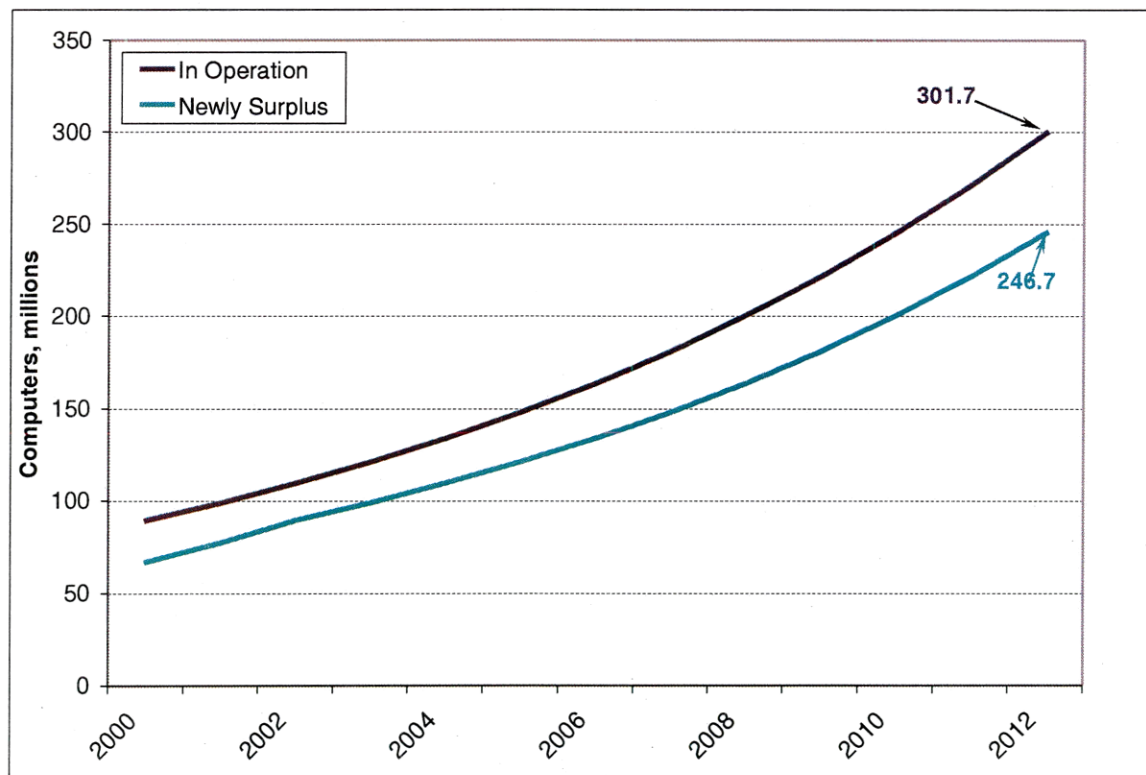


Figure 1.1 New and Obsolete Computers

It is estimated (Goodrich, 1999) that a full 75% of home computers that become obsolete are stored in a back closet due to the unit's perceived value. Business computers also tend to be retained for much the same reason, in addition to current laws surrounding computer disposal for

companies employing more than 120 persons. If one were to start with zero units in storage in 2002, an average of 75% retention applied to the projected growth of the computer population of the USA and Canada will result in some 348 million additional units in storage by 2006 and 582 million by 2008 (Figure 1.2). Eventually these units will be sent to landfill or recycled. These projections do not take into consideration market saturation, eventually slowing the sales of new units, nor does it take into consideration the eventual critical mass of obsolete units sitting in storage. As the number of computers in storage grows larger, the propensity of the average person to keep the unit in the back closet will lessen, resulting in a larger fraction of computers being added to the local landfill—not necessarily the best answer to the problem.

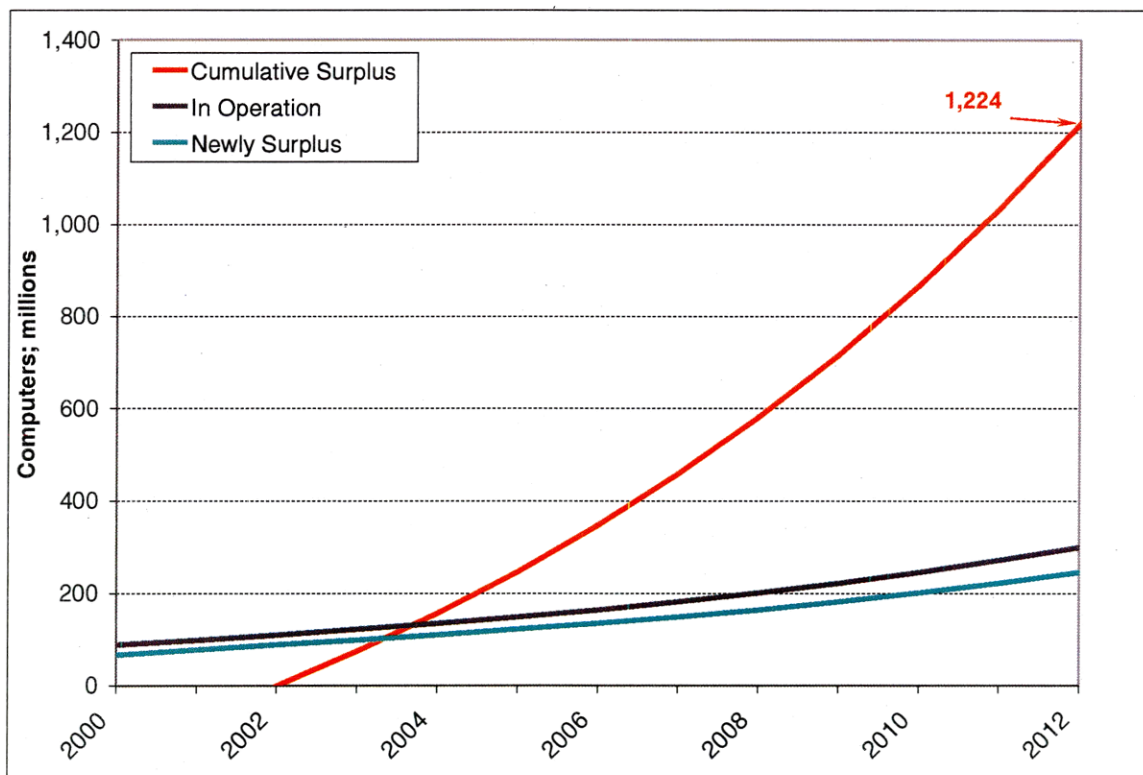


Figure 1.2 Cumulative Computer Resource

Evaluating the material in tonnage rather than number of units provides a better measure of the amount of material available. At 27.5 kg per computer, 3.7 million tonne of obsolete computer material would be generated in 2006 and an additional 4.5 million tonne in 2008.

1.3 Material Composition

Figure 1.3 provides a look as to the chemical make-up of the average 27.5 kg computer system broken down to its elemental constituents per tonne of waste. The presence of a CRT provides for a high level of lead (6.3%) and SiO₂ (10.8% Si corresponding to 24.9% SiO₂). The structural components present in a complete computer system are reflected in the high percentage of iron (20.4%) and aluminum (14.2%) as well as an increased level in elements used in alloying and decorative applications (Ni, Mn, Ti, Cr).

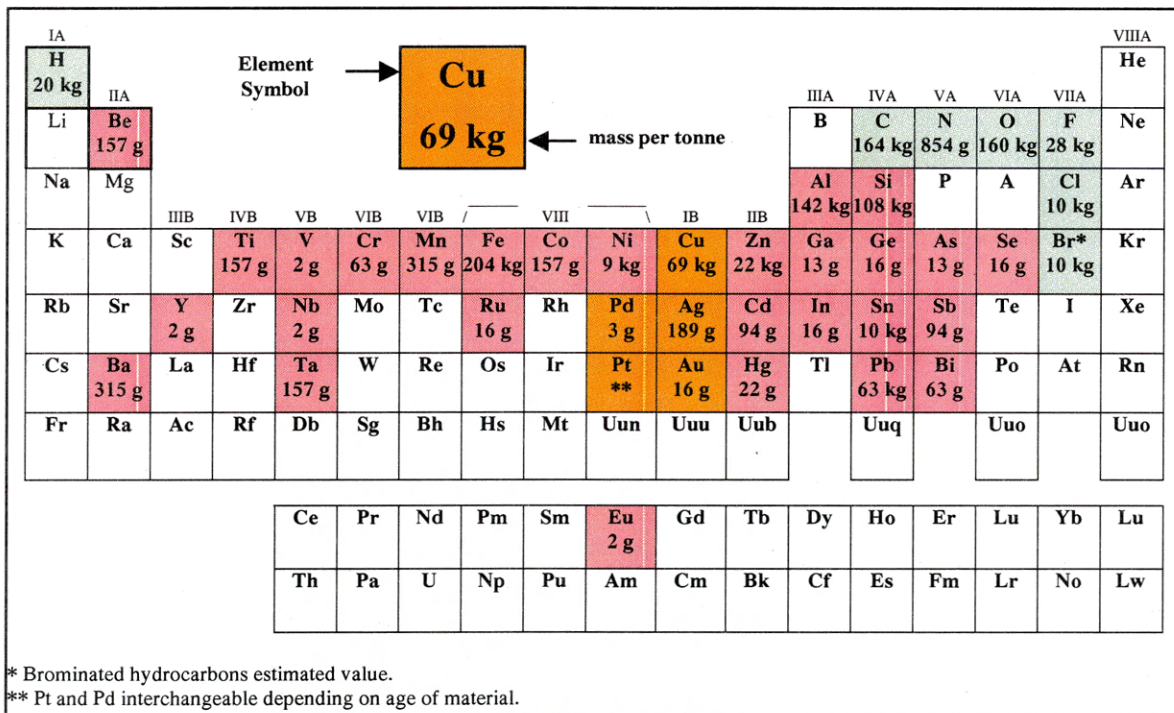


Figure 1.3 Element Distribution in a Desktop PC with Monitor

At 6.9% Cu, 16 g/t Au, and 189 g/t Ag, a desktop PC makes for a respectable polymetallic resource, although with some contaminants that make for a more difficult processing route. Knowing the distribution of elements within a PC is important in determining process applications. While some of the elements present are incorporated into components that are not easily separated, e.g., elements contained within a motherboard, some components may be

By eliminating CRT's and plasma displays from the discussion as well as the more readily recoverable components of a PC, i.e., plastic casing and metal frame, and focusing only on the internals of a computer system—populated motherboard, video, audio and network cards—one can estimate 0.75 kg e-waste per computer. This alternate composition represents roughly 2.75% of the initial mass. Relating this reduction in mass to the projected numbers of computers made obsolete and ending up in backroom storage gives 100,500 tonne of populated circuit boards in 2006 from obsolete computers alone. The amount of circuit boards accumulating in storage would reach 261,000 tonne by 2006 and 436,500 tonne by 2008.

This estimation of an e-waste assay also compares fairly well to an accepted general e-waste composition shown in Table 2.1 (Sum, 1991). As is often the case, the mantra of “One man’s waste is another man’s ore” can be applied here. A circuit board is primarily an oxide matrix with metal values and a moderate organic fraction. The metal fraction is copper, iron and tin with appreciable amounts of gold, silver and PGMs. Oxides are mostly silica and alumina. The organic fraction is, of course, plastics.

Table 2.1 General Printed Circuit Board Composition, Wt. %

Metal	40%	Refractory	30%	Organic	30%
Cu	20	SiO ₂	15	Polyethylene (PE)	9.9
Fe	8	Al ₂ O ₃	6	Polypropylene (PP)	4.8
Sn	4	Alk. & Alk. earth oxides	6	Polyesters	4.8
Ni	2	Titanates and mica.	3	Epoxies	4.8
Pb	2			Polyvinylchloride (PVC)	2.4
Al	2			Polytetrafluorethane (PTFE)	2.4
Zn	1			Nylon	0.9
Sb	0.4				
Ag	0.2				
Au	0.1				
Pd	0.005				

1.4 Material Value

Material composition varies based on age of the material as well as its source. Table 2.2 shows a number of e-waste assays from reference demonstrating a range of metal contents. As is often the case when dealing with secondary waste streams, one must know one's supplier. A hand-sorted sample will return a higher assay, but efficient processing will have to be based on a general sample with a minimum acceptable grade to ensure economically viable operation.

Table 2.2 Metal Assay of E-Waste—Literature Review

	Electronic Waste, Wt. %						tr-oz/st
	A ⁱ	B ⁱⁱ	C ⁱⁱⁱ	D ^{iv}	E ^{iv}	Avg.	
Cu	28.9	28.9	26.8	18.2	16.4	23.8	
Fe	11.5	11.5	5.3	37.4	27.3	18.6	
Sn	5.77	5.77	1.0	1.9	1.1	3.11	
Al	2.90	2.90	1.9	19.0	11.0	7.54	
Pb	2.89	2.89	-	1.6	1.4	2.20	
Zn	1.73	1.44	1.5	0.9	3.1	1.73	
Ag	0.106	0.289	0.33	0.0006	0.021	0.149	43.46
Au	0.054	0.144	0.008	0.0012	0.015	0.044	12.83
Pd (PGM)	0.003	0.007	-	-	0.002	0.004	1.17

i. Sum 1991

ii. Hoffmann 1992

iii. Lehner 1998

iv. Busselle 1999

At spot prices on 2 March 2006, the average value of copper and precious metals contained within the average e-waste was valued at around \$9,061 per short ton (\$9,988 per tonne) shown in Table 2.3. While this contained value reflects the run-up in metals prices currently being seen the global commodity markets, a valuation of contained metals using prices from January 1999 still returns a value of \$4,625 per short ton (\$5,098 per tonne).

Table 2.3 Average Valuation—Literature Review

	Avg. Wt. %	tr-oz/st	Spot Price*	Value/st
Cu	23.84		\$2.22 /lb	\$1,058.50
Fe	18.60			
Sn	3.11			
Al	7.54			
Pb	2.20			
Zn	1.73			
Ag	0.149	43.46	\$9.80 /oz	\$425.89
Au	0.044	12.83	\$564.25 /oz	\$7,241.21
Pd (PGM)	0.004	1.17	\$288.00 /oz	\$336.00
			Total	\$9,061.59

* 2 March 2006 (AMM 2006)

The thermal value of the contained plastics adds 7-8 million BTU heating value to each ton of waste (Table 2.4), valued at \$60 to \$70 when compared to the BTU value of natural gas. While the thermal value of oxidizing metal would be realized in a pyrometallurgical process, it is not included in this BTU valuation.

Table 2.4 Thermal Value

	Avg. Wt. %	BTU/lb	BTU/st waste
Polyethylene (PE)	9.90	19,900	3,940,200
Polypropylene (PP)	4.80	19,850	1,905,600
Polyesters	4.80	11,400	1,094,400
Epoxies	4.80	11,400	1,094,400
Polyvinylchloride (PVC)	2.40	7,700	369,600
PTFE	2.40	2,200	105,600
Nylon	0.90	13,200	237,600
Subtotal Organics-in-waste			8,747,400
	Coal (Delivered WA State)	\$1.22/MMBTU	\$10.70
	Natural Gas	\$6.50/MMBTU	\$58.81
Iron	8.00	1,650*	264,000
Aluminum	2.00	1,320,000*	52,800,000
Subtotal Metals-in-waste			53,064,000
		Total	61,811,400

* 2,420°F

1.5 Government Legislation

As the problem of e-waste generation gains attention in the recycling community, the need for a structured method for dealing with the collection, transport and reprocessing/disposal of the material becomes more essential. Due to the nature of modern electronics—low cost, high volume commodities—the production and distribution of the items are on a regional, if not national or global scale. Dealing with the material on a city or county level would be inefficient. Government involvement on at least a State if not Federal level would be needed to properly address the issue.

1.5.1 US State Government Legislaton

As with much of the waste material containing elements defined as “heavy metals” or “toxic,” political attempts to pass legislation to fix the problem abound. Four hundred and eight bills related to waste management, recycling, and product stewardship were introduced in US State legislatures in 2003 (Wu 2005). These legislative proposals include enacting bans on the disposal of waste electronics, study commissions, and full manufacturer responsibility programs. Over half of the States have considered bills regarding e-waste disposal.

Much of the attention goes to financial sources for collection and recycling of the material. Two options for the generation of funds most commonly considered are the Advance Recycling Fee (ARF), and Manufacturer Responsibility. The ARF is a fee added to the customer’s receipt at point of sale. Manufacturer Responsibility assigns the responsibility to manufacturers to collect and recycle their pro rata share of discarded products.

Three states, California, Maine, and Maryland, have passed laws requiring electronics recycling, yet with very different requirements for manufacturers and retailers. California’s legislation is based on the ARF model—known as SB 20 (2003), it imposes an advance disposal fee of \$6–10 on monitors, televisions and laptops at point of sale. Maine and Maryland have

adopted variations of the Manufacturer Responsibility model. Maine (Title 38, Section 1609) has implemented producer-financed collection, recovery, and recycling of electronic waste, to have begun January 2006. Maryland (HB-575) is mandating that manufacturers offer a take back program and pay a fee. Maryland's bill was to have taken effect July 2005. Other states have already banned disposal of CRTs, or have commissioned study committees to draft legislation. Several states, including Minnesota, Massachusetts and Wisconsin, are expected to take action on e-waste this year.

1.5.2 US Federal Government Legislation

With the states taking the lead on legislation, the federal government is being prompted to consider the issue. Fifty differing policies on waste remediation would have adverse effects on regional processing and interstate commerce.

Two bills have been introduced in the US Congress. The first (HR 425), by Representative Mike Thompson of California, would enact a national ARF of \$10 for new computers. The EPA would establish a national grant program to fund the collection and recycling of old computer systems.

The second bill (S.510), introduced in March 2005 by Senators Ron Wyden of Oregon and Jim Talent of Missouri, would establish tax incentives for consumers and businesses to recycle computers, monitors and televisions. The bill also would reduce the regulatory requirements for managing electronic waste to facilitate recycling, and compel the EPA to conduct a cost-benefit analysis of any potential national programs.

CHAPTER 2

RECYCLING OPTIONS

2.1 Reuse

Resale or donation to non-profit organizations is often touted as the answer to a large portion of the e-waste problem. This still requires a certain minimum performance for the system to be usable. One would be hard pressed to find a 486 or Pentium-based system in operation, unless it was used in the most mundane of applications. While non-profit operations are happy to accept donated systems that have some operational life remaining, this is not a permanent solution. This system's operational life may be extended by a year or two, but it will eventually return to the waste stream having little effect on the annual generation of e-waste.

2.2 Reprocess

Some examples of e-waste processing are given here. Depending on the background of the engineers involved in the process development, the focus is placed on different aspects of the complex waste material. Chemical engineers may focus on the recovery of the organic fraction as low molecular weight compounds, while metallurgists tend to focus on the metal recovery. The intent here is not to define the best current technology, as the financial burdens of each process are dependent on the location, relative supply/demand issues and metals contracts, but to take a look at where the engineering community is in relation to the issue of e-waste recycling, with an emphasis on high temperature processing.

When deciding on the appropriate recycling option, relying on the availability of capital from government sources is not the ideal. A truly successful process should be fiscally sound on its

own merits, without relying on Government subsidy. While a government policy that increases the availability of feed material may assist in the creation of a stable source of material, a self-sustaining processing must be able to handle the complex and varied chemistry that would be seen. While the primary value may be in the Cu and PMs, some value may be gained from other constituents as Pb (\$0.64/lb), In (\$1,000/kg) and Hg (\$700/flask-76 lb).

An integrated copper-lead smelter lends itself as an efficient processing option for e-waste. The lead circuits recover metals, deemed problematic in some applications, as products for reintroduction to the economy. Such operations are already designed to handle volumes of dust and offgas. The copper circuit allows for the recovery of high value metals—copper and precious metals.

A review of eight operations reprocessing e-waste has been undertaken, with a focus on the conditions presented to the waste and the relative stability of the individual elements present. The operations are: Adherent Technologies Inc.; Boliden Mineral; Teck Cominco Ltd.; Noranda Recycling, Inc.; Union Mineria; and (grouped together due to almost identical processing) Sabin Metal Corporation U.S., Pashelinsky Smelting and Refining Corp. U.S. and Engelhard Specialty Metals Division, U.K.

2.2.1 Adherent Technologies Inc.

Adherent Technologies has taken the approach of recovering low molecular weight organics from the polymers present in e-waste (Busselle, 1999). The waste is first processed via shredder/hammer mill. Ferrous metals are removed with magnetic belt and drum operation, with aluminum being removed via eddy current separation. These processes result in a reduction of the feed by 30%. The remaining polymer-rich material is transported through a pyrolysis chamber by screw conveyor. Thermal degradation of the material results in the evolution of low weight organic molecules that can be distilled to produce a number of saleable products. Adherent has demonstrated the ability to generate a phenol-rich liquid through vacuum

distillation of this gas stream. Reforming and other reactive distillation operations may then process this material producing commodity chemicals such as ethylbenzene, phenol or styrene. The resulting organic-free, metal-ceramic material can then be sent to conventional metallurgical processing.

2.2.2 Boliden Mineral

Boliden's Rönnskär smelter has incorporated e-waste as part of its secondary raw materials for some time. The operation consists of a lead flash smelter and refinery, a copper smelter and refinery, a sulphuric acid and sulphur dioxide plant, a slag fuming plant and a precious metals plant. The company estimates that its plant could consume 15,000-20,000 tons per year of PC scrap (Mark, 2000), based on test-runs of 10t/charge.

In a project sponsored by Boliden, The Association of Plastics Manufacturers Europe (APME) and The American Plastics Council (APC), the use of PC waste in the Zinc Fuming Furnace feed was studied as well as the current process of adding the e-waste to Boliden's Kaldo Furnace.

The e-waste investigated by Boliden was comprised of the entire personal computer (PC) with only selective removal of components that contained Hg. Processing of e-waste in this manner eliminates the need for complete disassembly of the components, reducing the cost of the scrap. Preparation of the PC waste was accomplished using a hammer mill with removal of iron via a magnetic separator, creating a more plastic-rich waste than was discussed above when considering circuit boards alone. The PC scrap is reduced to -30 mm and mixed with crushed revert slag in a 50:50 mixture to optimize bulk handling and silo feeding, avoiding blockages during feeding.

2.2.2.1 Zinc Fuming Furnace.

The fuming furnace is supplied with a mix of EAF dust, Revert Slag and PC waste. The plastics contained in the PC waste work with added coal fines to facilitate the fuming of zinc, lead, arsenic and related metals in addition to the contained halogens. This stream is sent to the clinker furnace.

The cleaned slag is tapped from the fuming furnace to a settler furnace where copper alloy and copper sulphide are separated. Precious metals from the e-waste follow the copper collector. In this way, almost complete recovery of the copper and precious metals from the e-waste can be obtained

2.2.2.2 Kaldo Furnace.

The total amount of secondary raw materials and lead concentrate processed by Boliden's Kaldo furnace is around 100,000 short tons per year. Kaldo technology has been practiced for over 15 years to recover cable scrap and printed circuit boards.

A skip hoist charges blended feed material. Oxygen lance supplies the needed O₂ for combustion with an oil-oxygen burner, if needed, to reach ignition temperature. At this point the value of the plastics within the PC waste is realized. With a thermal value on par with that of fuel oil, the polycarbonates supply the heat needed for the smelting operation. Offgases are subjected to additional combustion air at around 1,200°C in post-combustion. Standard gas handling system recovers thermal energy via a steam network.

The Kaldo furnace produces a mixed copper alloy that is sent to the copper smelter for recovery of metals (Cu, Au, Ag, Pd, Ni, Se, Zn) and dusts (containing Pb, Sb, In, Cd) are sent to other operations for metal recovery.

2.2.2.3 Plant Operation.

According to Mark, 2000, operational parameters (recovery, energy balance, product quality and emissions) were not affected by the addition of PC waste. Plastic additions accounted for 20% of the energy input (substituting for coal) without any appreciable change to the plant's output from either a chemical or thermal perspective.

2.2.3 Teck Cominco Ltd.

Tech Cominco is the largest producer of germanium and zinc in the world (Goosen, 2005). The company's Trail Metallurgical Complex operation, located in British Columbia, is a \$1 billion integrated zinc/lead smelter with capacity of 290,000 and 120,000 tonne per year of zinc and lead respectively. By-products include silver, gold and indium.

Facing a reduction in conventional feed material to their No.2 slag fuming furnace (SFF), electronic waste was considered as an alternative charge material. As an integrated zinc/lead operation, Teck can handle the typical elements found in electronic waste, thus making it simple to adapt the process for e-waste. In initial tests, the company processed 30 tonne (66,000 lbs) and 225 tonne (500,000 lbs) of shredded end-of-life electronic waste. The material is fed into the 24 m³ fuming furnace at 1,250°C, already containing a zinc-rich slag. Fumes of lead, zinc, cadmium, tin, germanium, indium and other elements are collected in the baghouse, while a slag of silica, iron and aluminum is left behind. The matte formed contains copper, nickel, gold, silver platinum and palladium.

In the process, the plastics contained in the electronic waste are used as a fuel source. The thermal energy is reclaimed through a boiler/steam generation. The offgas from the combustion chamber is further combusted through the addition of excess oxygen, destroying any dioxins, furans and brominated flame retardants that may remain. An extensive air monitoring program showed no increased emissions during the testing/demonstration program. In June of 2005, the

Canadian government approved the operation for the industrial treatment of electronic waste. The company estimates a 20,000 tonne per year capacity.

2.2.4 Noranda Recycling, Inc.

A unit of Falconbridge, Noranda Recycling operates six sampling and recovery plants in the United States, Canada and Asia focused on electronics recycling (Thomas, 2005). The plants in Tennessee, California, Rhode Island and Ontario have a capacity to process approximately 100 million pounds per year of electronic waste and other materials. This year, Noranda Recycling, Inc. opened an office in Penang, Malaysia. This office sources copper and precious metal-bearing scrap streams from electronics manufacturers in Asia, and are shipped for sampling to the recycling facilities in California and Rhode Island before being sent to the Horne smelter in Quebec.

The Horne Smelter, is located in Rouyn-Noranda, Quebec. The operation is a continuous copper smelter that processes both copper concentrates and copper metal bearing materials as its feedstock to produce a 99.1% copper. This copper is shipped to Noranda's Canadian Copper & Recycling (CCR) Refinery in Montreal-Ease, Quebec, to produce refined copper, precious metals and other by-products.

The copper smelter is capable of handling materials in various physical forms including shredding for over-sized materials. The Horne Smelter consists of three stages of refining: the reactor, the converters and the anode furnaces. Copper anode production capacity is approximately 700 short tons per day.

The CCR Refinery, located in Montreal, is a fully integrated copper and precious metals refinery. Copper produced by the Horne-Smelter, Gaspe Mines Division and other non-Noranda smelters are refined to 99.99%. The refinery can also process refinery slimes and dore anodes, producing gold/silver and palladium/platinum concentrates. Other by-products include selenium,

tellurium, copper sulphate and nickel sulphate. It is also equipped to receive blister, ingots, No. 2 and 3 copper and sweeps.

A series of shredders reduce e-waste materials to small pieces. While the majority of Noranda's process is a mechanical shredding and separation model, the first part is manual selection. Many hazardous components are removed, prior to introducing the hand-picked waste into a series of shredders to reduce piece size to -5 cm pieces. This size reduction allows for optimal material separation using technologies such as magnetic separation, eddy current separation and sand flow separation. In this way, the electronic scrap has been separated into various commodity streams. These commodities are then sent to the different Noranda operations. The copper and precious metal fines, circuit boards and copper/plastics are sent to the copper smelter to recover copper, silver, gold, platinum, palladium, selenium, tellurium, cadmium and nickel. While the steel output goes directly to a steel foundry, the aluminum goes directly to an aluminum smelter. Noranda Recycling, Inc. has the capacity to process approximately 70 million lbs (31,750 tonne) of electronic waste annually.

2.2.5 Union Mineria (UM)

UM's Hoboken site is comprised of copper/lead smelters and refining operations for complex non-ferrous raw materials with precious metals playing an important role (Felix, 1994). The Hoboken smelter treats 350,000 tonne per year of raw and recycled non-ferrous materials. Hoboken feed material is roughly 35:65 primary:secondary. The most important materials are:

- complex concentrates containing lead, copper and precious metals
- industrial by-products from other smelters and refiners (e.g. drosses, mattes, copper slags, flue-dust, speiss, tank house slimes, cements, lead sulphates)
- recycled products such as sweeps, spent catalysts, electronic scrap and film ashes

Organics are separated from the bulk through a two-stage pyrolytic furnace. This first oxygen-starved chamber pyrolyses the organics, which are sent to the oxidizing (post combustion) chamber. The furnace is equipped with its own emission system, including a venturi scrubber and two packed towers.

As with Boliden's operation, waste material can be fed to the flowsheet at various points, depending on the waste's assay and physical aspects—primarily Pb- and Cu-content as well as precious metals assay. For example, copper-rich (electronic) scraps can be treated in a converter, collecting precious metals in the blister-copper. Converter offgases are sent to the acid plant where any remaining hydrocarbons can be destroyed.

2.2.6 Sabin Metal Corporation (Sabin) U.S., Pashelinsky Smelting and Refining Corp. U.S. and Engelhard Specialty Metals Division, U.K. (Engelhard)

Sabin, of East Hampton, NY; Pashelinsky of Jersey City, NJ and Engelhard, of Cinderford, U.K. have approached the refining of e-waste in much the same manner. By applying accepted pyrometallurgical operations with sufficient control of process offgases, non-ferrous and precious metal recovery is obtained.

As with most secondary processing, scrap pedigree is important. Material must be inspected prior to processing to confirm the relative amount of iron, aluminum, copper and nickel present. It must also be inspected for such things as mercury relays and switches and possible radioactive contamination. Each customer's lot of e-waste is maintained as a separate batch, maintaining quality and fiscal responsibility.

E-waste is first processed via a low temperature rotary furnace with afterburner and baghouse systems, for ashing. The ashed e-waste has an average 36% weight reduction and 60% volume reduction. Milling and magnetic separation may be employed to further reduce the volume of waste prior to melting/smelting.

Sabin and Engelhard (Setchfield, 1987) then employ a rotary melting furnaces with appropriate fluxes and additional copper (collector for the precious metal) if required for separation of the copper and precious metals from the oxides. High iron content, if present, is removed through oxygen lancing and flux addition. Pashelinsky Smelting employs an electric furnace for standard metals processing.

2.3 Processing Summary

Currently applied processing options can be summarized in two operational systems: 1) Volatile removal/recovery—Pb, Zn, Hg, Cd providing for a lead/zinc-rich feed and 2) slagging/metal reduction— $\text{Al}_2\text{O}_3/\text{Fe}_x\text{O}_y$ rich slag; Cu, Au, Ag, Pd, rich metal. As stated previously, the current applied processes tend to be a function of the equipment on site, introducing the e-waste material as a supplementary feed. The construction of a large-capital metallurgical plant specifically for the reprocessing of e-waste would require a more integrated collection and shipping infrastructure, guaranteeing long-term accessibility to a sustained-value material stream. Given the complex nature of the feed material and the wide variety of recoverable metals, it is no surprise that lead or integrated lead-copper operations have been at the forefront of reprocessing of this material.

CHAPTER 3

EXPERIMENTAL TECHNIQUES

3.1 Research Parameters

As was stated previously, industrial sponsors have expressed an interest in the evaluation of processing options with the primary goal of defining operational parameters aimed at reducing and/or eliminating the formation of dioxins and furans during the pyrometallurgical processing of e-waste. Upon evaluation of the overall chemistry, a secondary issue of the possible creation of problematic metal halide compounds was also identified. It has been noted in previous work conducted at Colorado School of Mines (Patsos, 1982) that the presence of aluminum chloride in a mixed metal system can increase the mobility of other metal halide species. As is often the case when processing material which may contain sources of halides, the production of acids and the corrosion issues they can cause is also of concern. With these issues in mind, the investigation of pyrometallurgical processing of e-waste was undertaken with three goals:

- 1) Entrap/Sequester halogens to reduce dioxin/furan, metal halide and corrosive halide acid formation.
- 2) Operate in a reduced oxygen environment to reduce dioxin/furan formation
- 3) Operate at temperatures sufficient to decompose all solid organic species

3.2 Research Program

In exploring the e-waste system and allowing for the development of a process to accomplish the three goals described above, a number of theoretical and experimental programs were designed and executed:

- 1) Thermodynamic Modeling
 - a. E-Waste
 - b. E-Waste with Sequestering Agents
- 2) Polymer Behavior
 - a. Large Scale—Rotary Kiln
 - b. Small Scale—Tube Furnace
 - c. Milli-Scale: DTA, GC-MS
- 3) Sequestering Efficiency
- 4) Residue Processing

CHAPTER 4

THERMODYNAMIC MODELING

4.1 Direct Smelting: Metal/Metal Oxide

As was discussed in Chapter 2, a number of operations are finding some success with a mass combustion/fuming approach to the processing of e-waste. Many of these operations have the advantage of lead smelter access, allowing for the control and recovery of lead and related materials. Evaluating the regions of stability for each metal oxide through a combination of elevated temperature and relative degrees of oxidation provides for a general roadmap to the distribution of compounds in a high-temperature pyrometallurgical process. This thermodynamic evaluation is made via the following equation:



As any operator can attest, furnace operation tends to be more of an Art than a Science, unless the operation is “out of the box” new. Rather than showing a specific point of operation, a general area is shown, in Figure 4.1, relative to the thermodynamic equilibrium of elements and their oxides.

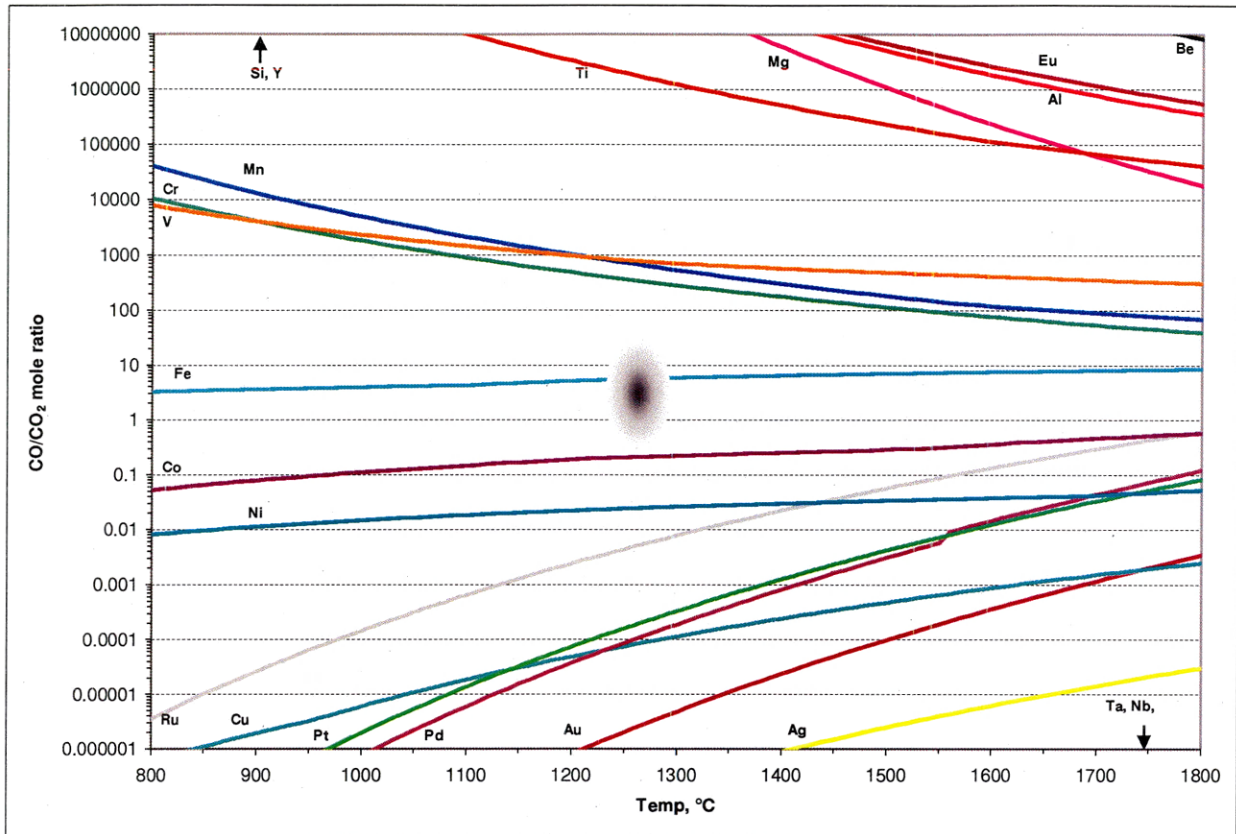


Figure 4.1 Oxide Stability vs. Oxidation Potential: Slag and Metal Elements

Figure 4.1 shows the elements that are expected to report to the both the slag and metal phases during a lead/zinc fuming operation with the general field of operation shown in the shaded region. Elements that would be expected to be removed from the bath via vaporization are shown in Figure 4.2. Without having to look at the thermodynamic data, one would expect Al, Mg and Ti to report to the oxide, as shown. Included in the slag phase would be oxides that that could be problematic. Beryllium has an oxidation potential greater than that of aluminum, indicating its thermodynamic propensity to report to a slag phase. A high level of other slag constituents (i.e. ~167 kg SiO₂/tonne e-waste) would possibly push the beryllium content to levels low enough to not be problematic. Final concentrations would, of course, be dependent on overall processing path, additional feed streams and fluxing agents. The more noble metal (Cu, Ag, Au, Pt, Pd, etc.) report, as expected, to the metal phase.

Figure 4.2 shows the group of elements that possess a substantial vapor pressure (Figure 4.3) or those that are routinely fumed off for value recovery. As an example, lead, zinc, cadmium, tin, germanium, indium and other elements may be collected at a typical smelter for recovery. Some of the elements indicate that they would exist in a form that possesses little or no vapor pressure; e.g. Hg_2O . It is important to keep in mind that any thermodynamic evaluation is a guide, not the final destination when it comes to complex metallurgical systems. While the final area of operation would suggest that all mercury will exist as a non-volatile oxide, the behavior of mercury on the path to the final area of operation results in the production of mercury gas, allowing for its recovery as a product stream.

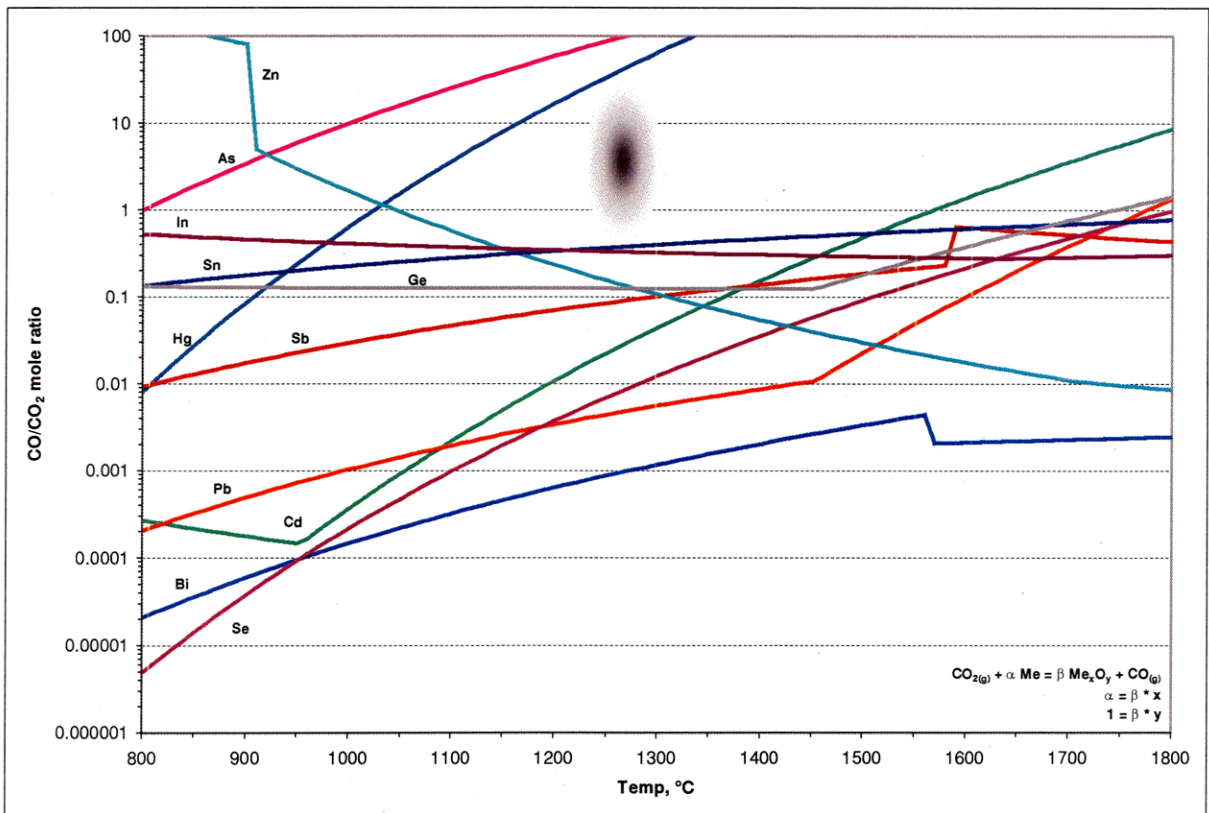


Figure 4.2 Oxide Stability vs. Oxidation Potential: Volatiles Elements

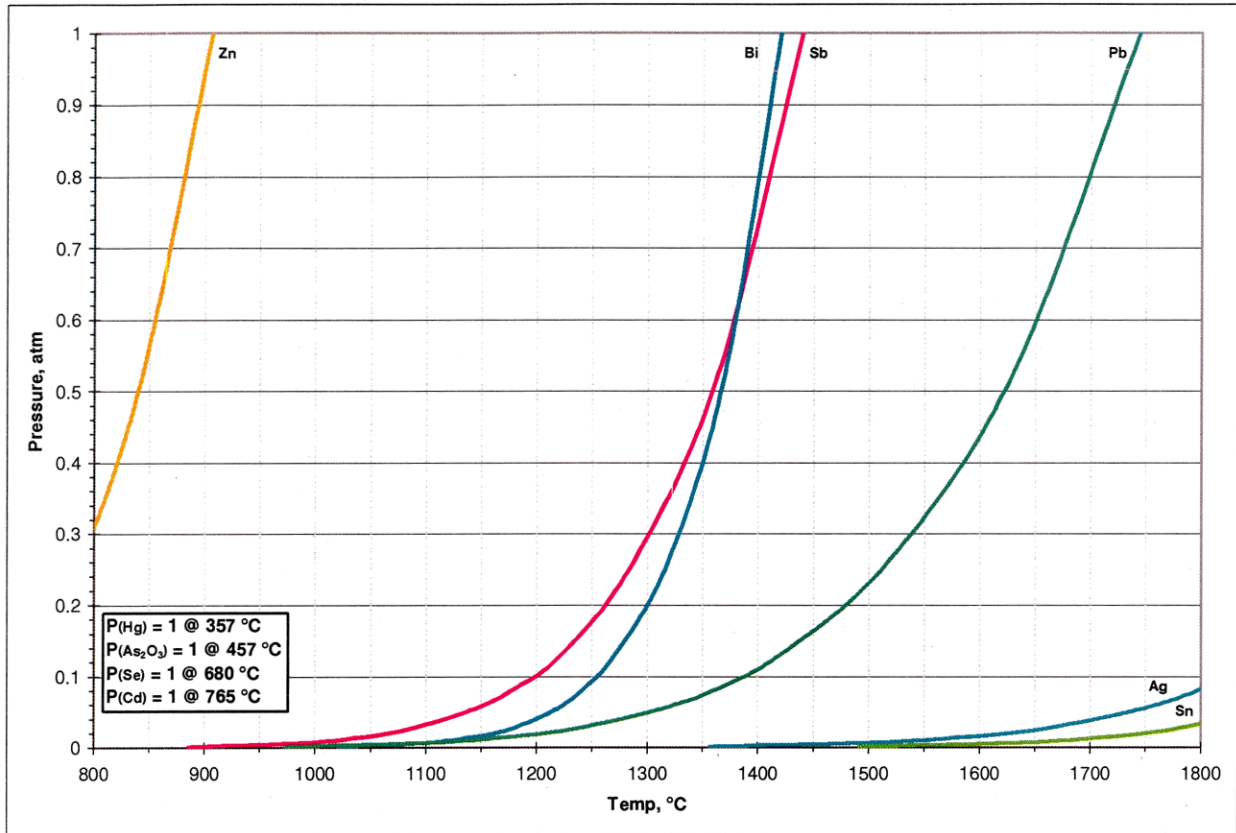


Figure 4.3 Vapor Pressures, (Perry, 1997)

Relative activities of elements within the metal and oxide phases will affect the actual behavior. As has been the case in the steelmaking industry, understanding of a complex mixed metal/oxide system requires detailed investigation to determine activity coefficients and final elemental distribution. Taking the stabilities shown in Figure 4.1 along with the composition detailed in Figure 1.2, prior to the inclusion of any additional fluxing agents, the idealized oxide and metal systems shown in Table 4.1 are produced.

Given these elemental distributions, it is plausible to envision the production of an intermediate tantalum-rich slag. If the appropriate equipment is in place, and market conditions are right, the economics of such an intermediate could be attractive.

Table 4.1 Idealized Metal and Slag Composition

Slag		Metal	
SiO ₂	35.73%	Cu	87.17%
FeO	24.49%	Ni	8.72%
Ta ₂ O ₅	21.43%	Ag	1.37%
Al ₂ O ₃	17.98%	Ru	1.16%
BeO	0.30%	Ga	0.94%
MnO	0.04%	Au	0.58%
TiO ₂	0.02%	Co	0.03%
Cr ₂ O ₃	0.02%	Pd	0.02%

While thermodynamics and empirical vapor pressure measurements over pure systems may indicate an inability to economically recover certain elements from a molten liquid, common operational systems prove otherwise. This is another indication that while such evaluations of a given system are useful in understanding operational possibilities, final process evaluation and design require the incorporation of many other areas of investigation, including tried and true, hands-on operation.

4.2 Thermal Processing: Metal-Halide Systems

Thermodynamic modeling was initially conducted with Outokumpu Oy's HSC 5.1 software. This type of simulation allows for a number of processing options to be explored for such a complex system. Utilizing this software package, the chemical composition of a desktop PC without monitor (shown in Figure 1.4) was evaluated to obtain the equilibrium composition. This represents the "worst case scenario" as no oxidant is present—Figure 4.4.

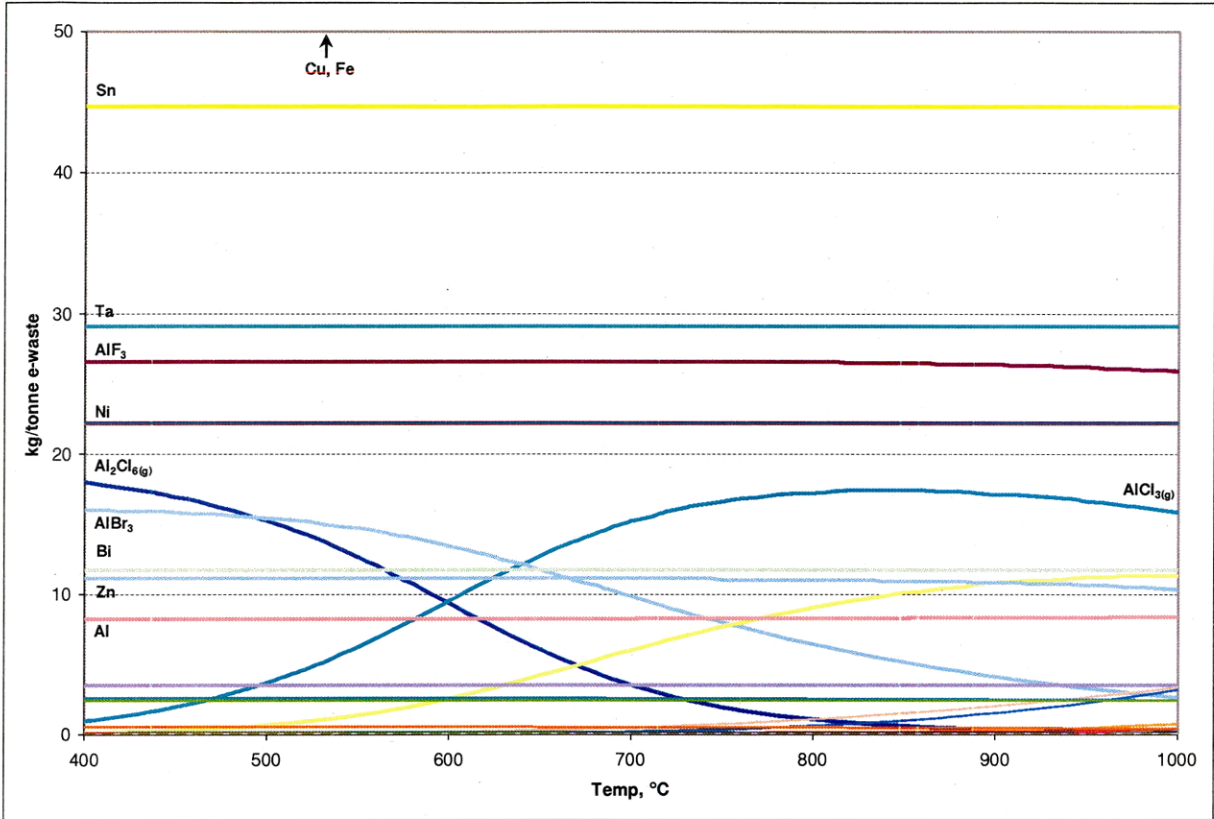


Figure 4.4 HSC 5.1 equilibrium composition of 1 tonne of e-waste, <50 kg/mt E-Waste

The most stable compounds present are aluminum halides. Other primary constituents (Cu, Fe, Sn, Ta, Ni and Zn) are present in metallic form. The dominant metal forming metal halide compounds is aluminum. At 600°C, the aluminum halides account for roughly 61 kg of material.

Taking a closer look at the system (Figure 4.5), metals other than aluminum form finite amounts of halides—Be, Mn and Cu. A look into lower levels of the equilibrium composition would show the existence of additional compounds, both gaseous and liquid, that might complicate high-volume processing of this waste stream. At 600°C, some of the metal halides in addition to Al expressed in kg/mt-e-waste are: Be-2.65 kg; Mn-0.52kg; Cu-0.16kg; and Zn-0.11kg, totaling some 65 kg of metal halides.

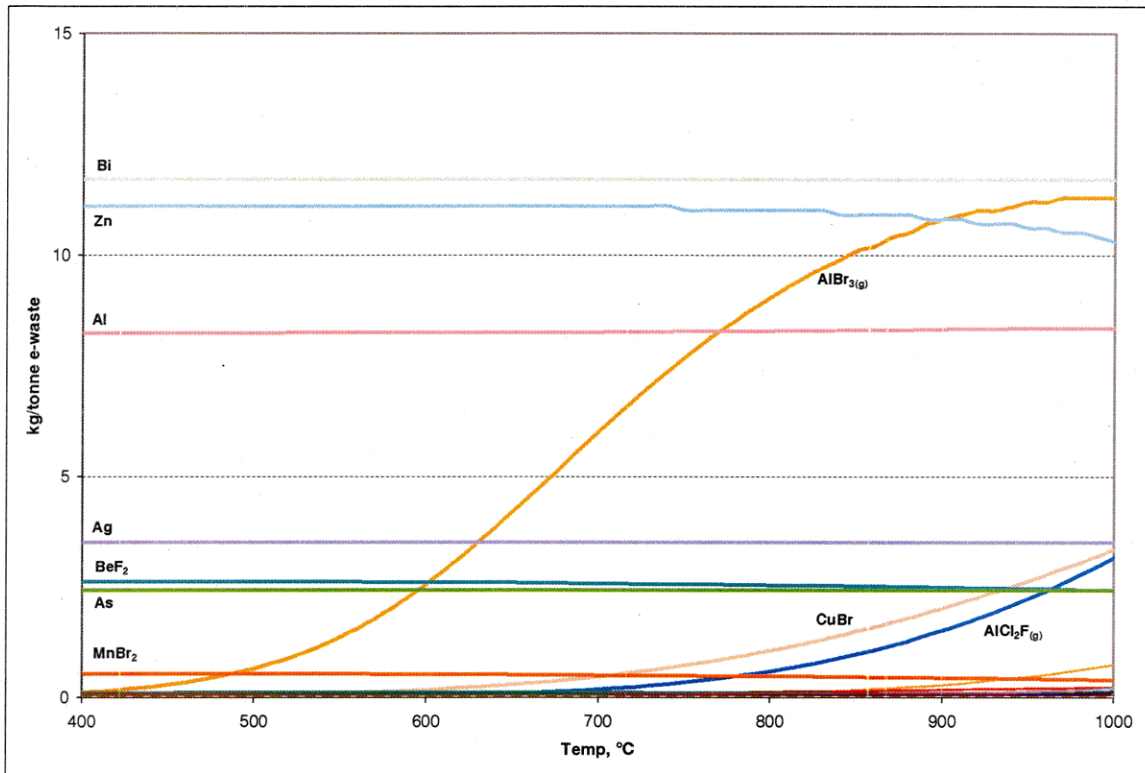


Figure 4.5 HSC 5.1 equilibrium composition of 1 tonne of e-waste, <15 kg/mt E-Waste

It is acknowledged that the system shown in Figures 4.4 and 4.5, as complex as it appears, is a simplified version of what may actually exist. The thermodynamic model assumes that all elements are available at all temperatures and calculated the minimum free energy of the system based on the compounds evaluated. The processing of mixed polymers with various decomposition temperatures would have chlorine and fluorine liberated in a specific temperature range. Figure 4.6 is an example of the previous system shown with fluorine available for reaction at 580°C (the temperature where pure PTFE has shown significant thermal degradation). Since the goal of this research is to eliminate all solid polymers contained within e-waste, generating a gas product with high heating value, processing temperatures will be above the decomposition temperature of all contained polymers. Therefore, the more simplified method of modeling shown in Figures 4.4 and 4.5 is suitable for evaluating the system composition.

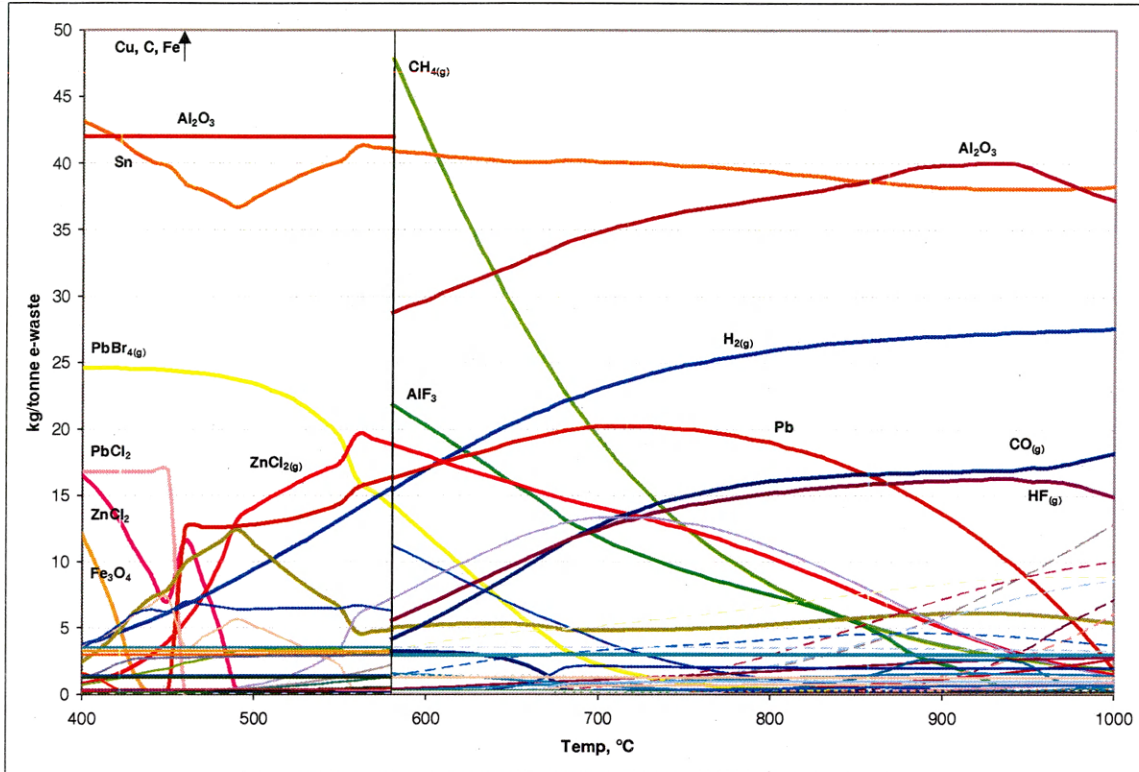


Figure 4.6 HSC 5.1 alternate equilibrium composition of 1 tonne of e-waste

A number of the reprocessing options being employed by industry (discussed previously) use excess oxygen to thoroughly combust the organics present. The intent is to eliminate the formation of dioxins/furans through complete destruction of the organics. The addition of large excesses of combustion air also could assist in the reduction of contaminants to levels below emission standards on a per cubic meter basis. The excess oxygen employed in an intense combustion operation may be beneficial in addressing the organic-related challenges of e-waste, but thermodynamic modeling (Figure 4.7) shows the formation of higher amounts of metal halides. This increase in overall metal halides is due to the oxidation of aluminum and the subsequent formation of heavier metal-halide compounds. At 600°C, 119 kg of metal-halides are present in this system. The dominant metal-halide compounds indicated in the model are tin-, lead-, and copper-based.

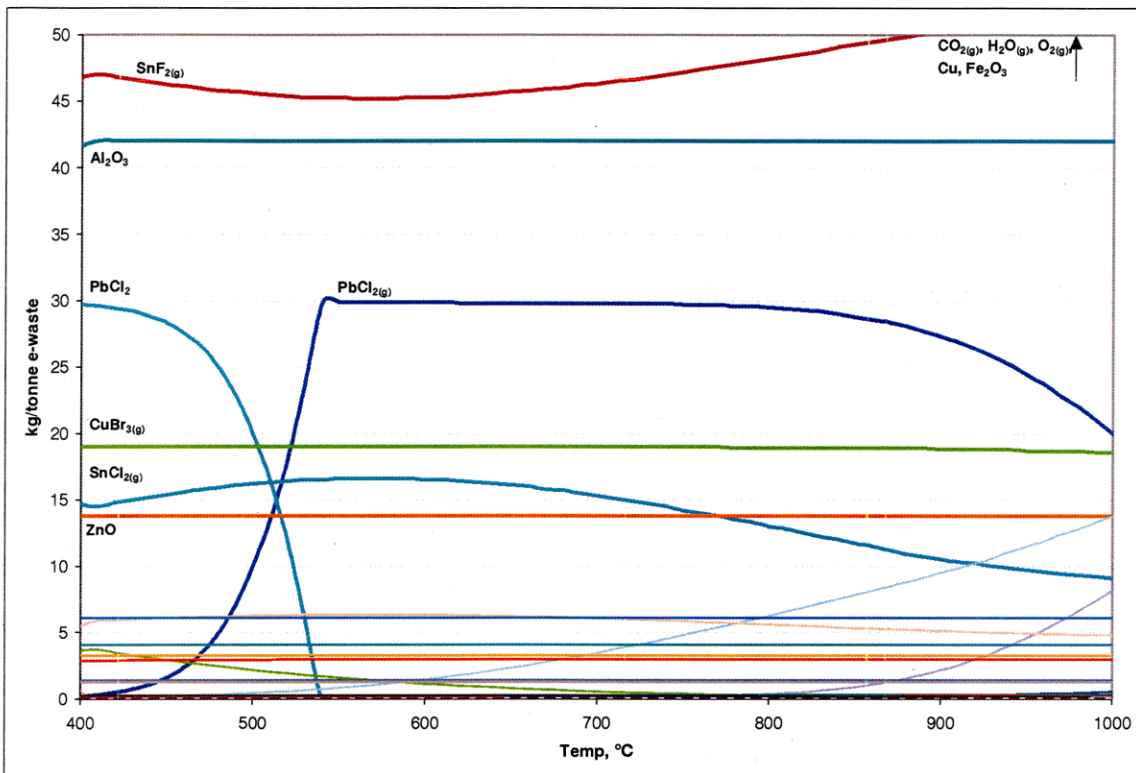
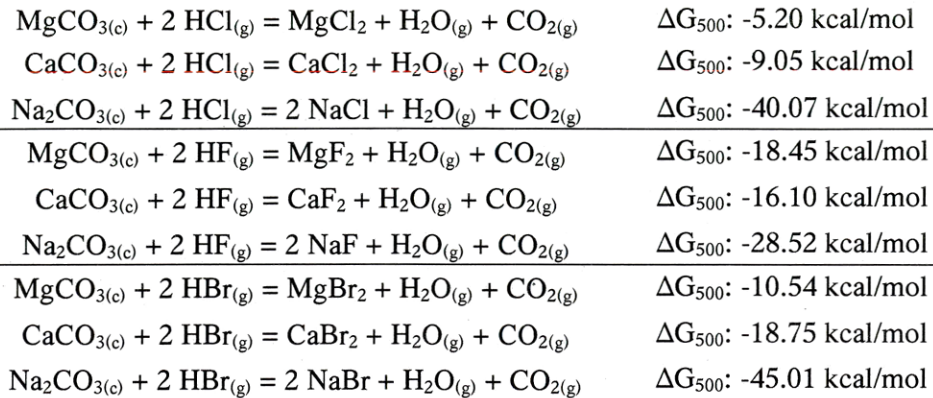


Figure 4.7 HSC 5.1 equilibrium composition of 1 tonne of e-waste and excess O₂

Based on the thermodynamic models shown in Figure 4.7, and the possible production of dioxin/furans in the presence of free halides, additional modeling was undertaken to evaluate the sequestering of halides in-situ through the addition of alkali and alkali earth carbonates.

4.3 Thermal Processing: Halide Sequestering Agents

A survey of sequestering agents was conducted to develop a listing of materials for study. Information was taken from literature as well as a survey of free energy, providing a list of complexing agents to be investigated: Ca²⁺, Mg²⁺, and Na⁺ in the form CaCO₃, MgCO₃ and Na₂CO₃. Thermodynamic data shown here were obtained from HSC 5.11.



Additionally, the model shown in Figure 4.7 was readdressed with the addition of the various sequestering agents shown above. Figure 4.8 gives the thermodynamic stability of the e-waste system with the addition of 1.8 times the stoichiometric amounts of MgCO_3 .

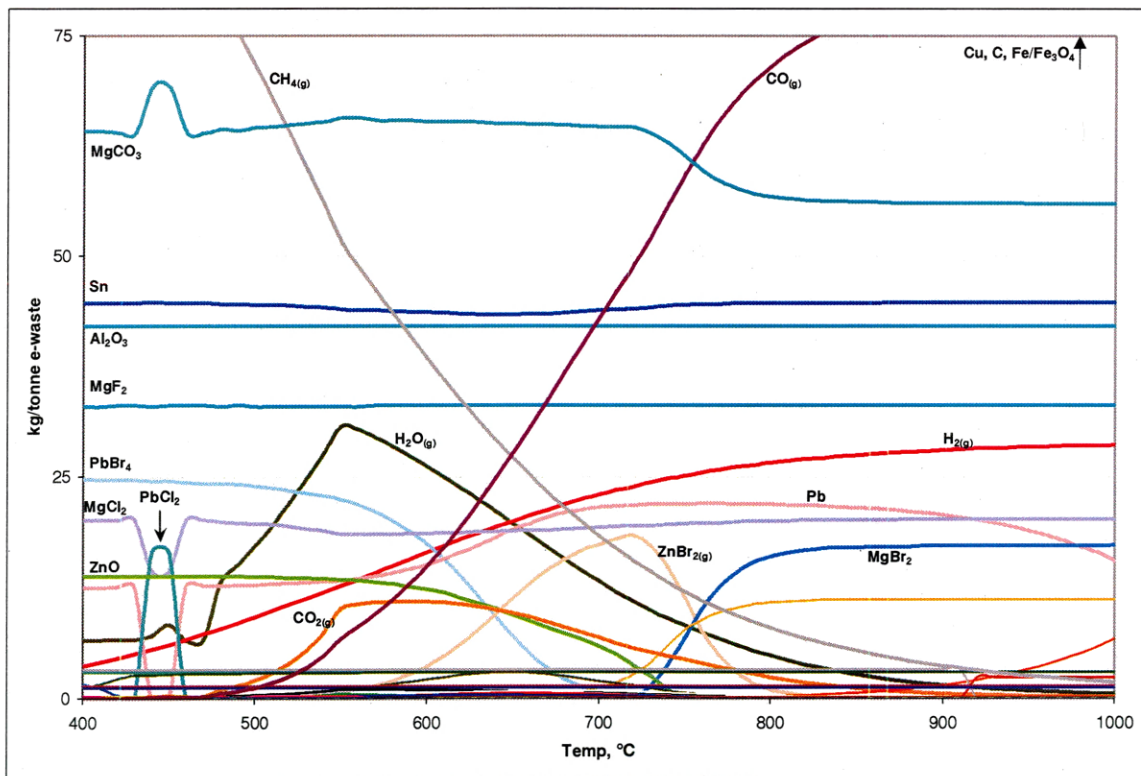


Figure 4.8 HSC 5.1 equilibrium composition of 1 tonne of e-waste and 1.8X MgCO_3

This model shows a moderate level of halide sequestering by the MgCO_3 Elements, such as lead and zinc, still show some stability as metal halide compounds. PbBr_4 shows stability up to 700°C while PbCl_2 possesses a region of stability from $\sim 430^\circ\text{C}$ to $\sim 470^\circ\text{C}$. $\text{ZnBr}_{2(g)}$ shows a region of stability from about 550°C to 800°C , before zinc degrades to $\text{Zn}_{(g)}$ at temperatures above 700°C .

Figure 4.9 gives the thermodynamic stability of the e-waste system with the addition of 1.8 times the stoichiometric amounts of CaCO_3 .

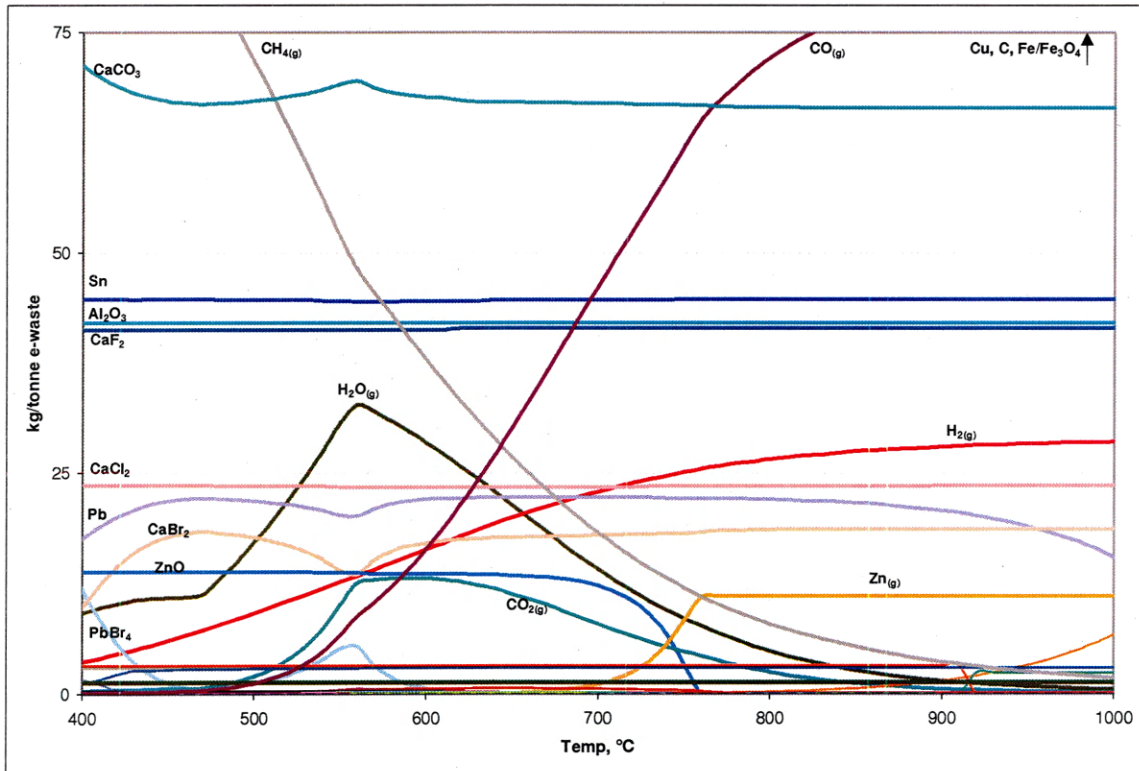


Figure 4.9 HSC 5.1 equilibrium composition of 1 tonne of e-waste and 1.8X CaCO_3

This model shows a higher level of halide sequestering by the CaCO_3 when compared to MgCO_3 . Zinc no longer shows a stable halide at any temperature. Lead, however, still shows some stability as a metal halide as PbBr_4 in various amounts up to 600°C .

Figure 4.10 gives the thermodynamic stability of the e-waste system with the addition of 1.8 times the stoichiometric amounts of NaHCO_3 . The erratic behavior of $\text{H}_2\text{O}_{(g)}$ and $\text{CO}_{2(g)}$ at 600°C is due to the alteration in oxidation potential of the system from the stability of iron oxides at temperature— Fe_3O_4 is stable below 600°C , FeO is stable from 600°C to 620°C and Fe is stable above 620°C .

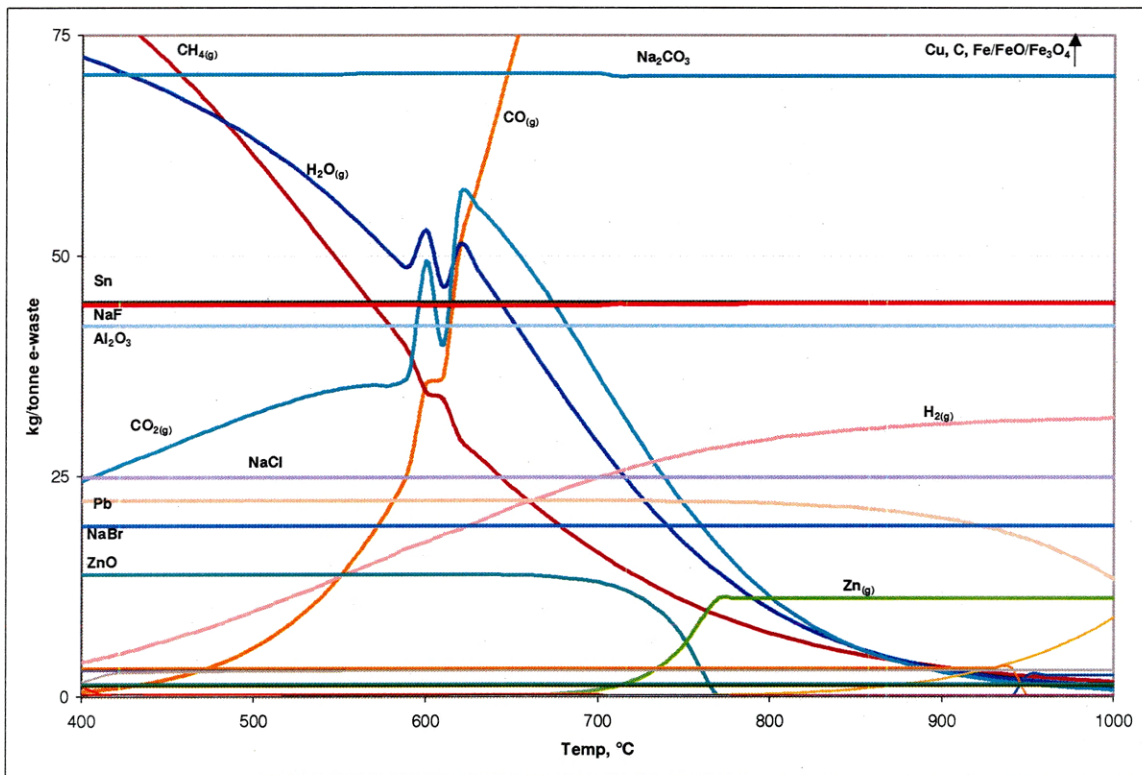


Figure 4.10. HSC 5.1 equilibrium composition of 1 tonne of e-waste and 1.8X NaHCO_3

This model shows that the presence of a sodium-based carbonate in the mixed metal/organic/halide system defining e-waste results in high level of stability of the halides as sodium salts. The weight percentages of fluorine, chlorine and bromine sequestered in the form of sodium salts, according to the thermodynamic equilibrium, are 99.38%, 99.92% and 99.93%, respectively.

4.4 Thermodynamic Modeling Results

In a system containing such a large number of elemental constituents, the number of compounds generated requires a computer application such as HSC to determine the thermodynamic stability within an acceptable amount of time. The ability to evaluate multiple chemical systems with a finite investment of resources allows for a quick survey of possible treatment scenarios. Entering into a research program with an understanding of the complex thermodynamic behavior can assist the researcher in avoiding pitfalls that may disrupt or delay a research program.

Based on the thermodynamic modeling work for the alkali and alkali-earth carbonates in the presence of the 39 elements present, an experimental system was developed for testing the applicability of three carbonate species. Work focused on sodium-based compounds as sodium showed the most stable halide salts, according to thermodynamic modeling. Calcium and magnesium were included for comparison.

CHAPTER 5

ORGANIC BEHAVIOR AT TEMPERATURE

5.1 Organic Behavior—Rotary Kiln Equipment and Procedure

Work was conducted to evaluate the behavior of the organic (plastic) components of various waste streams, including both automobile shredder residue and electronic waste under various conditions. Initial work dealt with the behavior of PE under conditions outlined in cooperative research with Paul Kruesi in support of patented technology (Kruesi, 2004). Understanding the vaporization and decomposition of various polymer materials in the presence of an added carbonate would assist in outlining the process parameters for e-waste and other waste-stream processing.

An experimental system was designed and assembled to evaluate the thermal processing of e-waste and other mixed waste materials (Figure 5.1). The system was comprised of six primary areas:

- 1) Control Panel
- 2) Pre-heat unit
- 3) Rotary Kiln
- 4) Condenser with collection reservoir
- 5) Particle Filter
- 6) Scrubber—5 liter volume

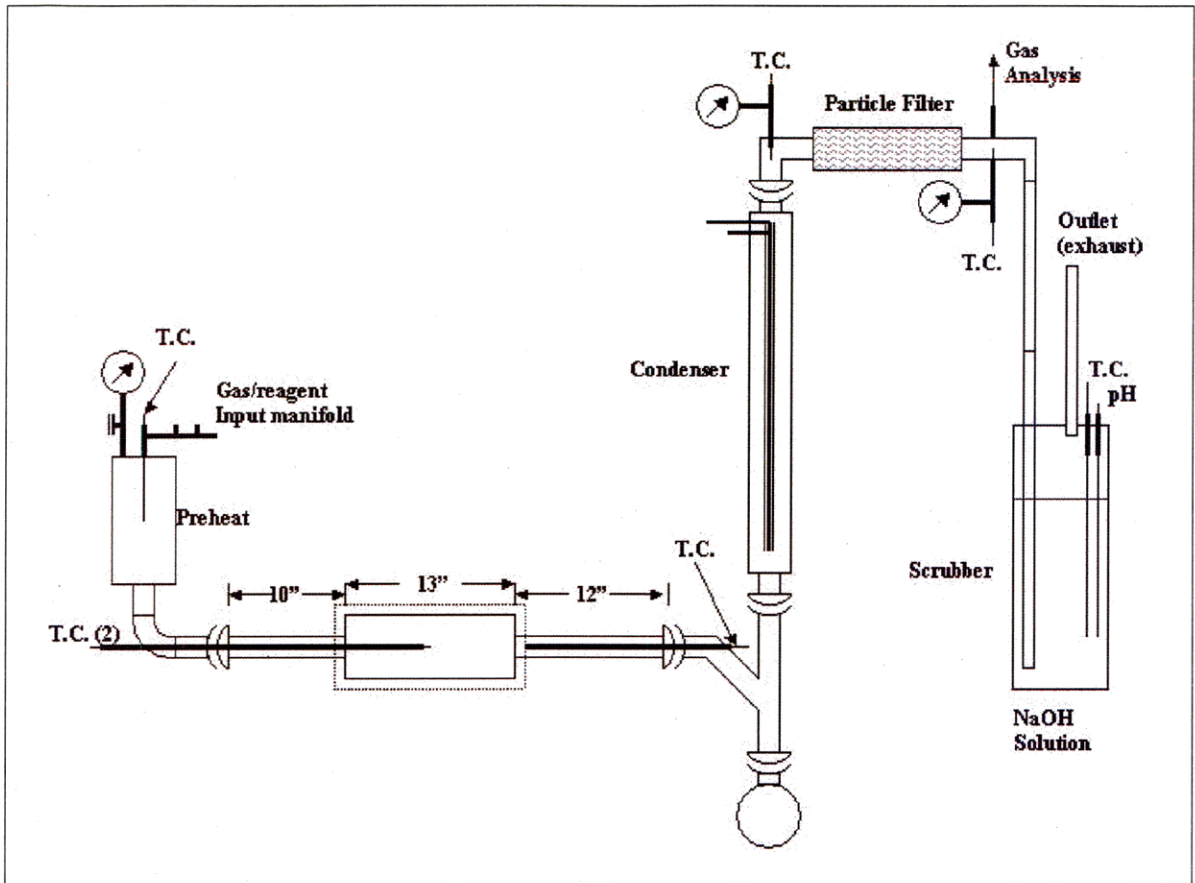


Figure 5.1 Experimental System-Schematic

- 1) Control Panel. The control panel (Figure 5.2) houses the Data Acquisition system, gas analysis, power supplies for the primary furnace and pre-heat system, flow meter module, gas mixing valves, and rotary kiln rotation control.
 - a. Data Acquisition. All relevant data are recorded via a computer data acquisition system. The system is comprised of a PC computer running Labview 7.1 connected to a National Instruments SCXI-1000 system fitted with the SCXI-1002 module and SCXI-1303 terminal block. This configuration allows for up to 32 channels of data to be recorded. Thermocouple measurements take advantage of the built-in cold-junction sensor in the National Instruments equipment. All data (Table 5.1) are recorded to "lvm" format, readable by MS Excel.

Table 5.1 Rotary Kiln Data Acquired

<ul style="list-style-type: none"> • Input gas flow <ul style="list-style-type: none"> ○ 0-5 slpm CO_(g) ○ 0-5 slpm CO_{2(g)} • Preheat chamber pressure • Preheat chamber temperature • Kiln body inlet temperature • Kiln body center temperature • Kiln body outlet temperature • Kiln furnace temperature • Condenser outlet (pre-filter) pressure • Condenser outlet (pre-filter) temperature 	<ul style="list-style-type: none"> • Post-filter (gas analysis sample port) pressure • Post-filter (gas analysis sample port) temperature • Gas analysis <ul style="list-style-type: none"> ○ 0-100% CO_(g) ○ 0-100% CO_{2(g)} ○ 0-25% CH_{4(g)} ○ 0-50% H_{2(g)} • Scrubber solution pH • Scrubber solution temperature • Exhaust flow: 0-10 slpm as air • Exhaust temperature
--	---

- b. Gas Analysis. Gas analysis is conducted via continuous sampling at ~0.61 slpm (liters per minute) (STP) to a NOVA Model 7904C-RM furnace atmosphere gas analyzer. Analyzer gases and ranges are as follows: CO_(g), 0-100%; CO_{2(g)}, 0-100%; CH_{4(g)}, 0-25%; and H_{2(g)}, 0-50%. Calibration is conducted prior to every experiment using industrial grade nitrogen (zero), CO_(g) (100%), CO_{2(g)}, (100%), and a calibration tank containing CH_{4(g)}, (25%); H_{2(g)}, (50%) and N_{2(g)}, (25%). Data generated is transmitted to the data acquisition system via 0-5V signals. Temperature and pressure data are taken at the gas sampling point positioned after the particulate filter. The gas stream first passes through a desiccant column and two filters supplied with the gas analyzer prior to entering the unit. The return-gas stream is directed back to the system prior to the scrubber.
- c. Power Supplies. Two power supplies with PID control are used to power the primary furnace, heating the rotary kiln, and the pre-heat, described below. The primary furnace is an Applied Test Systems (APS) Series 3210 Split Tube Furnace operated via a Barber Colman Series 2404 Temperature Controller. Pre-heat vessel is powered by a Brand Gaus Model 411 power supply controlled by a Watlow Series 96 controller.

- d. Flowmeter Module and Gas Mixing Valves. The flowmeter power supply is a Hastings Model 40, with the capability of operating four meters. Three HFM-200 meters are connected to the unit: CO_(g), 0-5 slpm; CO_{2(g)}, 0-5 slpm; and Air, 0-10 slpm. CO_(g) and CO_{2(g)}, meters combined with needle valves, allowing for accurate mixing of feed gas to the preheat module. The air meter is utilized to obtain a measurement of gas flow out of the system.
- e. Rotary-kiln Speed Control. A standard AC rotary speed control is employed to adjust kiln rotation.

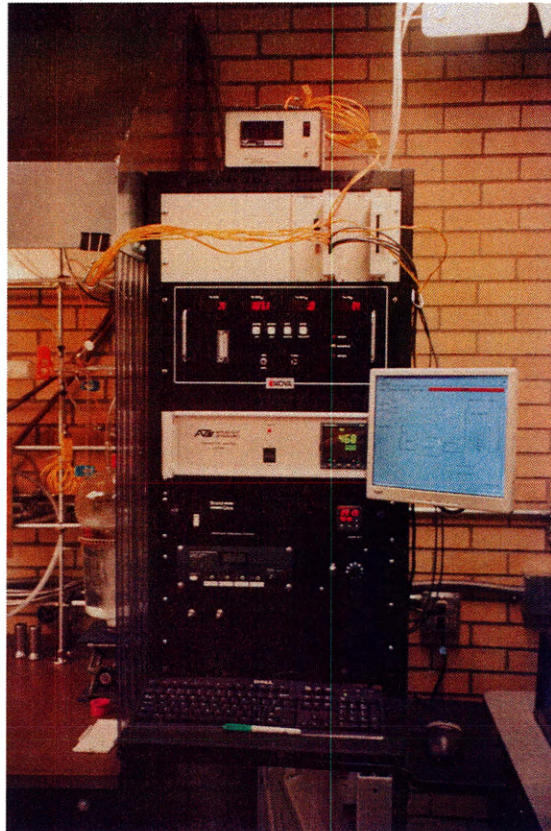


Figure 5.2 Data Acquisition and Control

- 2) Pre-heat. The pre-heat system is manufactured from 3" diameter, 306 stainless steel stock designed and filled with stainless steel wool to provide sufficient time, temperature and surface area to allow for the vaporization of any liquid reagents and

the heating of the feed gas to the required temperature, reducing or eliminating any quenching of the kiln due to the influx of reactants. The unit is fitted with a pressure transducer and centerline k-type thermocouple for power/temperature regulation. The preheat unit is attached to the rotary kiln via a 90° elbow and a 35/25 ball & socket joint. Heating of the unit is accomplished via three (3) Watlow band heaters. The unit is insulated with zirconium felt and silica insulation.

- 3) Kiln. The reaction vessel is designed to mirror preliminary experimentation, but on a larger scale. The kiln is manufactured from 306 stainless steel. The inlet and outlet to the kiln are a 10" long x 1" I.D. and a 12" long x 1" I.D. pipe respectively. The kiln body itself is a 13" x 5" I.D. stainless steel tube. The interior of the reactor is fitted with six lifters to ensure solids contact with the hot gas stream entering the reactor. One end of the reactor was designed to be removable, allowing for direct access to the interior, making charging and sample removal easier. The kiln is sealed using a copper gasket/o-ring. Center-point temperature of the kiln is monitored via a 1/4" k-type thermocouple 36" long, fed in through the pre-heat elbow. A 1/32" thermocouple is positioned along the large thermocouple, providing a temperature at the inlet of the kiln body. A kiln body outlet temperature is read via a third thermocouple fed in from the quartz outlet fitting. All temperatures, including the furnace, are recorded via data acquisition system.
- 4) Condenser. A standard condenser apparatus is fitted to the outlet of the kiln. Sufficient cold-water flow is maintained during all experiments to reduce the gas temperature to 25°C +/- 2°C. Inlet and outlet water temperatures are taken via data acquisition system. All glass equipment is shown in Figure 5.3.

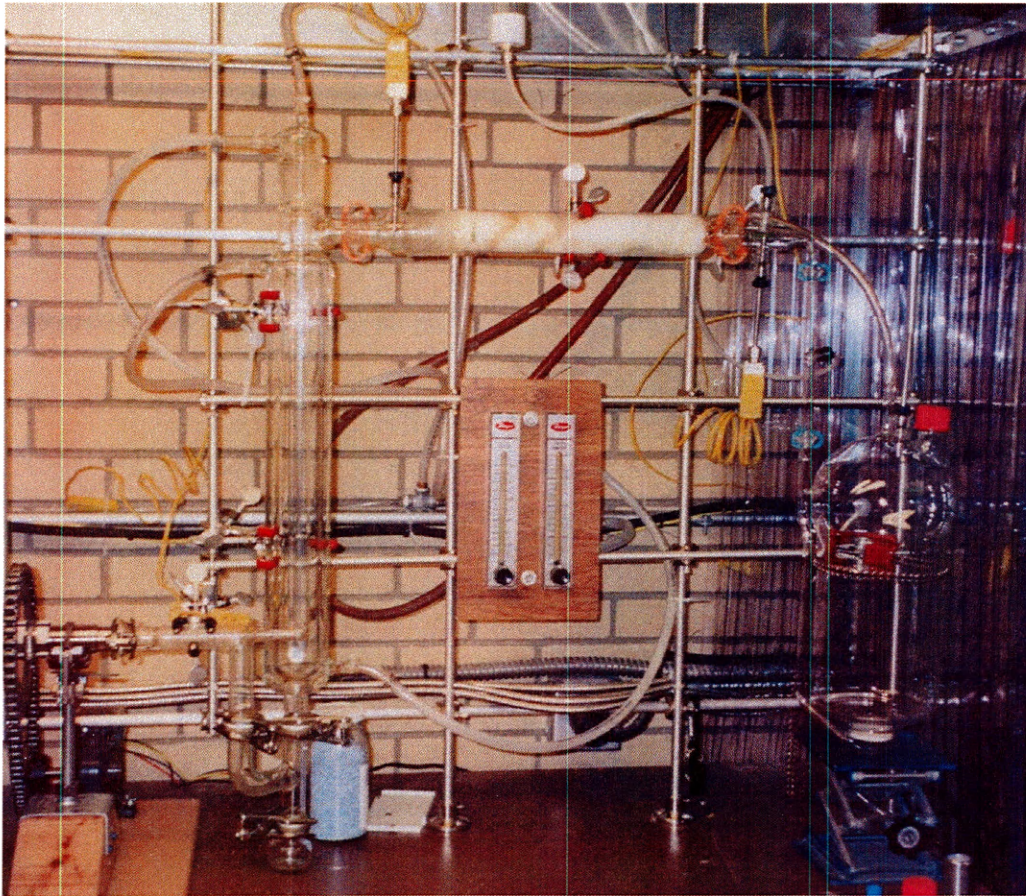


Figure 5.3 Condenser, Filter and Scrubber

- 5) Particle Filter. A 2" dia. glass vessel filled with fine glass wool serves as a particle filter, removing the majority of particles and entrained polymers from the gas stream prior to gas sampling and scrubbing. Temperature and pressure measurements are taken before and after the filter material.

- 6) Scrubber. Initial system design included a five-liter scrubber designed to accommodate the entrapment of chlorine liberated from a 200 g sample of PVC. Temperature and pH of the scrubbing solution is available to data acquisition. Gas flow from the scrubber is treated via a desiccant column prior to flow and temperature measurement.

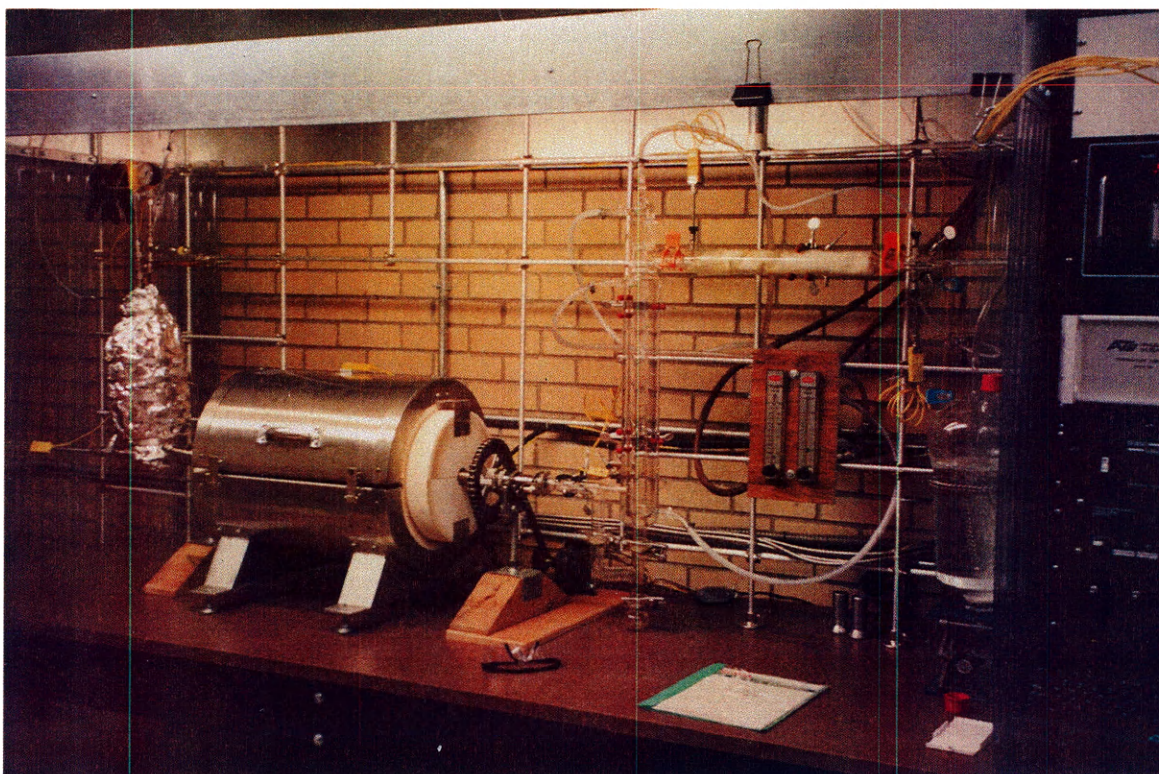


Figure 5.4 Experimental System

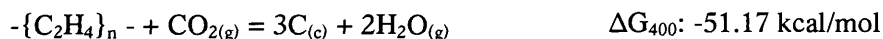
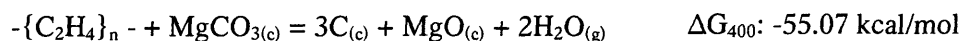
Polyethylene (PE) comprises ~10% of e-waste and was therefore selected as the first material for evaluation. Initial work focused on the decomposition of the polymer in the presence of a carbonate source. The selection of an atmosphere of $\text{CO}_{2(g)}$ was based on presumed full-scale operational parameters and the desire to minimize free oxygen. A temperature range of 350-500°C was outlined for investigation based on a survey of published decomposition temperatures for the organics present in e-waste (Table 5.2).

Table 5.2 Polymer Reference Data, in N_{2(g)}

		Melting Temp. °C	Decomposition Temp. °C
PE	-[C ₂ H ₄] _n -	170	350
PP	-[C ₃ H ₆] _n -	120	380
Polyesters	-[C ₁₀ H ₄ O ₄] _n -	260	300
Epoxies	-[C ₁₈ H ₁₂ O ₃] _n -	-	330
PVC	-[C ₂ H ₃ Cl] _n -	80	250
PTFE	-[C ₂ F ₄] _n -	335	360*
Nylon (6,6)	-[C ₁₂ H ₂₂ O ₂ N ₂] _n -	250	440

* Re-evaluated during subsequent experimentation

Experimental work using PE, spanned 65 experiments and focused on MgCO₃ given the instability of the carbonate in the temperature range selected, but also included CaCO₃ and MgCO₃Mg(OH)₂·3H₂O as carbonate sources. All PE experiments were conducted using post-consumer wire-sheath material. Work was designed to explore the possible validity of following reactions assisting the decomposition of PE (Data from HSC 5.11):



General Experimental procedure consisted of:

1. Loading of kiln. All measured sample material is placed into the rotary kiln, sealed and placed in primary furnace.
2. Pre-weights. All glassware on the outlet side of the kiln is weighed prior to the experiment to obtain a weight of "wax" produced.
3. Sealing of system. Thermocouples are inserted into the kiln through the attached equipment, sealing via Swagelock or ground glass fittings. Rotating fittings on either end of the kiln are sealed with vacuum grease and clamps. Cooling water to the condenser is set at >10 gallons per minute (gpm).
4. Purge and NOVA calibration. The entire system is purged with the desired gas (CO_{2(g)}). While the system is purging, The NOVA gas analyzer is calibrated using

industrial grade nitrogen (zero), $\text{CO}_{(g)}$ (100%), $\text{CO}_{2(g)}$, (100%), and a calibration tank containing $\text{CH}_{4(g)}$, (25%); $\text{H}_{2(g)}$, (50%) and $\text{N}_{2(g)}$, (25%). Upon completion of calibration, the system purging is checked by waiting until sampling shows ~100% $\text{CO}_{2(g)}$.

5. Data Acquisition and Preheat. Once the system is purged, all gas flow is set to zero. Data acquisition system is initiated and the preheat chamber is brought to temperature.
6. Kiln operation. Once preheat is to temperature, gas flow is resumed at the set flow and kiln heating is begun.
7. Shutdown. Once the desired time and/or temperature are reached, all flows are shut and power is turned off. The system is allowed to cool over night prior to emptying the kiln.
8. Sample weighing/collection. Glassware previously weighed is again weighed to obtain a weight of paraffin produced. The kiln is disassembled and solids removed and weighed. Solids attached to the inner surface of the kiln are removed with a brush or scrapper.
9. Solids analysis. Select solids are analyzed by X-Ray Diffraction (XRD) for characterization. A sample of the solids removed from the kiln is treated by an HCl digestion: 1-2 grams of solids were digested in 50 mls of pH < 1.0 solution for 10-30 minutes to remove soluble compounds. The residue is comprised of organic or carbon material. Some residues are treated to Pyrolysis in an oxygen-free atmosphere at 600°C, removing organic material and leaving the “free carbon” contained within the sample. This allows a carbon balance to be calculated.

5.2 Phase 1: High Flow System with Various Solid Carbonate Sources

Both magnesium carbonate and calcium carbonate were investigated for the effect on polymer decomposition. Magnesium carbonate has a decomposition temperature of ~310°C in a $\text{CO}_{2(g)}$ -free environment while calcium carbonate is stable over the temperature range under

investigation. Magnesium carbonate is also available as a basic carbonate ($\text{MgCO}_3 \cdot \text{Mg}(\text{OH})_2 \cdot 3\text{H}_2\text{O}$). Both calcium and magnesium carbonate will also be evaluated for halide sequestering in a later section of this thesis.

Experiments conducted with 200 g of PE and no carbonate source at temperatures from 300 to 600°C proved to generate excessive amounts of fume, reducing or eliminating any effective retention time (time-at-temperature). This resulted in a distillation effect, generating a large amount of wax-like residue in the condenser. Experiments conducted with small amounts of PE in a $\text{CO}_2(\text{g})$ atmosphere demonstrated the ability to distill the PE to various paraffin compounds in a more controlled manner with no detected gas emissions (Figure 5.5).

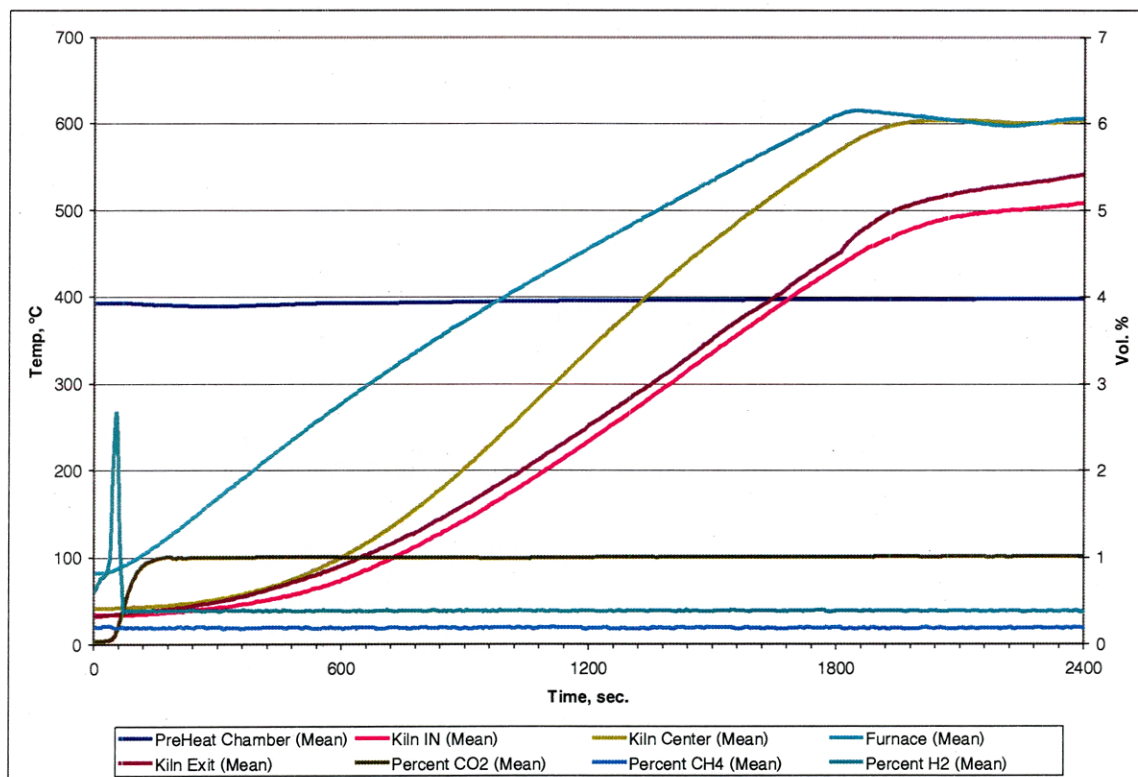


Figure 5.5 Exp 2: 1 g PE, 2 slpm $\text{CO}_2(\text{g})$

Due to the inconsistent heating observed within the kiln during the heating cycle, additional work was conducted with an alteration to the heating program. The system was first heating to

~330°C for 1 hour prior to a 1 hour slow ramp-up to the final experimental system temperature. This allowed for a more uniform heating of the entire kiln volume.

PE in contact with CaCO₃ in a CO_{2(g)} atmosphere produced minor CH_{4(g)} readings above 400°C (Figure 5.6), while the same experiment in N_{2(g)} produced no detectable gas emissions over the entire temperature range (Figure 5.7). These two experiments would suggest an interaction with the organic fume (vapor) and the CO_{2(g)} atmosphere, but does not necessarily indicate any carbonate/fume interaction.

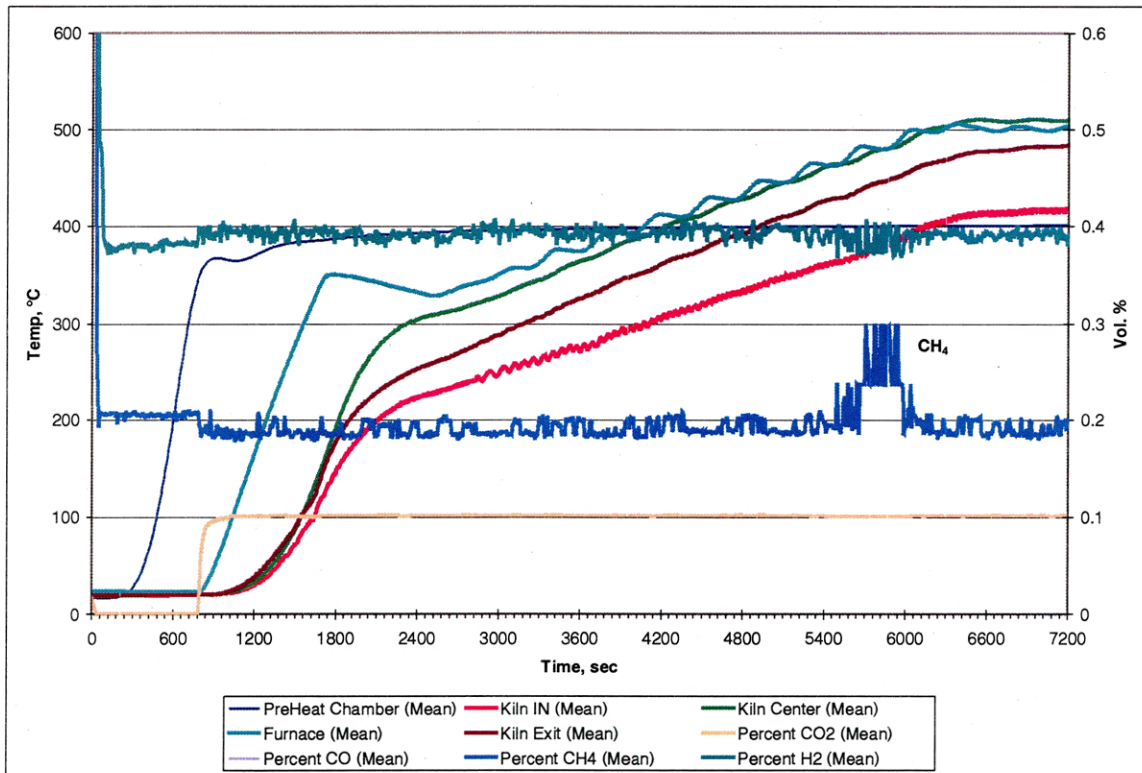


Figure 5.6 Exp 9: 10 g PE, 5.22 g CaCO₃, 2 slpm CO_{2(g)}

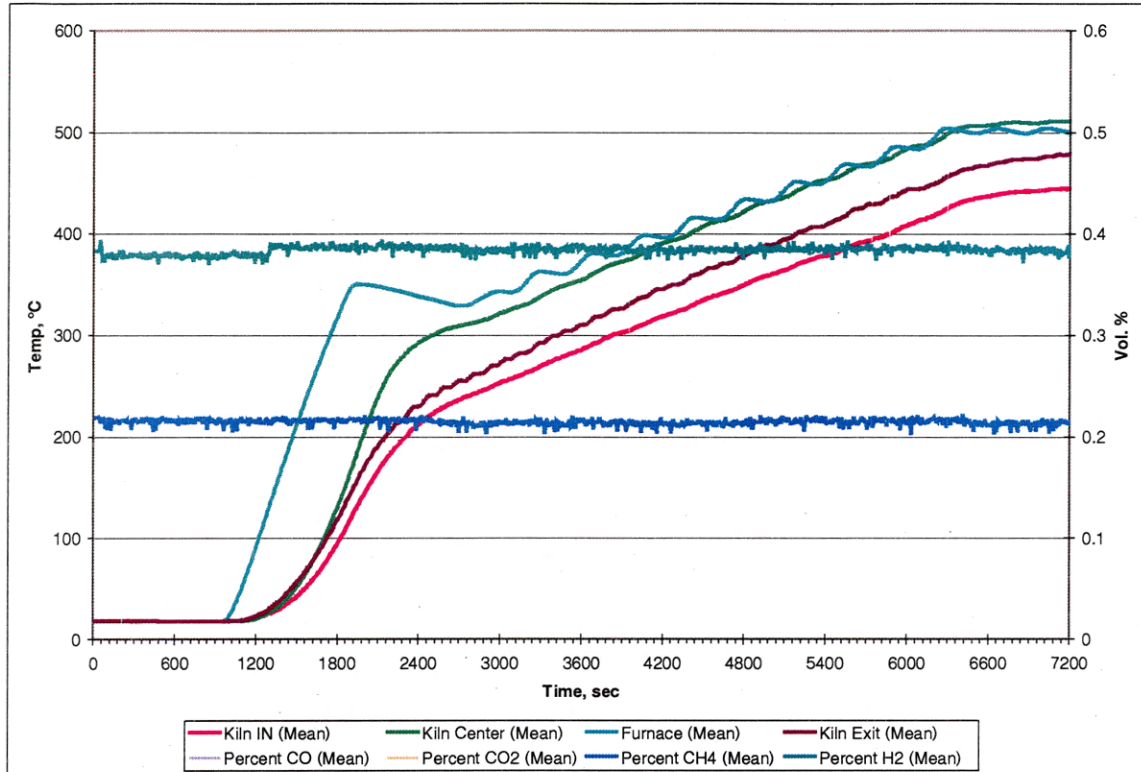


Figure 5.7 Exp 10: 10 g PE, 5.22 g CaCO₃, 2 slpm N_{2(g)}

Basic MgCO₃ (MgCO₃Mg(OH)₂·3H₂O) produced similar results, generating minor CH_{4(g)} readings in the presence of a CO_{2(g)} atmosphere, but emitting CO_{2(g)} over the temperature range 320-450°C in an N_{2(g)} atmosphere—decomposition of the carbonate solid (Exp A11 and A12). A combination of Basic MgCO₃ and CaCO₃ produced results similar to tests conducted separately, showing no increased reactivity as a mixture.

Conclusions of Phase 1: Evaluating the system under high flow (2 slpm) conditions and various carbonate sources resulted in a number of observations affecting the next stage of work. The gas flow of 2 slpm, in conjunction with the 4.1 liter volume of the kiln provided for a maximum gas retention time of 1.58 min. This is seen as the reason for excessive fume or wax formation, indicating that the materials are not being allowed long enough duration at the temperatures required for thorough reaction. With this in mind, a series of experiments was

devised with a closed (no gas flow) system, allowing for more accurate determination of the reactions taking place within the system.

5.3 Phase 2: Closed System with Various Solid Carbonate Sources

Phase 2 procedure alters the previous system procedure only by 1) eliminating both the preheat and NOVA gas analyzer, as there is no active gas flow into the system and 2) previously mentioned alteration to the heating program. The NOVA analyzer was still employed to ensure complete gas purge of the system before heating of the kiln is initiated. The following conditions were evaluated in Phase 2:

Final System Temperature, $T = 300, 400, \text{ and } 450^{\circ}\text{C}$

Solids/Carbonates: MgCO_3 , $\text{MgCO}_3\text{Mg}(\text{OH})_2 \cdot 3\text{H}_2\text{O}$, MgO , and carbon black.

Without active gas flow through the system, gas analysis was not possible, but reactions involving gas production or consumption could be detected via pressure change.

Based on previous experiments and the hypothesis that increased surface area may affect the degradation of the organic and, therefore, the increased production of short-chain organic gases, 60-mesh carbon was employed as an inert solid with high surface area to confirm/disprove this hypothesis. Carbon as the only solid in addition to PE, showed no effect to the system, based on pressure readings (Figure 5.8). The carbon was added to provide for a large surface area for the PE to coat and to reduce adherence of the PE to the inner surface of the kiln. Pressure readings showed only the initial expansion of gas within the vessel during heating.

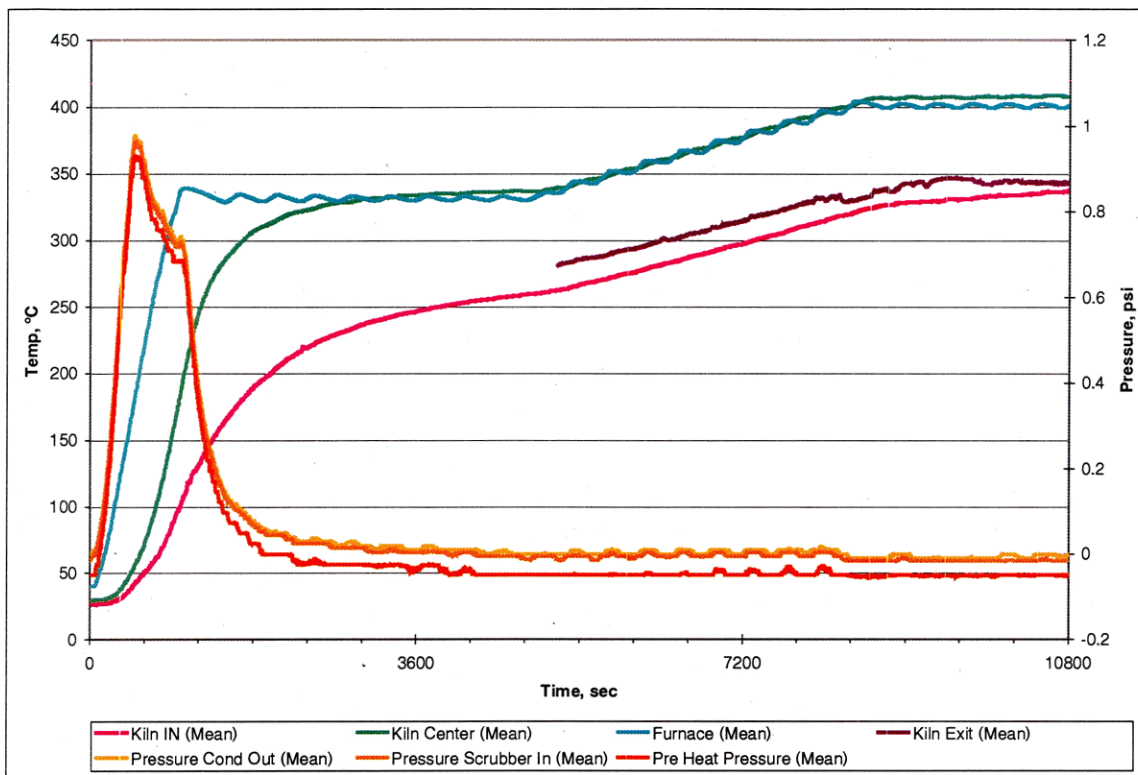


Figure 5.8 Exp 36: 5 g PE, 10 g C, CO_{2(g)}

Carbon in addition to MgCO₃Mg(OH)₂·3H₂O in the presence of PE added no detectable effect to the reactions taking place with MgCO₃Mg(OH)₂·3H₂O and PE. MgCO₃Mg(OH)₂·3H₂O both alone and with PE showed a second pressure wave generated at T = 150-250°C, indicating the release of H₂O (Figures 5.9 and 5.10). Additional slow temperature rise tests also showed a shallow pressure wave generated from 250-350°C. This increase in pressure is consistent with the beginning stages of carbonate decomposition.

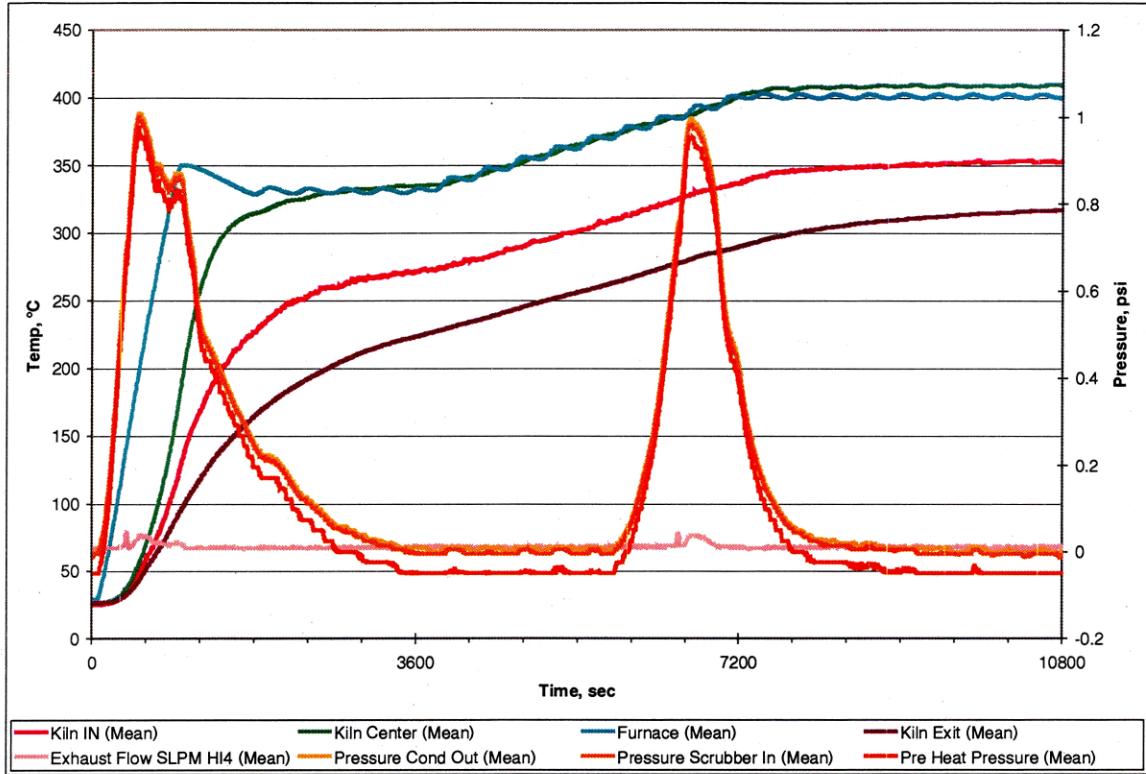


Figure 5.9 Exp 37: 5 g PE, 15 g C, 15 g $MgCO_3Mg(OH)_2 \cdot 3H_2O$, $CO_{2(g)}$

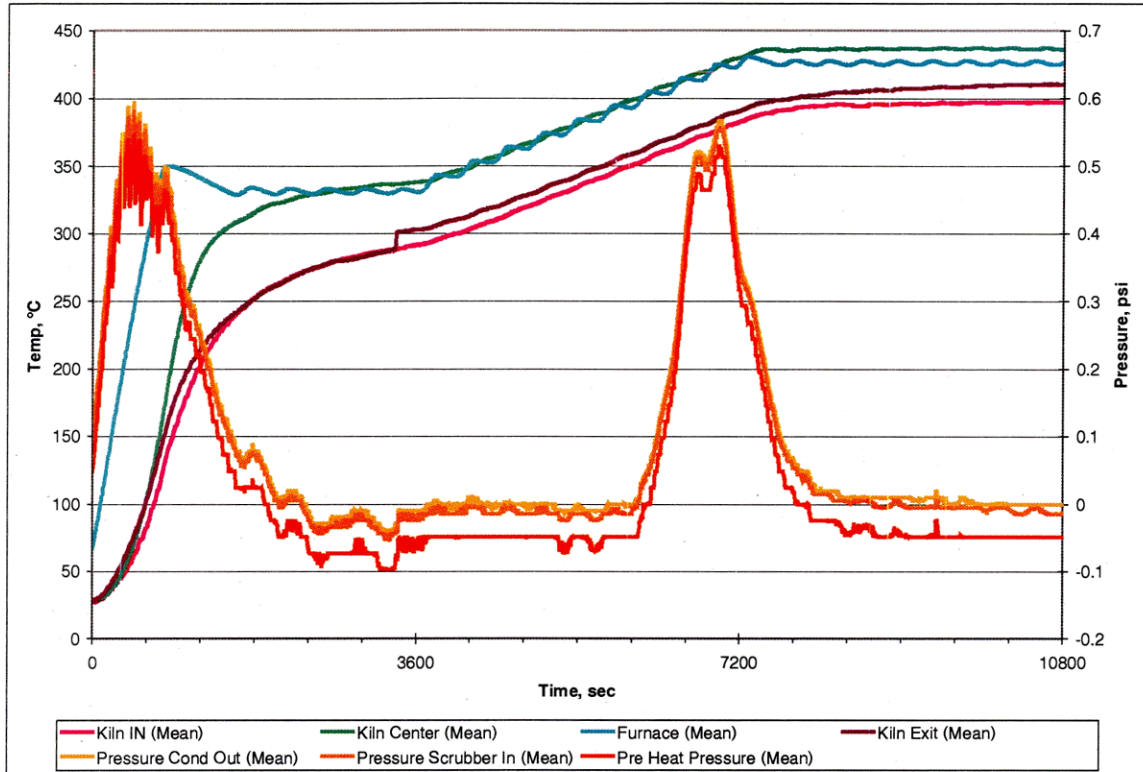


Figure 5.10. Exp 38: 5 g PE, 15 g $\text{MgCO}_3\text{Mg}(\text{OH})_2 \cdot 3\text{H}_2\text{O}$, $\text{CO}_2(\text{g})$

Tests that progressed to temperatures at and above 425°C showed an additional pressure wave that seems to relate to a more thorough degradation of the PE and, therefore, higher free carbon generation (Figure 5.11). This “reaction pressure peak” was less pronounced in experiments carried out with dry (reagent) MgCO_3 (Figure 5.12).

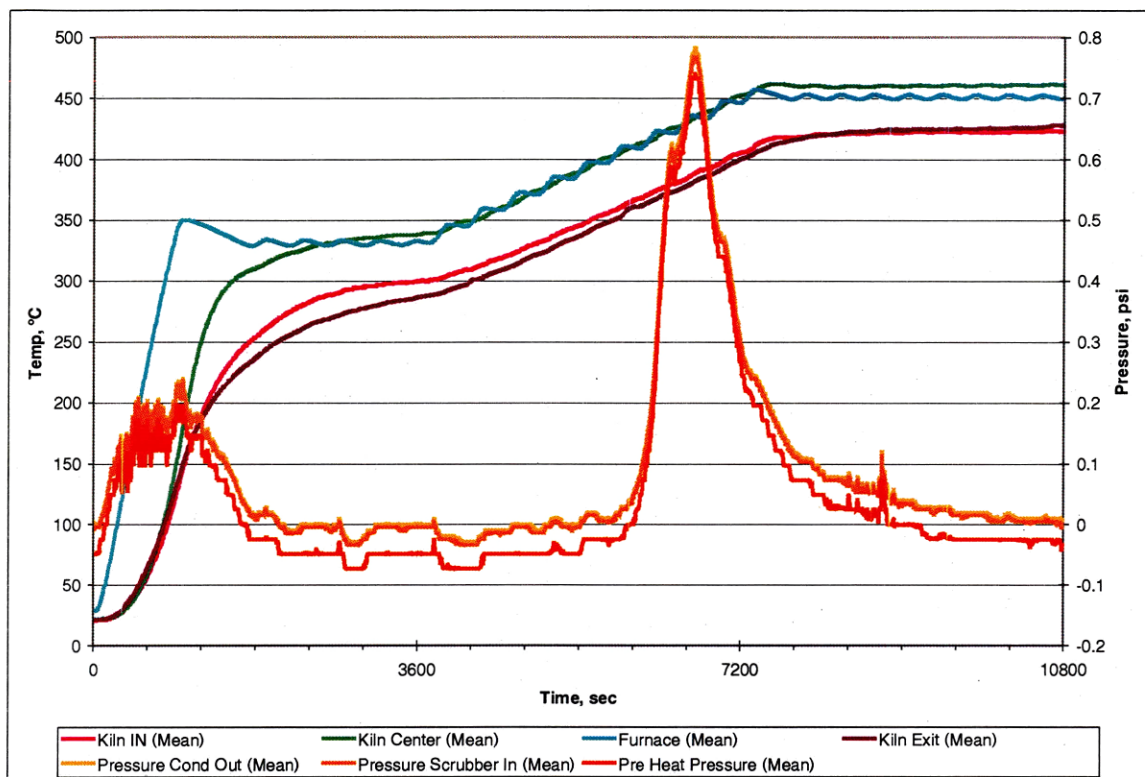


Figure 5.11 Exp 39: 5 g PE, 15 g $\text{MgCO}_3\text{Mg}(\text{OH})_2 \cdot 3\text{H}_2\text{O}$, $\text{CO}_2(\text{g})$

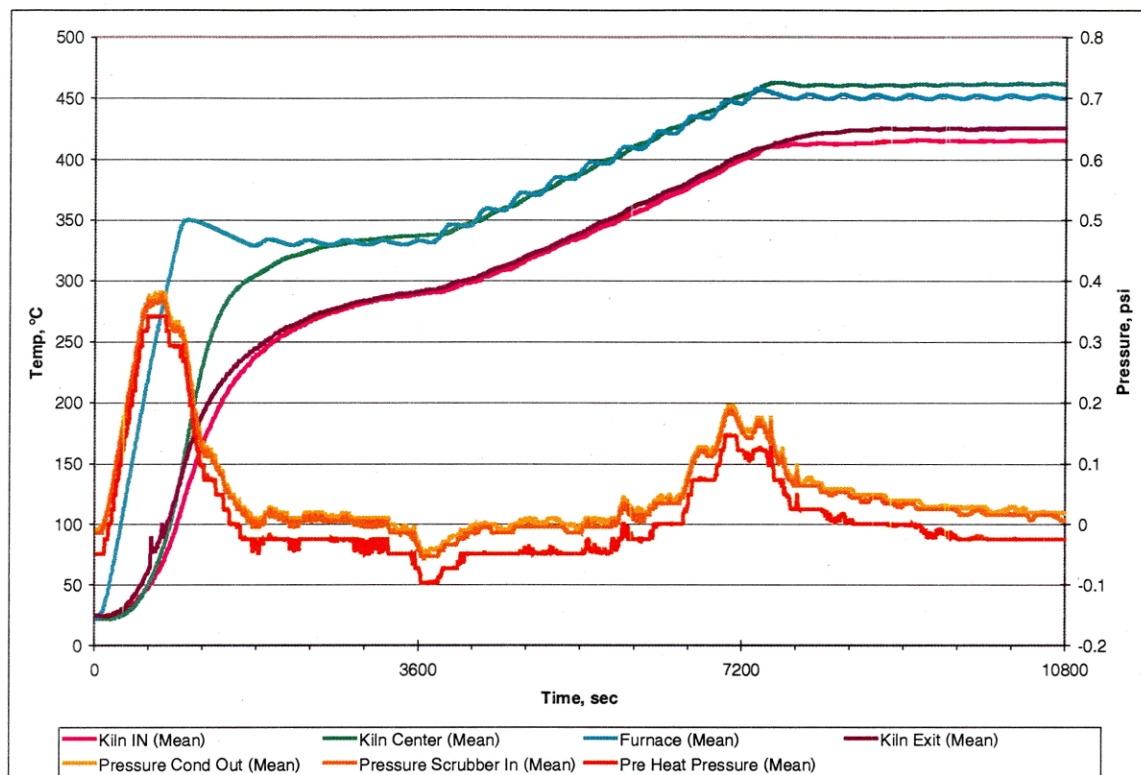


Figure 5.12 Exp 41: 5 g PE, 15 g MgCO_3 , $\text{CO}_2(\text{g})$

The solid carbonate sources $\text{MgCO}_3 \cdot \text{Mg}(\text{OH})_2 \cdot 3\text{H}_2\text{O}$ and MgCO_3 were compared over the temperature range 350-500°C, with the relative effectiveness based on non-digestible solids and overall carbon recovery from the PE. After each test, a sample of the solids was digested as described previously. The digested residue was then heated in an inert atmosphere to drive off any remaining organic. The remaining mass was deemed to be free carbon.

Figure 5.13 shows the amount of solids within the kiln that was not digestible via a pH 1.0 HCl digestion vs. final kiln temperature for both the basic magnesium carbonate and magnesium carbonate. While tests conducted at 375°C contained unreacted PE nodules, Tests conducted at 400°C resulted in an undigestible organic material. This organic residue is responsible for the higher recovery at lower temperatures. XRD analysis of this material showed the existence of a 6-carbon organic as part of the residue. This wax-like or paraffin residue may be unreacted

organic or material formed from back-reactions/condensation of fume remaining in the kiln during cool-down of the system.

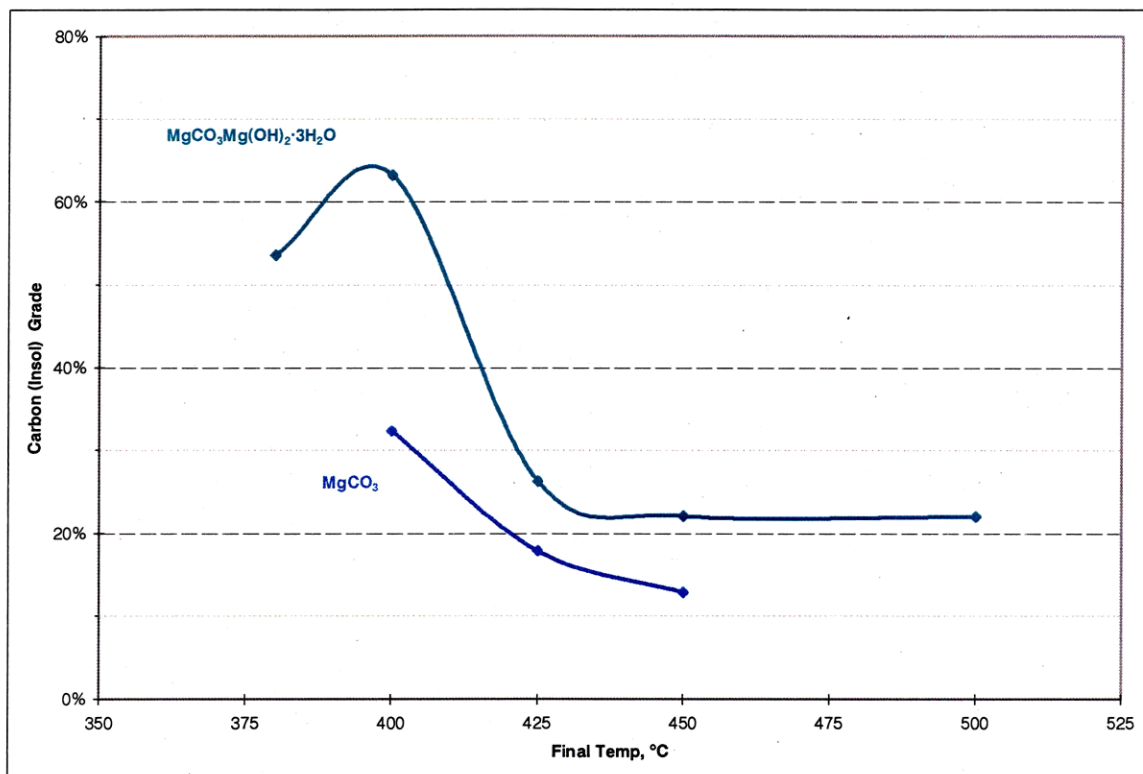


Figure 5.13 Acid Digestion Residue Recovery

Figure 5.14 shows the digested samples after pyrolysis (reported as Carbon Grade) indicating an increased degradation of PE in the presence of basic magnesium carbonate.

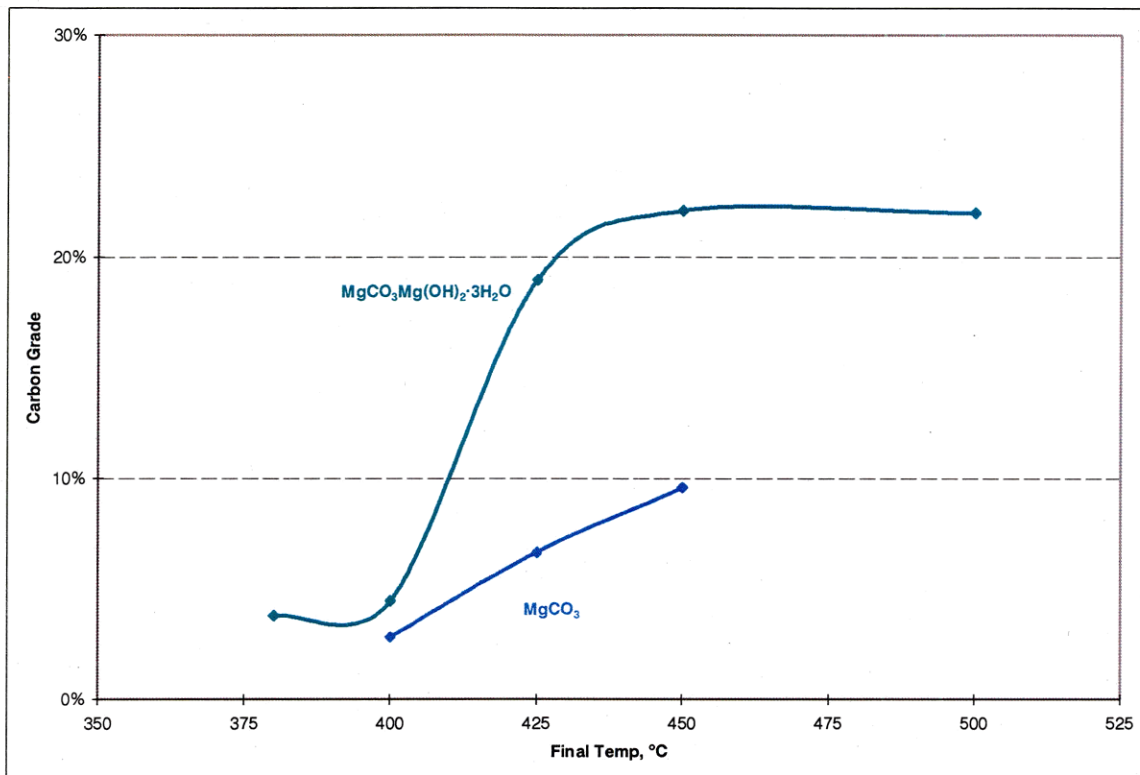


Figure 5.14 Carbon Grade of Residue

Conclusions, Phase 2: Based on the work conducted in Phase 2, the following observations were made:

- Magnesium carbonate and calcium carbonate both have a similar effect on the degradation of PE, increasing the relative degree of cracking of the polymer
- Basic magnesium carbonate ($\text{MgCO}_3\text{Mg(OH)}_2\cdot 3\text{H}_2\text{O}$) has a greater influence on the degradation of PE than does magnesium carbonate (MgCO_3)
- Despite a published decomposition temperature of 350°C , temperatures above 425°C allow for the conversion of PE to free carbon and shorter chain organics

5.4 Organic Behavior Study Results

A number of observations can be made from the initial study of PE in the presence of various carbonate sources. First, the degradation, or “cracking” of polymers will require a reactor volume based on fume retention time. The removal of the organic fraction from the metal and oxide fractions will occur in a relatively short time. The need to reduce the chain-length of the organic fume to the point that it is no longer a paraffin-like material will act as the limiting factor in equipment sizing.

Second, as is the case with most polymers, the distribution of molecular weights for any polymer sample does not allow for a unique reaction temperature at which all of the material will react to form the prescribed products. This is evident in attempting to correlate published temperatures of decomposition for a given polymer and the reactions seen in experimentation with post-consumer polymer material. As is also the case, the specific application of a given polymer may allow for the addition of filler material (metal or mineral) that may alter the thermal properties and stability of the host polymer. In the development of a process designed to consume a mixed material stream with varying composition, one must base operational parameters on highest operational temperature that may be required for any material processed. The effect of these realities can be seen in the processing of PE: even though degradation may begin at 350°C, process temperatures must exceed 425°C to ensure complete consumption of the material.

Third, the presence of a carbonate containing H₂O (MgCO₃Mg(OH)₂·3H₂O) has an increased effect on the degradation of a polymer when compared to a carbonate without H₂O (MgCO₃).

CHAPTER 6

SEQUESTERING AGENTS

6.1 Sequestering Agents—Tube Furnace Equipment and Procedure

Following work with the rotary kiln system and determining its advantages and disadvantages, a new experimental system was devised for more finite control. The second system is comprised of a simple tube furnace fitted with a quartz tube (Figure 6.1).

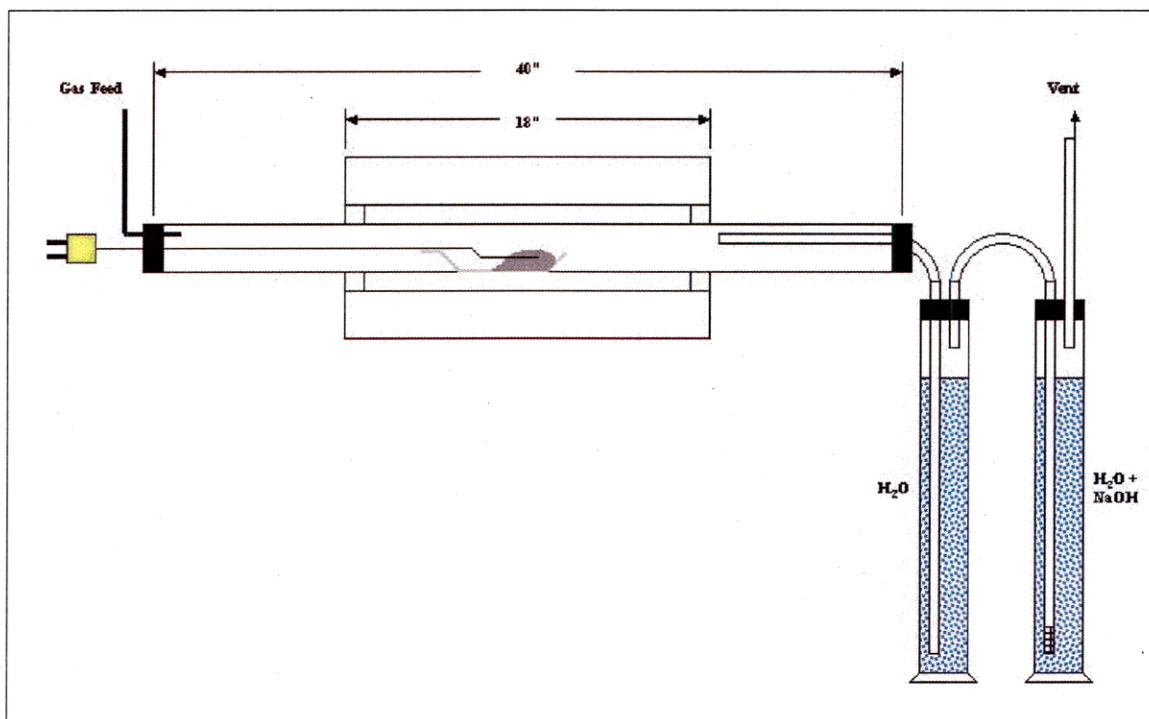


Figure 6.1 Tube Furnace System-Schematic

The tube ends are fitted with stoppers to ensure atmospheric composition while allowing for the injection of a known atmosphere and the collection and scrubbing of offgas from the system.

Gas flow is set at 1 slpm, giving an average velocity through the reactor, at temperature, of 3 cm/sec. The intent is to remove any gas or vapor product from the sample, allowing for the evaluation of the sequestering ability of the carbonate without reliance on any secondary reactions. Gases exiting the tube are first bubbled through water via a ½” glass tube to reduce the amount of condensable organic fume before being sparged through an alumina frit in a NaOH solution to recover any halides present. The ceramic sample boat is attached to a thermocouple allowing for the insertion of the sample to the hot zone of the furnace once the system has come to temperature. All relevant data are recorded via the computer data acquisition system described previously. One of two data acquisition arrangements is employed (Table 6.1). If chloride determination is desired, Mode 1 is employed (all exhaust gas is directed to scrubbing operation). If gas analysis is desired, Mode 2 is employed (all exhaust gas is directed to the NOVA gas analyzer). All data are recorded to “1vm” format, readable by MS Excel.

Table 6.1 Tube Furnace Data Acquired

Data Mode 1	Data Mode 2
<ul style="list-style-type: none"> • Input gas flow <ul style="list-style-type: none"> ○ 0-5 slpm CO_(g) ○ 0-5 slpm CO_{2(g)} • Furnace Temperature • Sample/Boat Temperature 	<ul style="list-style-type: none"> • Input gas flow <ul style="list-style-type: none"> ○ 0-5 slpm CO_(g) ○ 0-5 slpm CO_{2(g)} • Furnace Temperature • Sample/Boat Temperature • Gas analysis <ul style="list-style-type: none"> ○ 0-100% CO_(g) ○ 0-100% CO_{2(g)} ○ 0-25% CH_{4(g)} ○ 0-50% H_{2(g)}

General Experimental procedure consisted of:

- 1) Loading of sample. All weighed sample material is mixed in a mortar and placed into the sample boat, attached to the thermocouple, and placed in the “parked” position at the cold (inlet) end of the quartz tube. Furnace is heated to temperature.
- 2) Scrubbing system (Mode 1). NaOH scrubbing solution is prepared and placed in the second scrubbing cylinder. Water is placed in the first scrubbing cylinder. System is sealed and purged with selected atmosphere.

- 3) Data Acquisition (Mode 2). Once the system is purged, gas flow is set to desired flow rate. Data acquisition system is initiated.
- 4) Test Execution. Sample is inserted to a fixed location within the tube furnace for 20 minutes. This time frame allows for sample time-at-temperature of 10-15 minutes.
- 5) Shutdown. Once the required time expires, the sample is withdrawn to the “parked” position and allowed to cool before removal from the tube.
- 6) Sample weighing/collection. Boat weight is recorded for loss. Scrubbing solutions (if generated) are combined and titrated for Cl^- using the silver nitrate method.

6.2 Sequestering Agents—Experimental Matrix

A series of experiments were conducted to determine the relative effectiveness of in-situ sequestering of halogens generated from the decomposition of polymers. Samples of PVC and PTFE were acquired from a chemical supplier. Having a pure source of the polymers allowed for a more accurate measurement of entrapment efficiency. Pure sources of polymer also removed the question of filler materials used in polymer manufacture.

6.2.1 PVC behavior and Chloride entrapment

A series of experiments was conducted to determine the relative effectiveness of in-situ sequestering of chloride generated from the decomposition of PVC. All experiments were conducted under a $\text{CO}_{2(\text{g})}$ atmosphere, paralleling previous work designed at minimizing the dioxin and furan production through reduced oxygen potential, as well as having the effect of evaluating the sequestering agents under least favorable conditions from an atmosphere viewpoint. The formation of a sodium-halide salt results in the release of $\text{CO}_{2(\text{g})}$. Having a pure $\text{CO}_{2(\text{g})}$ should provide for the least favorable atmospheric conditions. Relative effectiveness was determined by titrating the scrubbing solutions for chloride. At a 1:1 stoichiometric ratio, relative effectiveness is shown in Table 6.2.

	400°C	450°C	500°C
PVC + CaCO ₃	-1.64%	-3.50%	2.07%
PVC + Na ₂ CO ₃	16.33%	16.33%	25.01%
PVC + NaOH	45.46%	42.36%	-
PVC + MgCO ₃	64.67%	54.76%	62.19%
PVC + NaHCO ₃	88.22%	85.13%	88.84%

PVC has a published decomposition temperature of 250°C, indicating that the final temperature (400, 450 or 500°C) should have little or no effect on the entrapment of the chloride. The only effect is the heating rate seen by the sample due to the temperature gradient present.

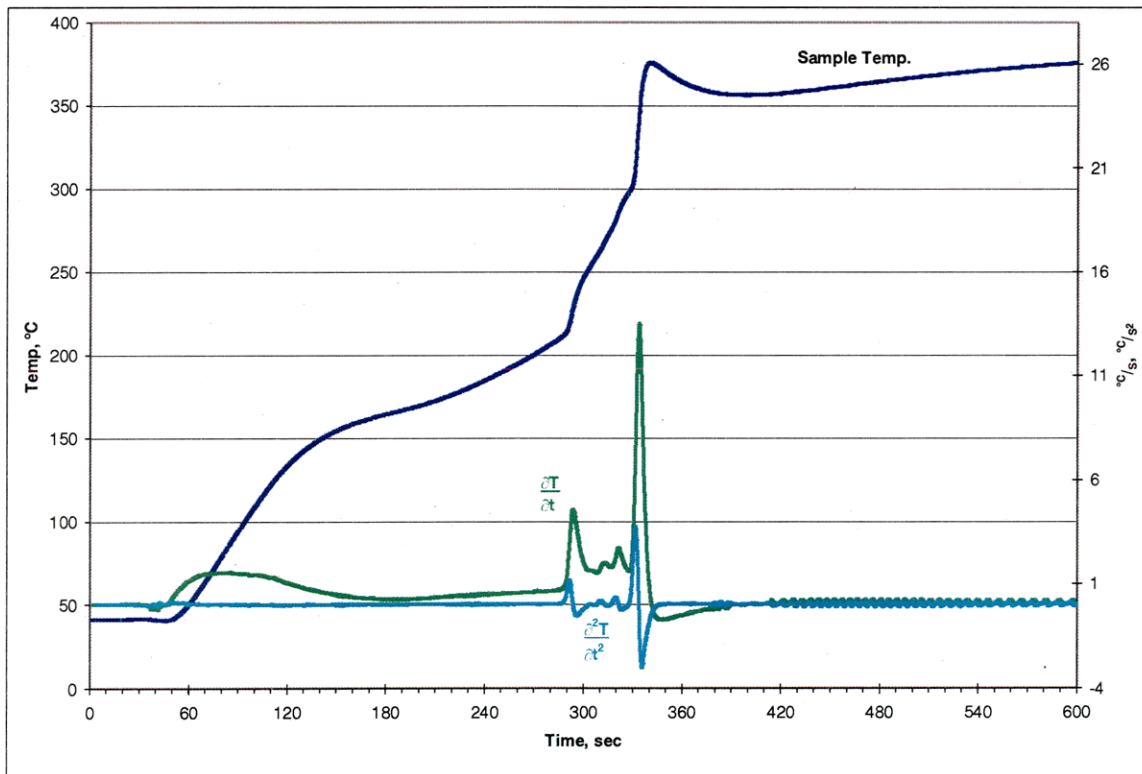


Figure 6.2 Sample Heat Curve of PVC + NaHCO₃

Figure 6.2 shows an example of the data recorded during experimentation. The initial decomposition of NaHCO₃ to Na₂CO₃ is evident from the decrease in the heating reate, beginning

at $T \sim 150^\circ\text{C}$. At $T \sim 216^\circ\text{C}$ evidence is seen of an exothermic reaction beginning to take place, as shown by both the first and second derivatives of the temperature curve. Even though this is below the published decomposition temperature of PVC, given the distribution of molecular weights present in a polymer, a temperature range for decomposition is expected. Once the temperature reaches 300°C evidence of another large exothermic reaction is seen.

What has proven surprising is the difference in the reactivity of the sodium compounds in relation to the entrapment of chloride. Thermodynamically, NaOH complexes with $\text{CO}_{2(g)}$ and NaHCO_3 decomposes to Na_2CO_3 before HCl is released from the organic at $T \sim 220^\circ\text{C}$. Yet when compared to Na_2CO_3 , adding NaHCO_3 to the PVC results in a five-fold increase in the entrapment of Cl^- while NaOH yields a 2-3-fold increase. This increased activity may be due to the surface activity of the newly generated Na_2CO_3 when compared to “out of the bottle” Na_2CO_3 .

6.2.2 PTFE behavior and Fluoride entrapment from mixed PVC, PTFE and PE

Following the results of the PVC evaluation of sequestering agents, NaHCO_3 was selected as the material of interest for further investigation due to its demonstrated efficiency for chlorine entrapment. Initial evaluation of PTFE with NaHCO_3 was conducted at 1:1 stoichiometric ratio over a temperature range of $500\text{--}600^\circ\text{C}$. Figure 6.3 represents the data generated from the first test of PTFE and NaHCO_3 at 550°C .

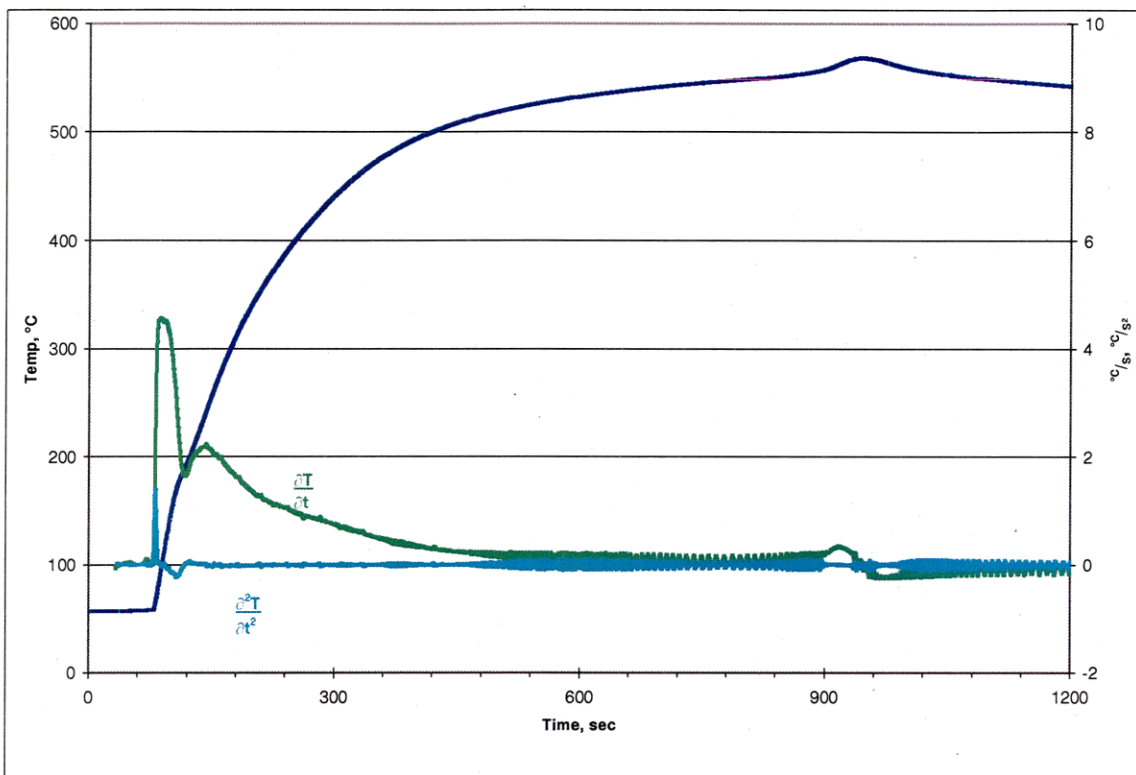
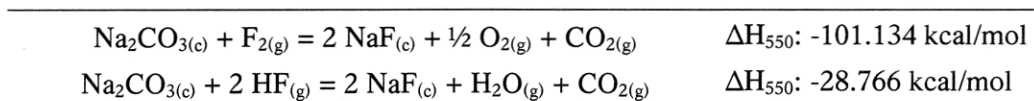


Figure 6.3 Teflon 1: 1.00 g PTFE, 3.36 g (1X) NaHCO₃, 1.0 slpm CO_{2(g)}, 550°C

The increase in temperature at $t \sim 500$ and the increase in the first derivative of this curve show an exothermic reaction taking place as the sample reaches $\sim 550^\circ\text{C}$. This is expected with the formation of NaF from either HF_(g) or F_{2(g)}—data from HSC 5.11:



During these initial tests, a sample of PTFE alone was also subjected to the tube furnace test at $T = 545\text{--}555^\circ\text{C}$. The temperature profile showed no anomalies (Appendix B, Figure B25), but the residue remaining in the sample boat maintained the look and feel of PTFE albeit with a loss of over 52% of its mass and no longer in the form of granules. Evaluation of the residue from test Teflon 1 via XRD (Figure 6.4) showed the existence of the expected NaF, but also gave indication of residual PTFE. A sample of the PTFE granules being used for experimentation was

analyzed via XRD (Appendix C, Figure C3) to provide a physical reference and support the calculated $-(C_2F_4)_n-$ reference #47-2217.

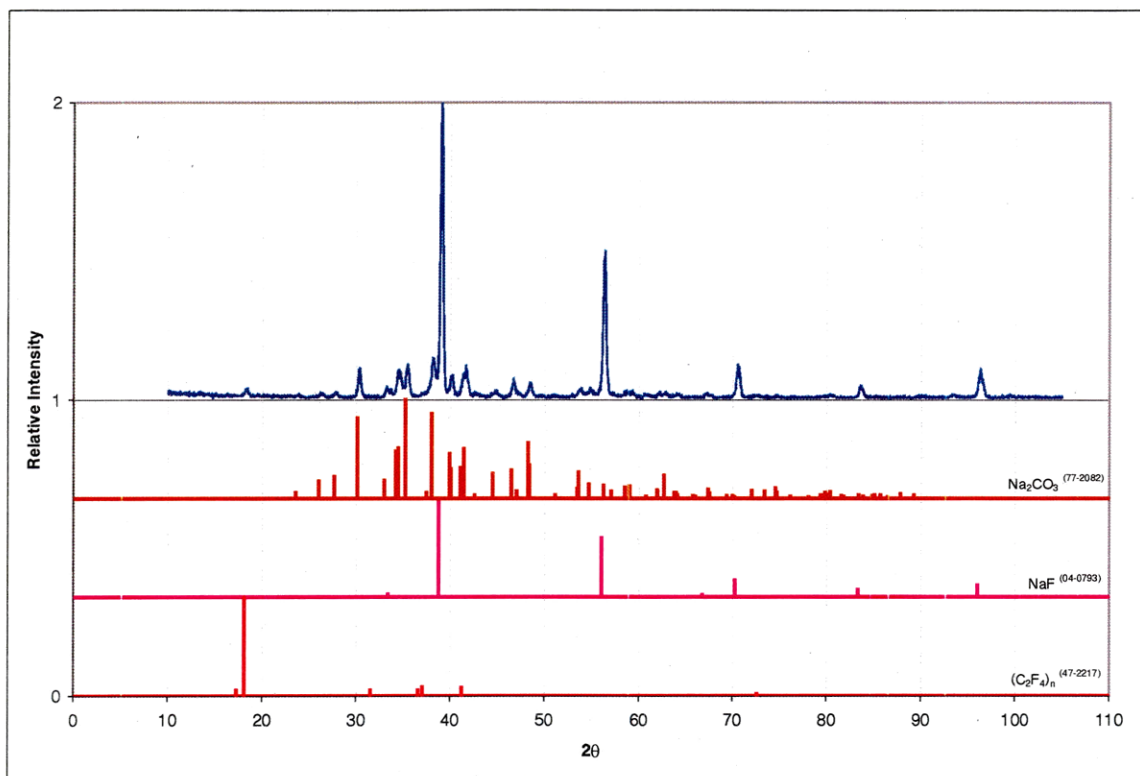


Figure 6.4 Teflon 1 XRD: 1.00 g PTFE, 3.36 g (1X) $NaHCO_3$, 1.0 slpm $CO_{2(g)}$, 545°C

Another experiment conducted at the slightly higher temperature of 550°C (Teflon 3 shown in Appendix B, Figure B29) produced a residue displaying a less defined, if barely discernible PTFE pattern via XRD (Appendix C, Figure C21) giving the indication that pure PTFE in the presence of sodium carbonate derived from $NaHCO_3$ will be decomposed at temperatures at or above 550°C. In comparison, the same experiment conducted at 555°C with Na_2CO_3 (Appendix B, Figure B28) produces a residue with a substantial PTFE signature (Figure 6.5). This result may be due to the previously seen increased reactivity of sodium carbonate derived from $NaHCO_3$ compared to Na_2CO_3 or, as seen with the behavior of PE in the presence of $MgCO_3$ and $MgCO_3 \cdot Mg(OH)_2 \cdot 3H_2O$, the effect of water or hydroxide radicals on the structure of the polymer.

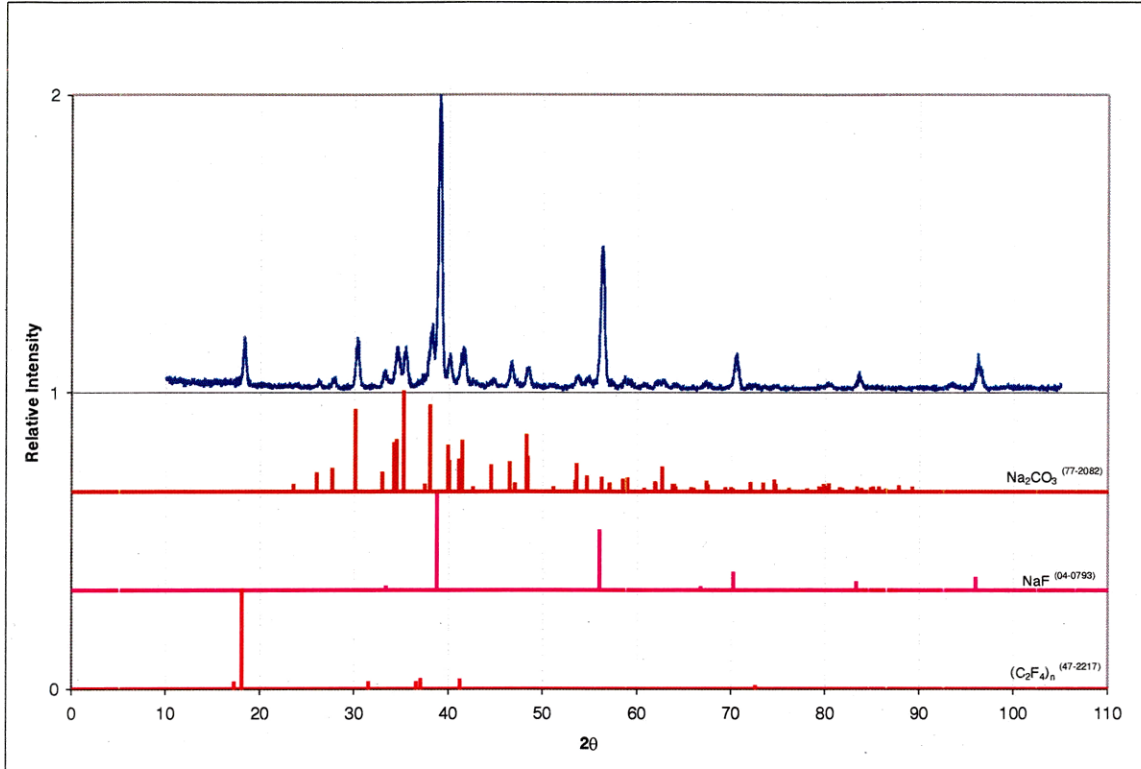


Figure 6.5 Teflon 2: 1.00 g PTFE, 2.12 g (1X) Na_2CO_3 , 1.0 slpm CO_2 , 555°C

Experiments conducted at 600°C (Teflon 5 shown in Appendix B, Figure B31) produced a much higher temperature spike during the formation of NaF. The higher and sharper temperature profile seen at experiments conducted at 600°C compared to 550°C leads one to surmise a more complete reaction of fluorine with the sodium carbonate present at ~600°C. XRD analysis of the residue from this test showed no trace PTFE pattern (see Appendix C, Figure C23). Scrubber solution samples were kept for fluorine determination employing a fluoride-specific electrode.

6.2.3 Mixed polymer (PVC, PTFE and PE) behavior and Halide entrapment

To more closely evaluate the complex nature of e-waste, a number of differing polymer mixture samples were assembled from pure sources. Samples of PTFE alone, PTFE with PE and mixtures of PVC, PTFE and PE were investigated. As the structure of PTFE is made of only carbon and fluorine ($-(C_2F_4)_n-$), the release of fluoride may be affected by the presence of PVC or PE. A source of hydrogen could alter the degradation path of the PTFE. Therefore, mixtures of PTFE:PVC:PE investigated are at 1:1:1 and 1:1:4 weight ratios—1:1:4 is the ratio that the organics are present in e-waste.

While the desire is to keep the process temperature as low as possible while maximizing the decomposition of organics present, the temperature of 600°C was selected for further investigation to ensure complete decomposition of PTFE. $NaHCO_3$ additions were increased to 1.5X stoichiometric ratio to maximize halide entrapment. Table 6.3 represents weight ratios of polymer mixtures investigated:

Table 6.3 Mixed Polymer Matrix

PTFE g	PVC g	PE g	$NaHCO_3$ Stoic. Ratio
1			1.5
1		1	
1	1	1	
1	1		
1		1	1.5
1	1	1	1.5
1	1		1.5
	1		1.5
	1	1	
	1	1	1.5
1		4	
1	1	4	
1		4	1.5
1	1	4	1.5
	1	4	
	1	4	1.5

Using a thermocouple in the sample material, data taken via data acquisition were able to show the behavior of the system with a high degree of detail. Figure 6.6 shows the data taken from a mixture of PVC:PTFE:PE at a 1:1:1 weight ratio. The first derivative of the temperature shows a decrease in the volatilization of the PVC in the temperature range of ~240-373°C. Another drop in the heating rate over the temperature range of ~460-540°C accounts for the volatilization of PE. The final drop in the heating rate at ~560°C corresponds to the volatilization of PTFE. The temperatures observed are above those for decomposition acquired from literature.

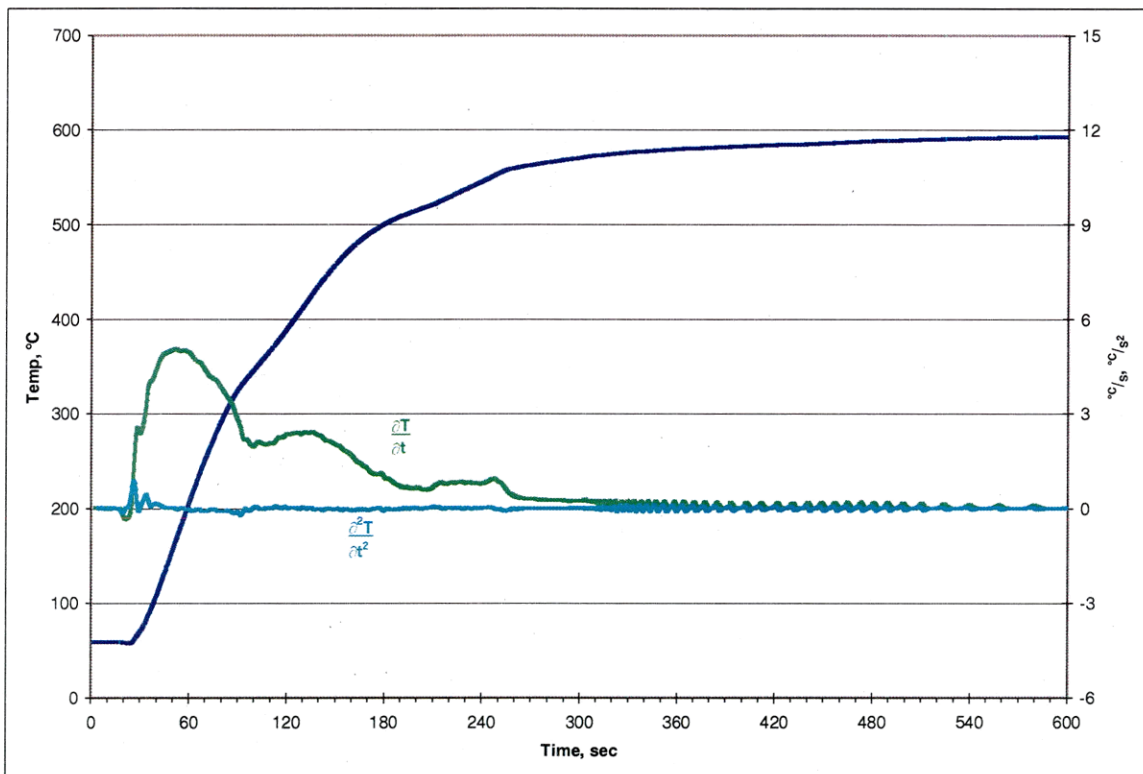


Figure 6.6: Teflon 17 Redo II: 0.5 g (PVC, PTFE, PE), 1.0 slpm CO₂

A prime example of the complex nature of the mixed polymer samples is experiment Teflon 21 shown in Figure 6.7. Experiment Teflon 21 represents a mixture of PVC:PTFE:PE of 1:1:1 with 1.5 times stoichiometric ratio NaHCO₃. During heating, a small drop in the heating rate occurs just below 100°C, indicating the volatilization of water (added for static control when needed). The decomposition of NaHCO₃ to Na₂CO₃ is seen at the expected temperature of

~170°C. The reaction of $\text{HCl}_{(g)}$ with the Na_2CO_3 (as seen in Figure 6.2) tends to be lost in the data, but the acceleration of heating in conjunction with the increasing heating rate (between 250°C and 350°C) can be seen as this reaction. The abrupt drop off of the heating rate seen at 350°C is the completion of any PVC/ Na_2CO_3 reaction. The dramatic spike in the temperature, correlating to the velocity and acceleration are indicative of the PTFE/ Na_2CO_3 reaction.

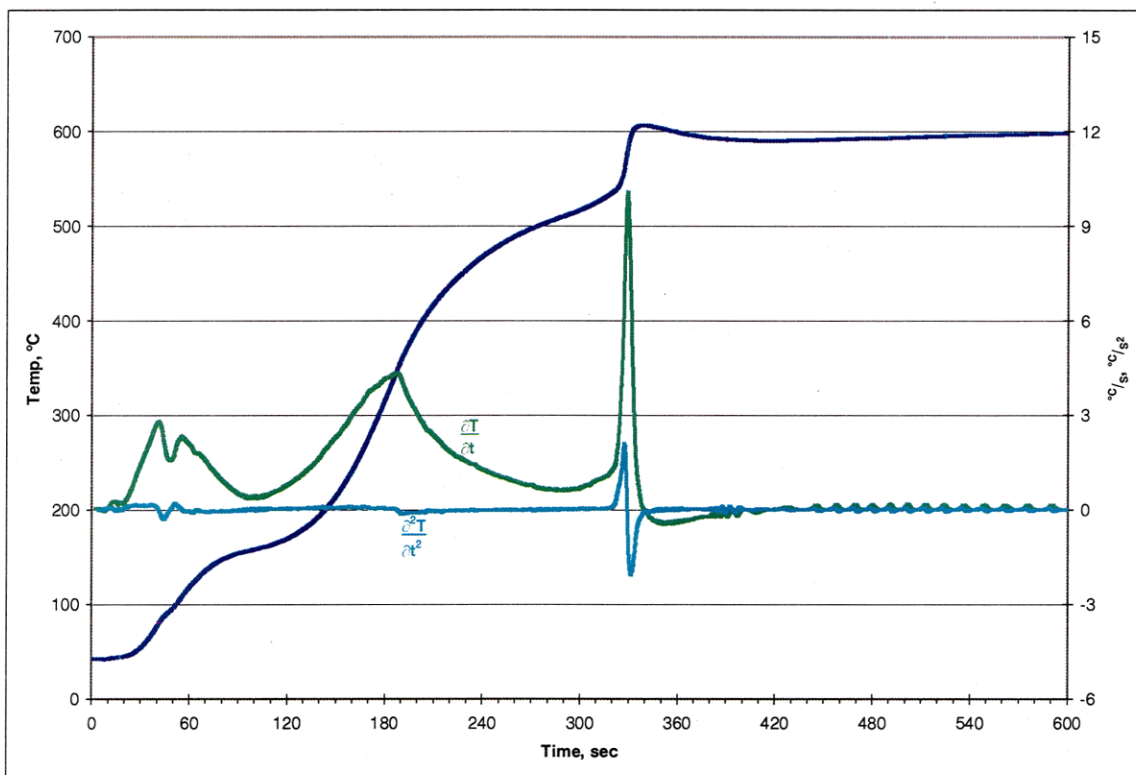


Figure 6.7: Teflon 21: 0.5 g (PVC, PTFE, PE), 3.5 g (1.5X) NaHCO_3 , 1.0 slpm $\text{CO}_{2(g)}$

6.2.4 Decomposition Temperature Depression in Polymer Mixtures

In reviewing the data generated from the mixed polymer tests, it was observed that the temperature at which halide-containing polymer began to react with Na_2CO_3 has a dependence on composition. For example, in evaluating the temperatures at which the reaction of PTFE with Na_2CO_3 begins, based on the increase in acceleration of the heating of the sample, it can be seen

that the temperature decreases as the mole fraction decreases (Figure 6.8). The temperature at which PVC begins to react follows a similar pattern. Based on the surveyed mixture of 1:1:4, the mole % for PVC and PTFE are 9.5% and 5.9% respectively. Calculating the relative mole % of PVC and PTFE with the inclusion of all organics shown as constituents in Table 2.1 (polypropylene, polyester, etc.) would yield 6.7% and 4.2% respectively.

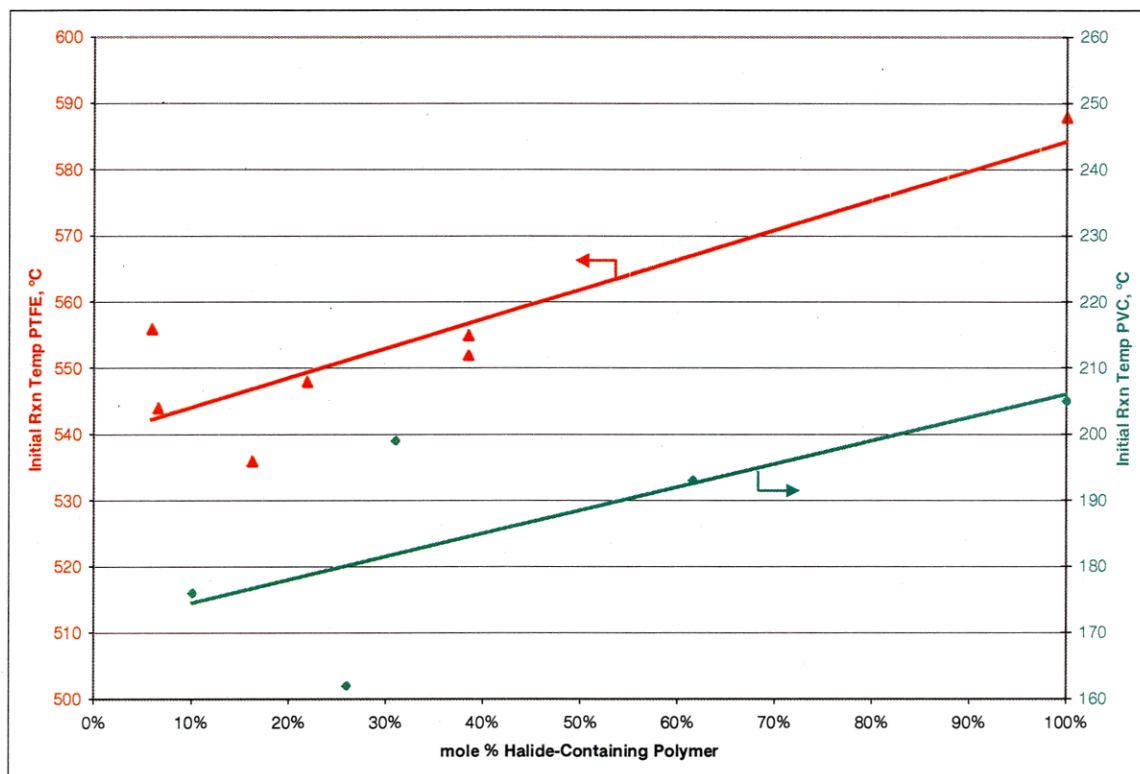


Figure 6.8 Halide Polymer Reaction Temperatures

Based on the observation of the reduction in the initial decomposition temperature of the halide containing polymers with decreased molar fraction, additional experiments were conducted at temperatures below 600°C to further explore the minimum temperature required for complete consumption of the PTFE. Extended retention time was also explored. A residue produced from the 1:1:4 PVC:PTFE:PE mixture at 550°C at 20 minutes total time (5 min. at temperature) showed no residual PTFE when evaluated with XRD (Appendix C, Figure C37). Operating at this lower temperature, required 450 sec. for initial PTFE/ Na_2CO_3 reaction, compared to 300 sec.

when operating at 600°C (Figure 6.7 above). With the decreased reaction temperature seen in the mixture, two additional experiments were conducted at a temperature of 500°C. The first experiment was held at temperature for five minutes (Appendix B Figure B59) and the second was at temperature for 20 minutes (Appendix B Figure B61). XRD patterns for both residues showed evidence of unreacted PTFE, in addition to NaF, NaCl and Na₂CO₃ (Appendix C, Figures C36 and C38).

6.2.5 Halide Sequestering Efficiency

The efficiency of halide sequestering was again measured by the amount of chlorine and fluorine remaining in the solid residue. This is determined through analysis of the scrubber solution and subtracting from the known amount of halide in the measured sample. Chlorine determination is made through silver nitrate titration. Fluorine determination is made with a fluoride-specific ion electrode. Values calculated for the experiments are shown in Table 6.4.

Table 6.4 Mixed Polymer Halide Sequestering

		PTFE	PVC	PE	NaHCO ₃	Temp	Cl in Residue		F in Residue	
		g	g	g	g	°C	%	+/- %	%	+/- %
1	Teflon 13	0.5			2.52	600			99.16	2.28
2	Teflon 16	0.5		0.5		600			98.76	2.37
3	Teflon 17	0.5	0.5	0.5		600	0.84	6.82	96.68	2.84
4	Teflon 18	0.5	0.5			600	-9.08	6.82	92.25	3.83
5	Teflon 20	0.5		0.5	2.52	600			99.37	2.23
6	Teflon 21	0.5	0.5	0.5	3.53	600	92.21	6.80	99.69	2.17
7	Teflon 22	0.5	0.5		3.53	600	86.54	6.80	99.26	2.26
8	Teflon 14		0.5		1.01	600	90.79	6.80		
9	Teflon 15		0.5	0.5		600	0.84	6.82		
10	Teflon 19		0.5	0.5	1.01	600	69.54	6.81		
11	Teflon 24	0.25		1		600			98.96	1.16
12	Teflon 25	0.25	0.25	1		600	32.00	13.63	98.30	1.24
13	Teflon 27	0.25		1	1.26	600			99.13	1.14
14	Teflon 28	0.25	0.25	1	1.76	600	74.50	13.61	99.00	1.16
15	Teflon 23		0.25	1		600	87.25	13.60		
16	Teflon 26		0.25	1	0.50	600	70.25	13.61		

In general, the chlorine sequestering for the 1:1:1 mixtures of PVC:PTFE:PE with 1.5X stoichiometry met or exceeded the values obtained with PVC alone (86-92% +/- 6.80%). Mixtures of 1:1:4 PVC:PTFE:PE retained less chlorine in the solid residue (70-74% +/- 13.60%). The increased error is due to the smaller samples used for halide-containing polymers in the 1:1:4 mixtures. The decreased halide sequestering can be attributed to the increased volume of halide-free polymer (PE) reducing the contact between the carbonate present and the halogenated polymer of interest. Measurement of fluorine sequestered within the solid residue proved to be problematic. The reactivity of $\text{HF}_{(g)}$ or $\text{F}_{2(g)}$ produced from the polymer sample was evidenced by the pitting within the experimental system.

6.3 Atmosphere Effects

All experiments to this point have been conducted with a $\text{CO}_{2(g)}$ atmosphere. In order to gauge any possible effect of changing atmosphere, a series of experiments was designed based on the 1:1:1 PVC:PTFE:PE polymer mixture with 1.5X NaHCO_3 . This mixture was selected as it contains all of the materials being evaluated, but with higher relative levels of halide for detection. All tests were conducted at the standard 1 slpm flow rate. Each test was run twice; once to obtain a scrubbing solution for halide determination and a second time to obtain NOVA gas analysis. As before, chloride titration was accomplished via silver nitrate titration (Table 6.5). An attempt was made to obtain fluoride concentration with the ion specific electrode with the same level of success as seen before. Overall, the atmosphere had little effect on the solid residue produced. The five atmospheres investigated, with residue and chlorine data, were:

Table 6.5 Atmospheres Investigated

Test #	Atmosphere	Test Name	Residue, %	Cl in residue, %	+/-, %
1	100% CO _{2(g)}	NOVA 2, Comp 2	44.99	92.21	6.80
2	50:50 CO _(g) : CO _{2(g)}	NOVA 4, Comp 3	44.07	91.50	6.80
3	100% CO _(g)	NOVA 5, Comp 4	44.31	91.50	6.80
4	50:50 N _{2(g)} : CO _{2(g)}	NOVA 1, Comp 2	44.37	91.50	6.80
5	100% N _{2(g)}	NOVA 3, Comp 1	44.38	95.75	6.80

Temperature profiles and NOVA gas analysis for the tests listed above can be found in Appendix B, Figures B62-B75. In reviewing the data on gasses produced (summarized in Table 6.6), a number of observations can be made:

1. In samples where CO_{2(g)} was not a constituent and finite changes in CO_{2(g)} could be measured, two discharges of CO_{2(g)} occurred, corresponding to the decomposition of a halide-containing polymer (PVC and PTFE).
2. In samples where CO_(g) was not a constituent and finite changes in CO_(g) could be measured and having 50 or 100% CO_{2(g)}, finite amounts of CO_(g) were detected, corresponding to the decomposition of PTFE.
3. Increasing amounts of CO_(g) increases CH_{4(g)} production.

The primary effect seen in gas products generated in relation to atmosphere was an increase in CH_{4(g)} production with an increase in CO_(g) in the system's atmosphere.

Table 6.6 Gas Production vs, Atmosphere

Test #	Atmosphere	CH _{4(g)} peak, %	CO _(g) Peak, %	CO _{2(g)} Peak, %
1	100% CO _{2(g)}	2.5	1.25	
2	50:50 CO _(g) : CO _{2(g)}	5.6		
3	100% CO _(g)	26.0		18, 13
4	50:50 N _{2(g)} : CO _{2(g)}	4.5	1.25	
5	100% N _{2(g)}	4.0		17, 10

6.4 Sequestering Agents Study Results

The application of NaHCO_3 to a mixed polymer system demonstrated its ability to sequester the halides present. Measurement of chlorine retained in residue treated with NaHCO_3 indicated high levels of sequestering as NaCl . While direct measurement of the fluorine present had some difficulty, XRD analysis of the solid residues produced indicated substantial amounts of both NaCl and NaF .

While total sequestering efficiency approached, but did not meet 100% for chlorine in the tube furnace experiments, the aggressive experimental procedure was designed to evaluate the materials under discouraging conditions, resulting in a more robust processing option. Applying the carbonate of choice (NaHCO_3) to a rotary kiln reactor with extended retention time would allow for multiple contact between carbonate material and gasses and fumes generated that may not have had interaction during initial volatilization. Operational temperatures required for the removal of organic material was shown to be lower for the mixed polymer samples than those seen in pure samples but within the range of 550-600°C.

CHAPTER 7

DTA-MS EVALUATION

With an understanding of the system behavior in relation to polymer decomposition and halide sequestering, a study was undertaken using Thermogravimetric (TG) Analysis/Differential Thermal Analysis (DTA) – Mass Spectrometry (MS) in a $\text{CO}_{2(g)}$ environment to further outline the system behavior. This work was conducted with the cooperation of researchers with the Norwegian University of Science and Technology (NTNU). Samples were prepared at Colorado School of Mines (CSM) and placed in glass vials for shipment to NTNU. Glass vials were used to reduce or eliminate any loss of sample within the vessel, as would be expected in a plastic zip-top style sample bag. Nineteen samples were prepared from PVC, PTFE, PE, NaHCO_3 and Na_2CO_3 , with pure components and mixtures being evaluated. An initial list of compounds for Mass Spectrometry was compiled [(MW) molecule]: (15) $\text{CH}_{4(g)}$, (18) $\text{H}_2\text{O}_{(g)}$, (28) $\text{C}_2\text{H}_{4(g)}$, (36) $\text{HCl}_{(g)}$, (68) furan/dioxin, (78) benzene- $\text{C}_6\text{H}_{6(g)}$, and (81) $\text{TFE}_{(g)}$. After the first batch of samples was evaluated, (20) $\text{HF}_{(g)}$ was added to the list of compounds to be detected. A list of the initial samples subjected to TG/DTA–MS evaluation is shown in Table 7.1 Data obtained from the MS was without calibration for quantitative determination. The information was applied in qualitative determination of reactions occurring in the system. The data did allow for a correlation and confirmation of the data produced from the experiments conducted at CSM using the tube furnace equipment.

TG/DTA data from all samples containing NaHCO_3 showed the endothermic decomposition of NaHCO_3 to Na_2CO_3 beginning at $\sim 120^\circ\text{C}$. A prime example of NaHCO_3 decomposition can be seen in Figures D2a and D2b. The decomposition of PVC, resulting in a mass loss, was shown to begin at $\sim 218^\circ\text{C}$ with the exothermic formation of NaCl beginning at $\sim 250^\circ\text{C}$ —best seen in Figures D4a and D4b. PVC containing samples also demonstrated another mass-loss (endothermic) between $375\text{--}520^\circ\text{C}$. This is attributed to a chlorine-free polymer residue

decomposing at this temperature range—similar to PE. A mass loss attributed to the decomposition of PE tends to begin at ~330°C with substantial change in weight at ~400°C. A mass loss attributed to the decomposition of PTFE begins to show at ~490-500°C with the exothermic formation of NaF showing at ~490°C. Both the PE and PTFE effects are best seen in Figures D10a and D10b. All PTFE-containing samples showed a distinct endotherm representing the melting of PTFE at ~340°C, correlating with the published 335°C melting temperature.

Table 7.1 Mixed Polymer/Carbonate Samples - TG/DTA-MS

	Mix	Na ₂ CO ₃	NaHCO ₃	PVC	PTFE	PE
		g	g	g	g	g
1	PTFE	0.01				
2	NaHCO ₃		0.0150			
3	Na ₂ CO ₃	0.0150				
4	NaHCO ₃ + PVC		0.0040	0.003		
5	Na ₂ CO ₃ + PVC	0.0025		0.003		
6	NaHCO ₃ + PTFE		0.0101		0.003	
7	Na ₂ CO ₃ + PTFE	0.0064			0.003	
8	NaHCO ₃ + PVC + PE		0.0040	0.003		0.006
9	Na ₂ CO ₃ + PVC + PE	0.0025		0.003		0.006
10	NaHCO ₃ + PTFE + PE		0.0101		0.003	0.006
11	Na ₂ CO ₃ + PTFE + PE	0.0064			0.003	0.006
12	NaHCO ₃ + PVC + PTFE		0.0141	0.003	0.003	
13	Na ₂ CO ₃ + PVC + PTFE	0.0089		0.003	0.003	
14	PVC			0.01		
15	PVC + PTFE			0.01	0.01	
16	PVC +PE			0.005		0.01
17	PTFE +PE				0.005	0.01
18	PVC +PTFE +PE			0.005	0.005	0.01
19	PE					0.01

Qualitative information regarding the evolution of short-chain or “cracked” organics taken from the MS data provide for an increased understanding of the system’s behavior.

- Samples containing PVC produced HCl and benzene concurrent with the primary decomposition of PVC and exothermic formation of NaCl
- Samples containing PTFE produced TFE during decomposition
- Samples containing PVC and PE produced both $\text{CH}_{4(g)}$ and $\text{C}_2\text{H}_{4(g)}$ from the decomposition of the polymers. PVC generates these compounds from the decomposition of both primary polymer and secondary Cl free residue
- The majority of the samples without NaHCO_3 (including those with no sodium compounds at all) showed the production of $\text{H}_2\text{O}_{(g)}$, demonstrating the reactivity of $\text{CO}_{2(g)}$ with contained polymers

As the processing path of the TG/DTA is similar to the tube furnace system, direct correlation of the data between the two systems is possible. The generation of TFE during the decomposition of PTFE is seen as one of the causes for the inability to measure fluorine in NaOH scrubbing solutions. The presence of molecules such as TFE, C_6H_6 and $\text{C}_2\text{H}_{4(g)}$ again show the need for prolonged residence time with gas/solid interaction to allow for the thorough decomposition of the organic material and capture of the contained halides.

CHAPTER 8

PROPOSED PROCESS

8.1 E-Waste Processing

Having obtained an understanding of the primary polymers in the e-waste system, based on relative stability (PE) and halogen-containing (PTFE and PVC), a number of small and large-batch e-waste experiments were conducted. Two experiments (with and without NaHCO_3) were designed for the system used for sequestering agent evaluation (tube furnace). Data from these experiments would be directly comparable to other data generated from that equipment. Two tests were then designed for application to the rotary kiln employing a continuous feed system to simulate a continuous operation. For all four tests, a 0.8 kg sample of e-waste was compiled and cut to $-0.25''$. This size reduction allowed for the feeding of material into the rotary kiln via an auger or screw conveyor as well as provided a 150 g sample via standard riffle splitting operation. It is acknowledged that the sample may not be representative to a high degree of certainty as would be expected in standard mineral processing operations. This is due primarily to the physical constraints of the experimental system and the bulk density of e-waste. The calculated variance of a 150 g sample based on organics fraction is on the order of 6%, while a 6 g sample approaches 30% variance.

The sample of e-waste was assembled to reflect what would be expected of a scrap or obsolete computer system complete with audio, visual and network capabilities. A picture of the material is shown in Figure 8.1 The sample was comprised of: Pentium-based ATX-Form Factor Motherboard, circa 1998; 2 X 16MB SIMM Memory modules; 1 PCI 8MB Video Card; 1 PCI SoundBlaster brand Audio Card and 1 PCI Ethernet Network Card.

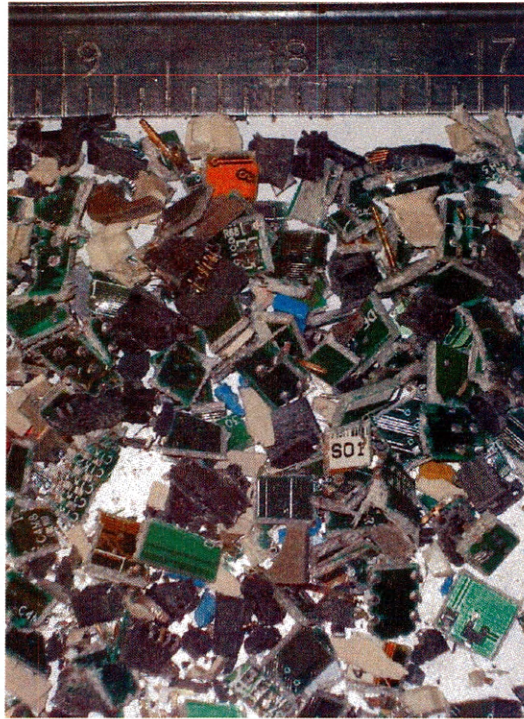


Figure 8.1 E-Waste Sample

After manual size reduction, the sample was split into five 150 g samples for use with the rotary kiln with 50 g remaining for use with the tube furnace. 6.3 g samples (limited by sample boat volume) were taken from this 50 g lot for tube furnace work.

8.1.1 Tube Furnace E-Waste Experiments

The two tests conducted using the tube furnace system employed the NOVA gas analyzer to obtain information on the gasses produced. Atmosphere was set at 1 slpm $\text{CO}_{2(g)}$ reflecting the majority of the work conducted previously. Test 1 was comprised of 6.3 g e-waste, test 2 was comprised of a mixture of 6.3 g e-waste and 1.26 g NaHCO_3 . Experimental procedure was the same as employed previously.

The temperature curve generated from the sample of e-waste (Figure 8.2) reflects curves obtained for polymer samples. The decrease in the first derivative at time ~100 sec. is indicative of melting or vaporization as seen in earlier experiments.

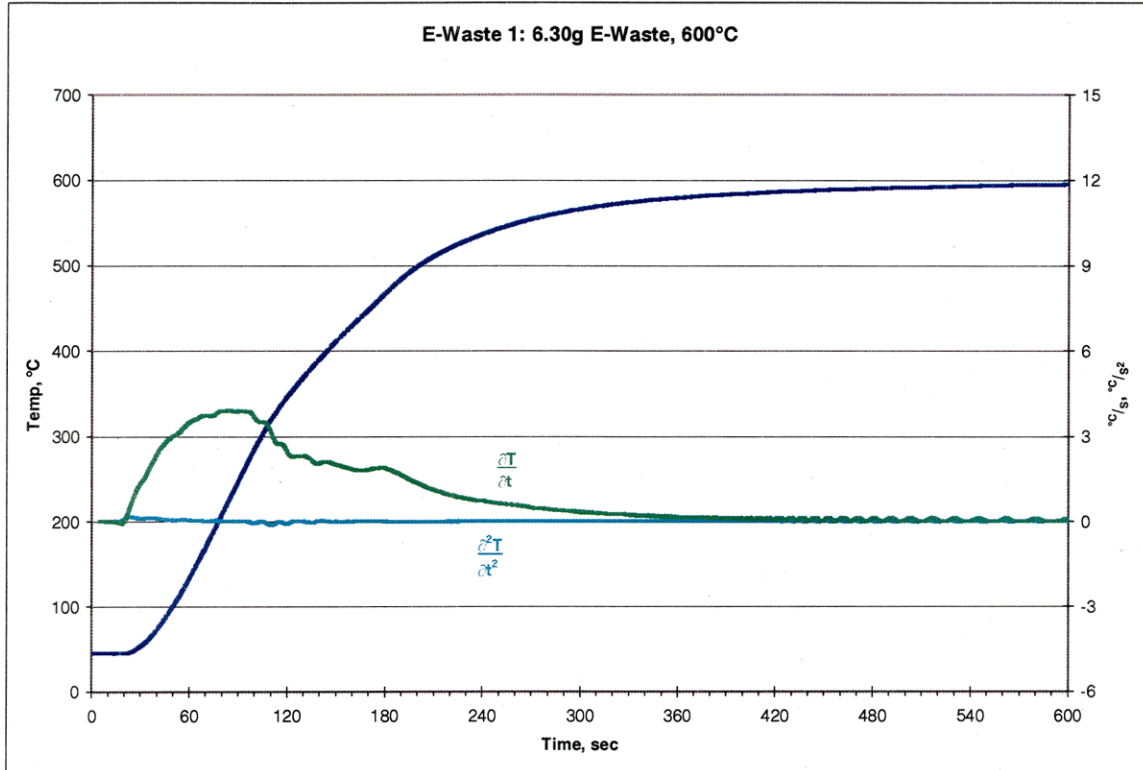


Figure 8.2 E-Waste Temperature Data

Gas analysis data (Figure 8.3) shows the generation of gasses after ~120 sec. when the sample reaches 300°C. Maximum gas levels attained are: 3.5% CO_(g), 2.4% CH_{4(g)} and 1.4% H_{2(g)}. Integrating the data for 1.0 slpm flow gives total volumes of 45.3 cm³ CO_(g), 30.1 cm³ CH_{4(g)} and 11.6 cm³ H_{2(g)}. The flow of 1.0 slpm represents the flow into the system. Without accurate data for flow out of the system, this integration will contain some error. Data obtained from the larger-scale rotary kiln experiments will provide more accurate data on total gas produced. Solid residue of 4.46 g shows a loss of 29.22% of initial mass, correlating well with the general composition of e-waste shown previously indicating a 30% organic component.

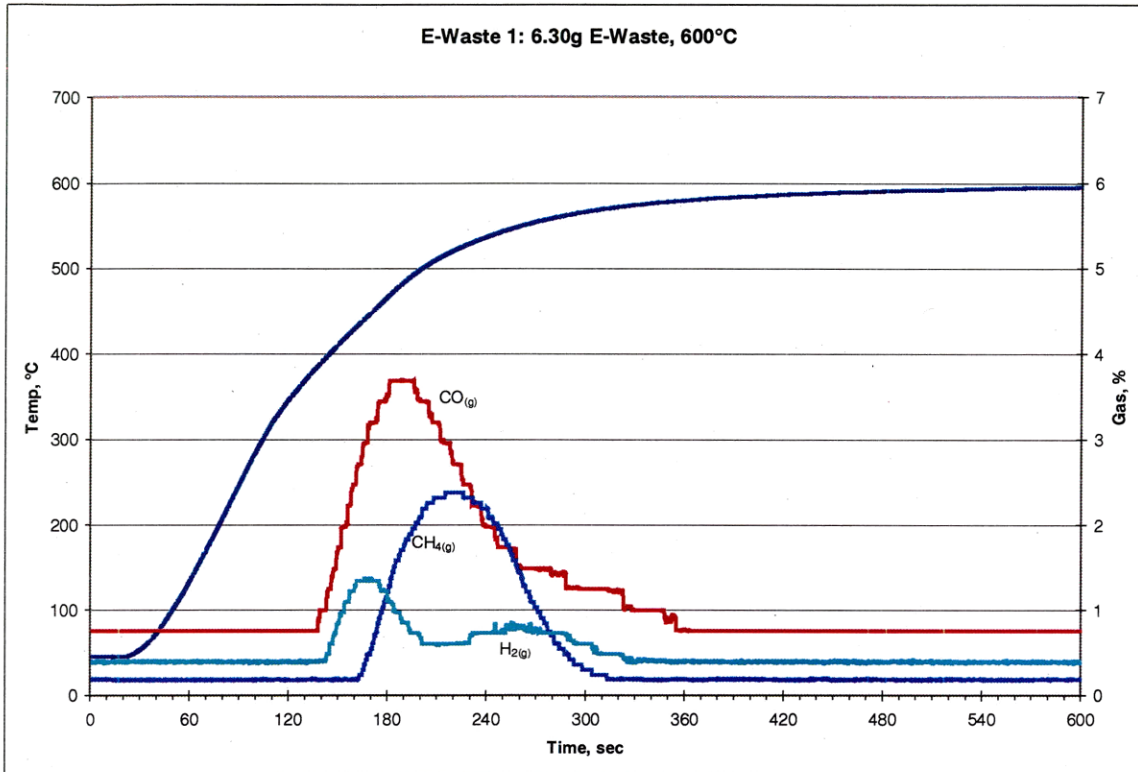


Figure 8.3 Gas Analysis, 6.30 g E-Waste

The temperature curve generated from the sample of e-waste treated with the addition of 20% by weight NaHCO_3 (Figure 8.4) reflects curves previously obtained for mixed polymer/ NaHCO_3 samples. Most notable is the similarity between these data and that obtained for experiment Teflon 19 (Appendix B, Figures B46 and B47). Teflon 19 was a sample of PVE and PE treated with NaHCO_3 . With the complex composition of the bulk e-waste sample, the fluctuations in the heating rate over the time range of 50-90 sec. can be attributed to the melting and vaporization of various polymers (endothermic) and the formation of sodium-halide salts (exothermic).

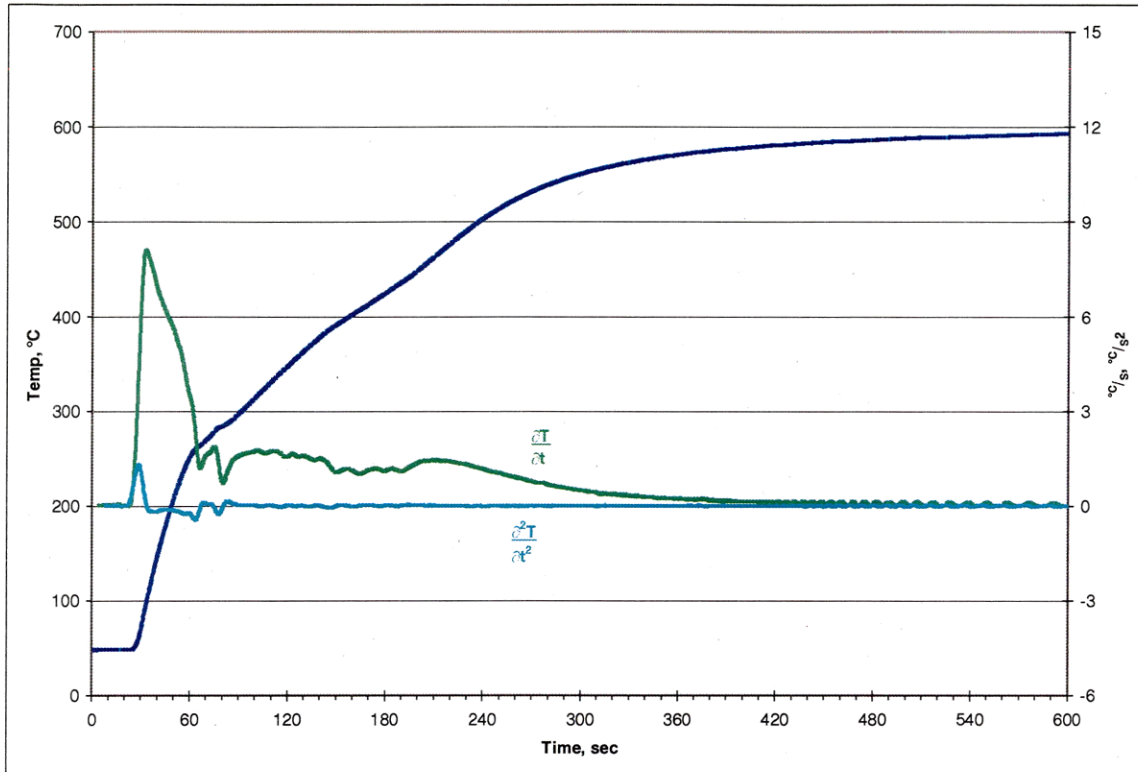


Figure 8.4 6.30 g E-Waste, 1.26 g NaHCO₃

Gas analysis data of the e-waste with NaHCO₃ (Figure 8.5) show the generation of gasses after ~160 sec.—some 40 sec. later than seen in the experiment without NaHCO₃. This can be caused from the slower heating rate seen by the bulk sample due to the endothermic decomposition of NaHCO₃. More notably, the maximum gas levels attained in the sample with NaHCO₃ are: 3.2% CO_(g), 3.2% CH_{4(g)} and 0.6% H_{2(g)}. This amounts to a 0.3 point (8.5%) decrease in CO_(g), a 0.8 point (30.8%) increase in CH_{4(g)} and a 0.8 point (57.1%) decrease in H_{2(g)}. Integrating the data for 1.0 slpm gives total volumes of 45.6 cm³ CO_(g) (0.7% increase), 43.5 cm³ CH_{4(g)} (44.5% increase) and 1.4 cm³ H_{2(g)} (87.9% decrease), respectively. Solid residue accounted for 78.95% of the initial value after accounting for residual Na₂CO₃ in the sample. The residue was 8% higher than that seen in material processed without NaHCO₃. This increase in residue mass is accounted for by the sodium-halide salts remaining in the solid residue.

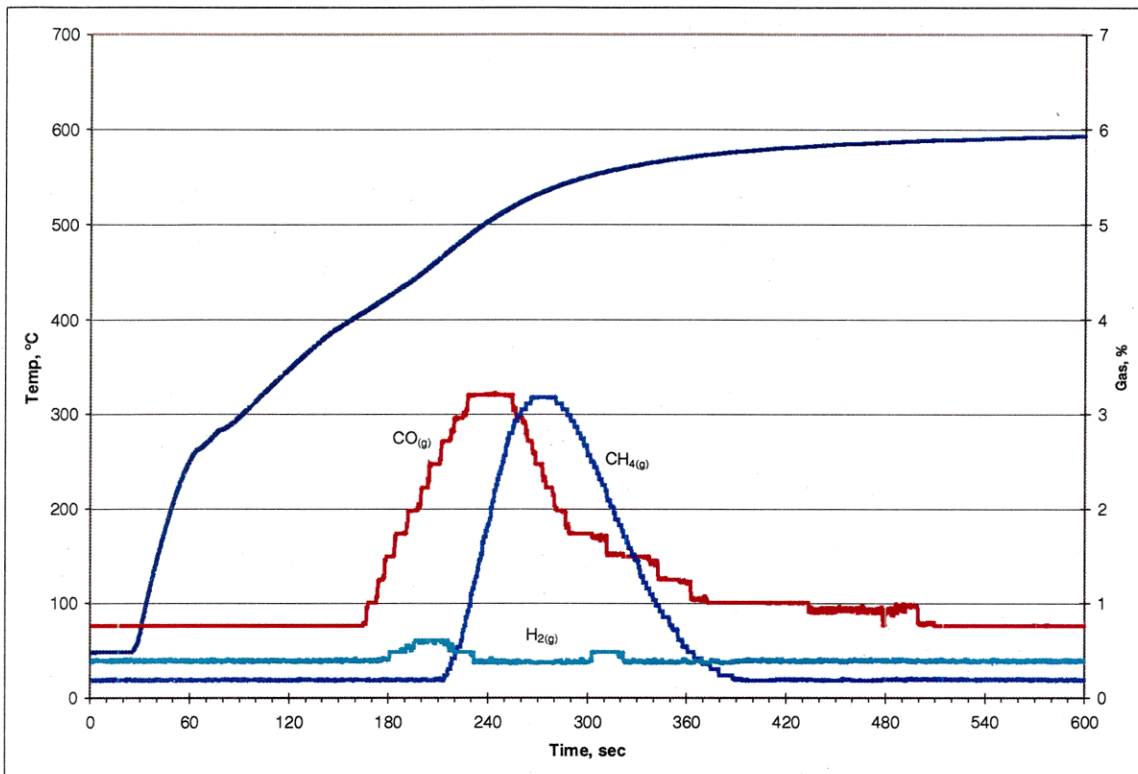


Figure 8.5 Gas Analysis, 6.30 g E-Waste, 1.26 g NaHCO₃

Comparing the gasses produced from both samples (summarized in Table 8.1), it can be seen that the sample processed with NaHCO₃ produced an offgas with higher carbon content—CH_{4(g)}. The subsequent calorific value of the gas streams (per kg of e-waste at 600°C) are: -67.3 kcal for Test 1 (E-Waste) and -81.4 kcal for Test 2 (E-Waste + NaHCO₃)—a 21% increase.

Table 8.1 Comparable Gas Products-E-Waste Tube Furnace

	CO _(g) , cm ³	CH _{4(g)} , cm ³	H _{2(g)} , cm ³
Test 1, E-Waste	45.3	30.1	11.6
Test 2, E-Waste + NaHCO ₃	45.6	43.5	1.4

XRD analyses for both samples are shown in Figure 8.6. The pattern for the sample processed without carbonate addition shows a primary amorphous pattern with some very minor peaks with loose correlation to SiO₂, BaTiO₃ and other oxides. More importantly when comparing the two

sample's XRD patterns, one can see a strong set of peaks for NaBr among the residual Na_2CO_3 peaks in the sample of e-waste treated with NaHCO_3 . As bromine is used in many different polymers as a flame retardant, where chlorine and fluorine are constituents of specific types of polymer (PVC and PTFE, respectively), it is no surprise that NaBr is more readily seen. As shown previously, NaBr is more stable than the two other sodium-halide salts. The formation of NaCl and NaF are dependent on the presence of PVC and PTFE, respectively. The formation of NaBr is dependent only on the presence of a polymer doped with a brominated flame retardant. Also, any NaF or NaCl that may have formed may be of too low of a concentration to be seen via XRD.

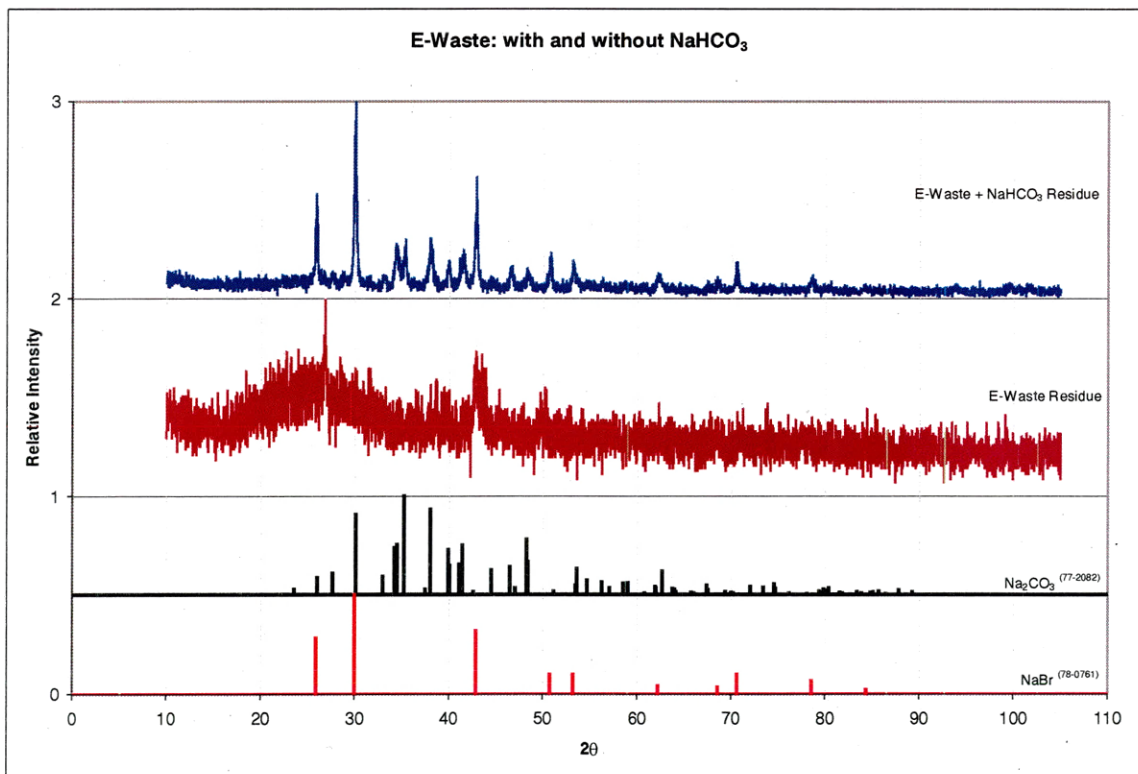


Figure 8.6 XRD Analysis of E-Waste with and without NaHCO_3

8.1.2 Rotary Kiln E-Waste Experiments

To simulate a continuous operation, the 150 g samples were fed into the rotary kiln system described previously at a feed rate of 1.5 g/min after the kiln had been heated to 600°C. The solid sample was fed into the kiln with a gas flow of 0.10 slpm N_{2(g)}. The gas flow was designed to hinder any clogging of the screw feeder and ensure some minimal flow through the kiln. With a minimum flow of 0.10 slpm, a kiln volume of 4.1 liters and an operating temperature of 600°C, the maximum residence time was calculated as 14 min. Upon evolution of the gas from the kiln, an additional 0.90 slpm was introduced to the stream, transporting the gas products through condenser/filtration and on to the NOVA gas analyzer. The 1.0 slpm N_{2(g)} was also needed to dilute kiln production gas to within the NOVA gas analyzer's range (0-25% CH_{4(g)}, 0-50% H_{2(g)}). Experimental procedure for these tests was the same as described previously in Chapter 5.1 with three slight alterations:

1. Sample was charged into the screw conveyor hopper (rather than the kiln)
2. Sample feed commenced with gas flow through the system once the kiln has come to desired temperature (one hour).
3. Resin module located on exhaust stream in place of scrubber for dioxin/furan analysis via EPA Method 23 analysis conducted by an outside lab.

8.1.2.1 Rotary Kiln E-Waste

The first experiment (Final 4) was conducted on 150 g sample of raw e-waste. Due to a problem with heating of the screw conveyor, sample feeding was interrupted after 50 min. resulting in processing of only a small portion of the 150 g sample. After disassembly and a correction of the heating issue, the processed portion of the sample was returned to the kiln with the remaining unprocessed material deposited into the screw feeder. A second test (Final 4B) was then conducted and the data were combined with that obtained from the first. The first partial test is shown in Figure 8.7 with the second part shown in Figure 8.8.

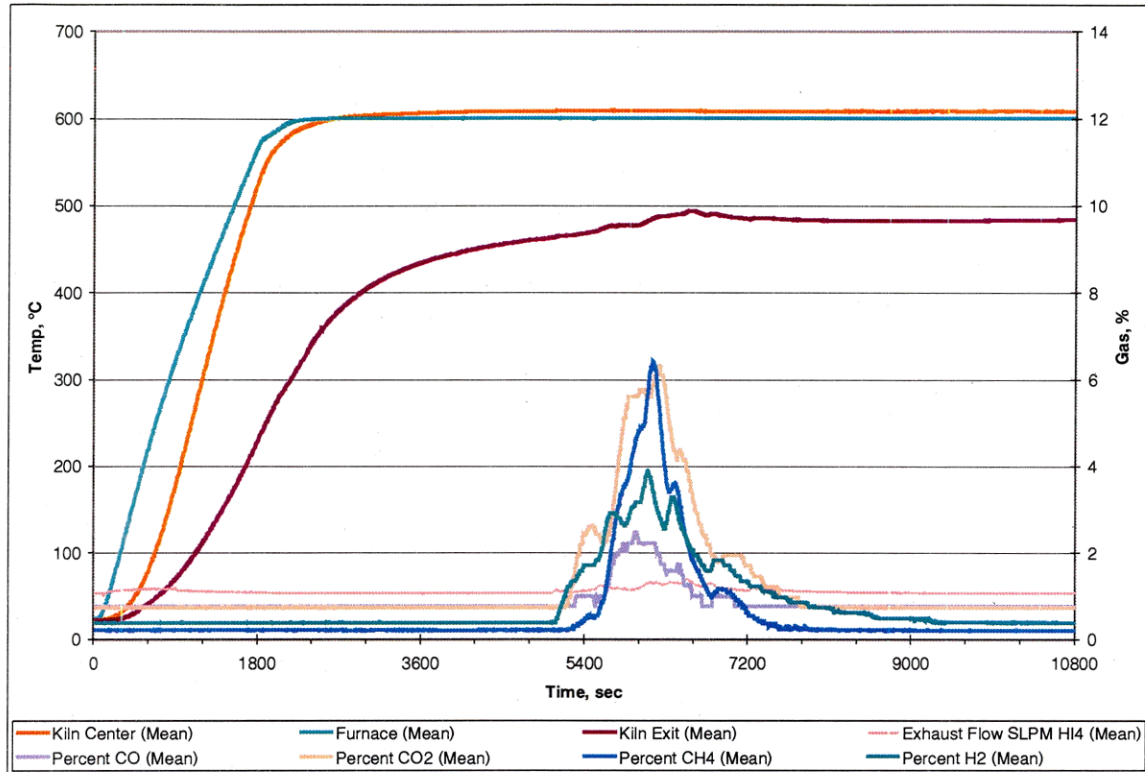


Figure 8.7 Continuous Feed Rotary Kiln: E-Waste (Final 4 Part 1)

Using a $N_{2(g)}$ atmosphere, $CO_{2(g)}$ produced from the e-waste can be measured in addition to the other gasses measured in the tube furnace tests. Knowing the increase of flow out of the system, measured as a dry gas, against the flow of dilution gas into the system allows for the calculation of gas production for the four gasses measured (Table 8.2.)

Table 8.2 Comparable Gas Products: E-Waste Rotary Kiln

	$CO_{(g)}$, liter	$CO_{2(g)}$, liter	$CH_{4(g)}$, liter	$H_{2(g)}$, liter
Test 4a, E-Waste	0.36	0.82	0.57	0.54
Test 4b, E-Waste	0.80	1.49	0.98	1.31
Test 4 Total	1.16	2.31	1.55	1.85

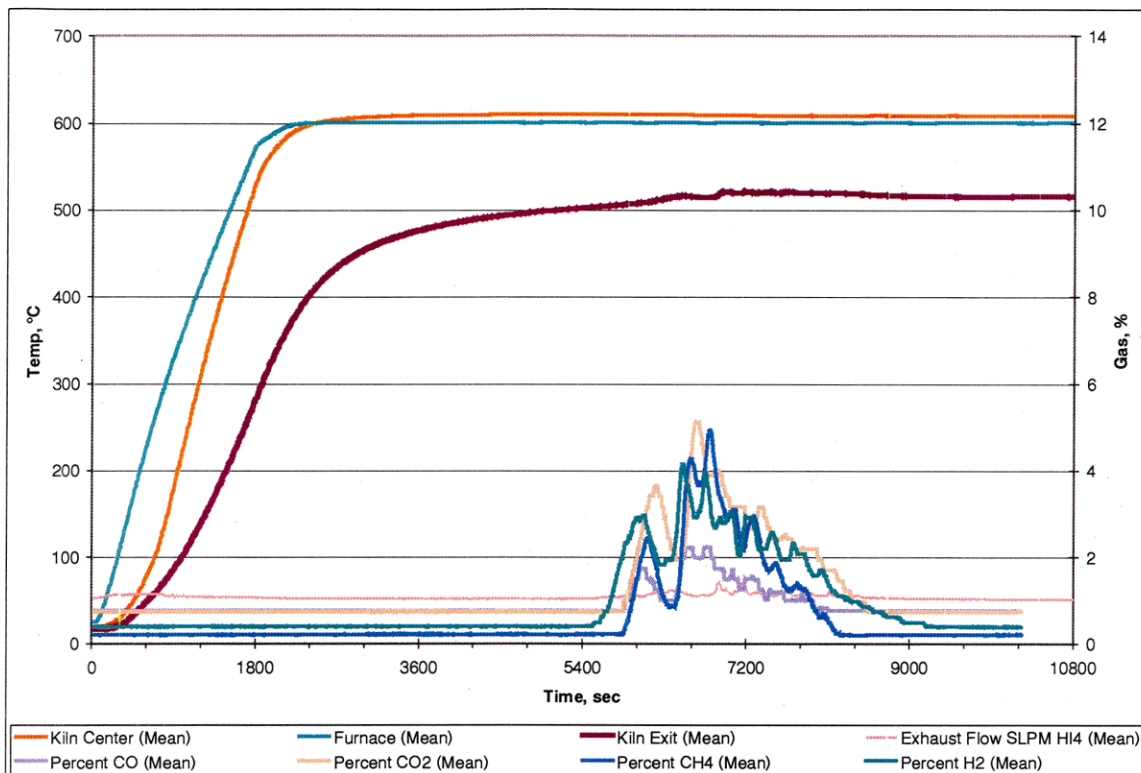


Figure 8.8 Continuous Feed Rotary Kiln: E-Waste (Final 4 Part 2)

Products generated from the 150 g of e-waste amounted to 102.65 g ashed waste, 12.37 g distillate and 7.27 g gas for a total of 122.29 g (27.71 g deficit). $H_2O_{(g)}$ generated from the reaction of $CO_{2(g)}$ with polymers, as seen in the Mass Spectroscopy work, is not included. Water vapor was removed from the gas stream via desiccant columns prior to gas analysis or flow measurement. Without a measurement for water, the mass balance is 81.53%

8.1.2.2 Rotary Kiln E-Waste + $NaHCO_3$

Processing with $NaHCO_3$ (Experiment Final 5) was accomplished with the same procedure used for Final 4, with the addition of 30 g $NaHCO_3$ to the 150 g e-waste sample. In this manner, carbonate would be introduced to the kiln along with the e-waste material. A fresh resin module was located on the exhaust stream in place of the scrubber for dioxin/furan analysis.

Data generated from the processing of e-waste treated with NaHCO_3 (Final 5) is shown in Figure 8.9. The volume of gas produced from this test is calculated in the same manner as before (Table 8.3). The first difference noticed in the gasses produced is the high level of $\text{CO}_{2(g)}$. This is due to the decomposition of NaHCO_3 to Na_2CO_3 , evolving $\text{CO}_{2(g)}$ and $\text{H}_2\text{O}_{(g)}$. It also is noticed that the level of $\text{CH}_{4(g)}$ detected is much higher than the level for $\text{H}_{2(g)}$, compared to the data generated without NaHCO_3 where the level of $\text{CH}_{4(g)}$ detected remained close to the level of $\text{H}_{2(g)}$. While the disruption in the previous test makes direct comparison less exact, viewed in conjunction with the e-waste tube furnace tests, increased combustible gas production using NaHCO_3 is evident.

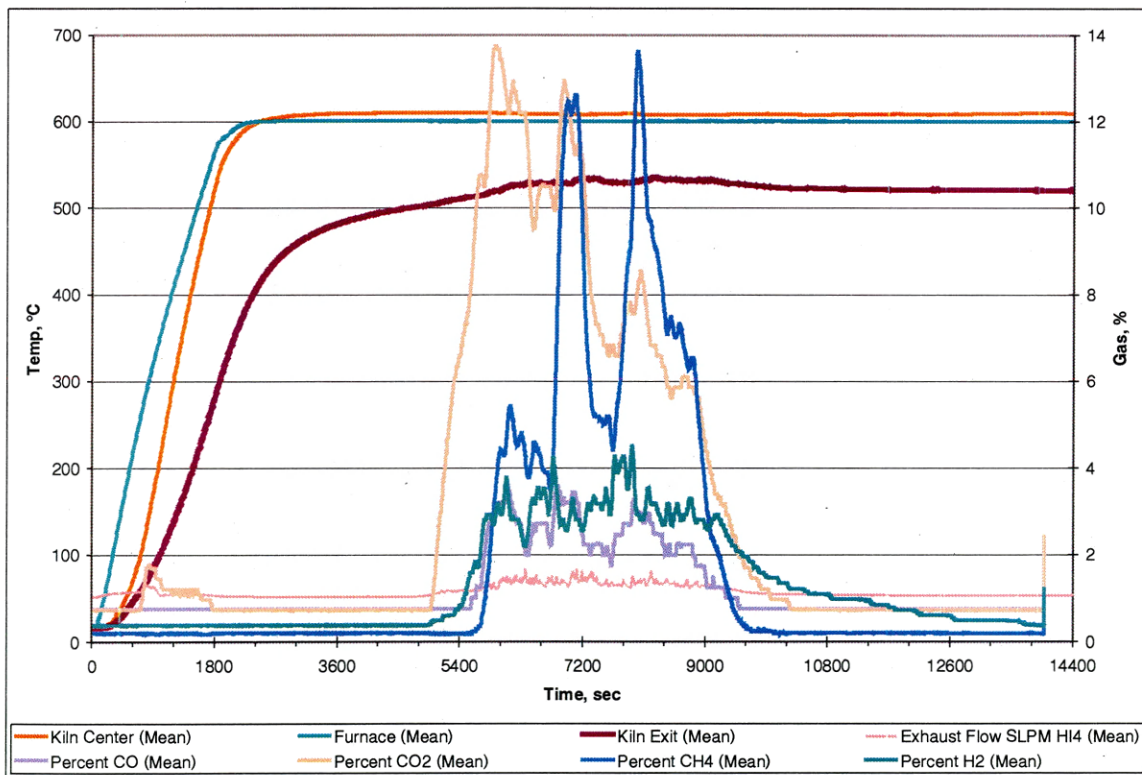


Figure 8.9 Continuous Feed Rotary Kiln: E-Waste with NaHCO_3 (Final 5)

Table 8.3 Comparable Gas Products: E-Waste + NaHCO₃ Rotary Kiln

	CO _(g) , liter	CO _{2(g)} , liter	CH _{4(g)} , liter	H _{2(g)} , liter
Test 5, E-Waste + NaHCO ₃	2.39	8.30	5.32	3.13
from 30 g NaHCO ₃		4.00		
Test 5 Total	2.39	4.30	5.32	3.13

Products generated from the 150 g of e-waste + 30 g NaHCO₃ amounted to 123.58 g ashed waste, 16.08 g distillate and 23.46 g calculated gas for a total of 163.12 g (16.88 g deficit). Of the 123.58 g of ashed material, only 18.9 g could be attributed to Na₂CO₃, assuming no sodium halide salt formation. As before, water vapor is not included. Without a measurement for water, the mass balance is 90.62%. The reduced deficit in mass balance (measured in grams as well as percent) is affected by the formation of sodium salts, evidenced by XRD analysis. The chlorine, fluorine and bromine, which would be evolved in the form of an acid without the presence of a sodium source, are retained in the residue, attributing to a higher ashed residue weight. A sample of the final ashed waste is shown in Figure 8.10.

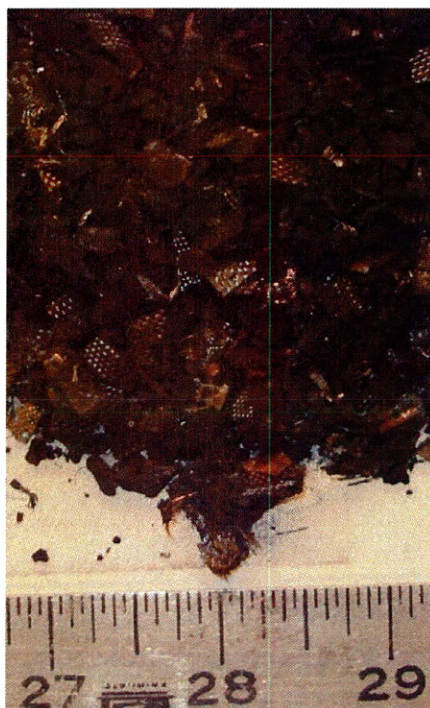


Figure 8.10. Processed E-Waste Sample

The subsequent combined calorific value of the gas streams produced from each rotary kiln test (per kg of e-waste at 600°C) are: -144 kcal for Test 4 (E-Waste) and -406 kcal for Test 5 (E-Waste + NaHCO₃)—a 282% increase.

8.1.2.3 Measured Dioxin/Furan Reduction in Rotary Kiln Experiments

Data obtained from the Dioxin/Furan analysis via the resin modules show the existence of five chemicals from the dioxin/furan family. They are listed here with their respective Toxic Equivalency Factors (TEF)—a weighting factor relating to the chemical's toxic effect:

- Octochlorodibenzo-p-dioxin (TEF = 0.001)
- 2,3,7,8-Tetrachlorodibenzofuran (TEF = 0.1)
- 2,3,4,7,8-Pentachlorodibenzofuran (TEF = 0.5)
- 1,2,3,4,7,8-Hexachlorodibenzofuran (TEF = 0.1)
- 1,2,3,6,7,8-Hexachlorodibenzofuran (TEF = 0.1)

The data (Table 8.4) shows a reduction in the level of dioxins produced by 67.5% through the addition of NaHCO₃ to the e-waste. It is also important to note that one of the furan (1,2,3,6,7,8-Hexachlorodibenzofuran) was eliminated entirely while the most toxic compound found (2,3,4,7,8-Pentachlorodibenzofuran) was itself reduced by 69.5%.

Table 8.4 Dioxin/Furan Results for Kiln Experiments

	OCDD (0.001)	2,3,7,8 TCDF (0.1)	2,3,4,7,8 PeCDF (0.5)	1,2,3,4,7,8 HxCDF (0.1)	1,2,3,6,7,8 HxCDF (0.1)	Total w/ TEF*
	pg/kg e-waste					
e-waste	81.19	89.27	22.58	33.49	20.70	25.72
e-waste + 200 g/kg NaHCO ₃	56.43	34.91	6.89	13.65	0	8.36

* Toxic Equivalency Factors (TEF)—a weighting factor relating to the chemical's toxic effect

A reduction of 67.5% in the dioxin/furan production is an excellent start. Additional research surrounding equipment design to maximize solid/solid and solid/gas contact is needed to

minimize, if not eliminate dioxin/furan production. Maximizing residence time to facilitate complete cracking of the organics to $\text{CH}_4(\text{g})$ and $\text{H}_2(\text{g})$ will also assist in the control of the unwanted dioxin/furan compounds.

8.2 E-Waste Processing Summary

Tests conducted in both the small-scale batch tube furnace and the continuous feed rotary kiln at an operational temperature of 600°C demonstrated the ability to produce a gas stream with heating value. These results parallel those obtained with pure reagent polymer sample materials in previous work. Tests conducted with NaHCO_3 produced higher levels of combustible gasses. An increase in combustible gasses can be attributed to an increased degradation in the polymer species in the presence on a carbonate, as seen in work described in Chapter 5 Overall, the data obtained from processing of e-waste confirmed the data generated from processing of known polymers.

8.3 Flowsheet-Heat and Material Balance

Using data obtained primarily from the continuous feed rotary kiln experiments, in conjunction with thermodynamic data, a unit operation can be modeled for the processing of e-waste. As a first order design of a unit operation, one tonne per hour of e-waste will be modeled using equilibrium compositions calculated from the HSC thermodynamic calculations.

Assuming the consumption of computer internals (motherboard, etc), a plant consuming 1 tonne per hour, 330 days/yr would consume 7,920 tonne or 7.8% of the estimated e-waste generation. Each tonne of e-waste would require 186.3kg NaHCO_3 or Trona [$\text{Na}_3\text{CO}_3(\text{HCO}_3)\cdot 2\text{H}_2\text{O}$]. The thermodynamic modeling for kiln processing is shown in Table 8.5 The thermal deficit without any addition of oxygen is 101,582 kcal/mt e-waste. It should be noted that a number of the volatile metals are expected to enter the gas stream in this operation, including mercury, selenium and arsenic.

Table 8.5 Heat and Mass Balance: Initial Kiln operation

MATERIAL IN @ 25°C				
1 mt e-waste + 186.3 kg NaHCO ₃				
MATERIAL OUT @ 600°C				
Gas	kg	kg mole	Vol, m ³ (STP)	Vol %
H _{2(g)}	17.3	8.58	192.24	57.0724
H ₂ O _(g)	43.3	2.40	53.84	15.9837
CH _{4(g)}	36.5	2.28	50.96	15.1302
CO _(g)	27.2	0.971	21.75	6.4577
CO _{2(g)}	31.4	0.713	15.98	4.7447
N _{2(g)}	1.23	0.0437	0.980	0.2909
Hg _(g)	4.08	0.0203	0.455	0.1352
Se _{2(g)}	2.93	0.0186	0.416	0.1234
As _{4(g)}	2.34	0.00780	0.175	0.0519
As _{2(g)}	0.0718	0.00048	0.0107	0.0032
Cd _(g)	0.0408	0.00036	0.00813	0.0024
SbO _(g)	0.0376	0.00027	0.00611	0.0018
Zn _(g)	0.0108	0.00017	0.00370	0.0011
Se _{3(g)}	0.0256	0.00011	0.00242	0.0007
GeO _(g)	0.00276	3.12E-05	0.00070	0.0002
Se _{4(g)}	0.00753	2.38-05	0.00053	0.0002
Total	166.48	15.04	986.45	m ³ @ 600°C
Solids	kg	Solids	kg	
Cu	222.00	In ₂ O ₃	3.59	
C	203.00	Ag	3.50	
SiO ₂	166.82	Ga ₂ O ₃	3.24	
Fe	88.97	Ru	2.97	
NaBr	51.45	Ge	2.96	
Sn	44.70	Au	1.48	
NaF	44.33	BeO	1.40	
Na ₂ CO ₃	39.17	MnO	0.177	
Ta ₂ O ₅	35.53	TiO ₂	0.114	
NaCl	24.69	Co	0.0682	
Ni	22.24	Pd	0.0556	
Al	22.24	Cr	0.0274	
Pb	22.20	Nb ₂ O ₅	0.0012	
ZnO	13.80	Eu ₂ O ₃	0.0010	
Bi	11.70			
		Total	1,032.44	
Heat Balance	101,582 kcal	(118.0 kW-hr)		

Based on the volume of gas produced at 600°C, and a desired retention time for the gas/vapor phase of 14 min. minimum (the maximum seen in the continuous feed rotary kiln), kiln dimensions calculate to be 2 m-dia. by 20 m length. Initial calculations (summarized in Table 8.6) are based on no introduction of air to the kiln, operating in a completely indirectly heated mode, minimizing gas volume within the kiln. The introduction of in-situ heat generation would require an increase in the size of the equipment to maintain sufficient retention time for thorough degradation of the organics present. Figure 8.11 represents a description of the unit operation.

Table 8.6 Operational Parameters and 1st Order Kiln Design Specifications

Feed	Gas Flow Out	Temp.	Retention Time	Kiln Dia.	Kiln Length
1 mt/hr E-Waste 186 kg/hr NaHCO ₃	941.39 m ³	600°C	14.9 min.	2 m	20 m

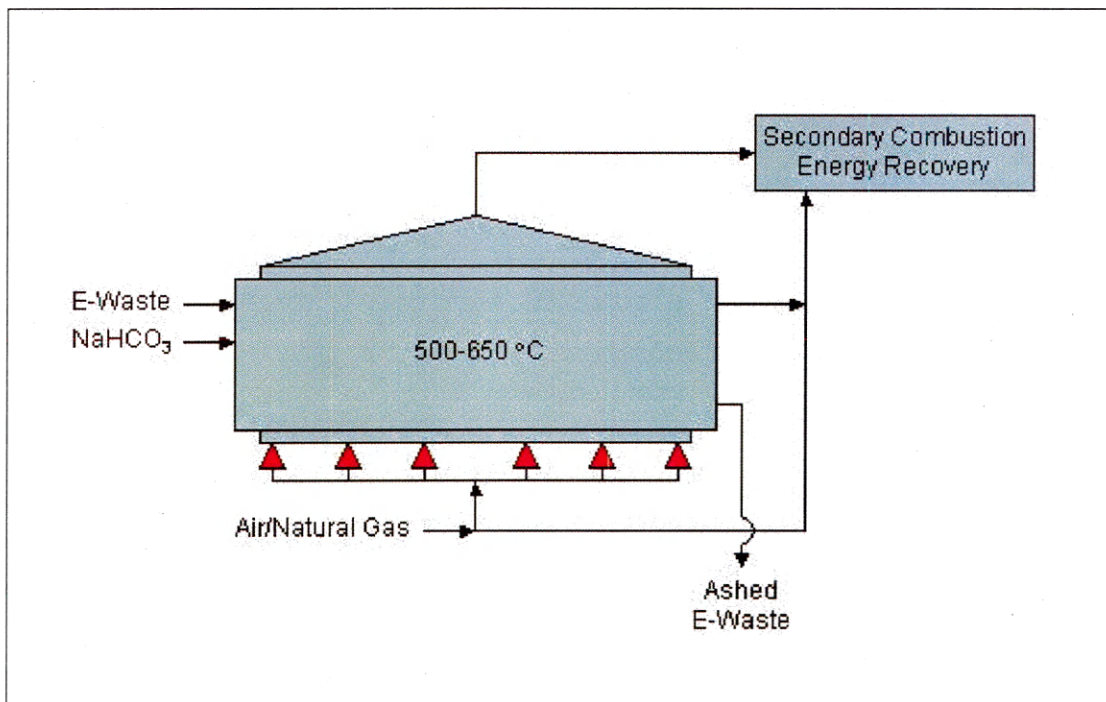


Figure 8.11 Proposed Unit Operation

Both the solid and gas products contain high thermo values to be reclaimed as a portion of the value inherent in e-waste. A determination as to the amount of energy remaining in the solids was conducted with an eye on the degree of oxidation of the slag phase being produced. Of

primary interest was determining if the solids contained sufficient thermal value for subsequent melting/converting operations. Solids leaving the kiln and entering the melt were evaluated at 550°C, accounting for some heat loss in transport. The standard 20.99% O_{2(g)} air stream at 25°C was employed as the oxidant source. The heat and mass balance for combustion and melting the solids residue from the processing of one tonne of e-waste is shown in Table 8.7 and 8.8.

Table 8.7 Solids Combustion Inputs, Energy Recovery

MATERIAL IN @ 25°C				
Combustion Air	kg	kg mole	Vol, m ³ (STP)	Vol %
O _{2(g)}	454.38	14.2	318.1	20.99%
N _{2(g)}	1,497.35	53.5	1,197.3	79.01%
MATERIAL IN @ 550°C				
Solids	kg	Solids	kg	
Cu	222.00	In ₂ O ₃	3.59	
C	203.00	Ag	3.50	
SiO ₂	166.82	Ga ₂ O ₃	3.24	
Fe	88.97	Ru	2.97	
NaBr	51.45	Ge	2.96	
Sn	44.70	Au	1.48	
NaF	44.33	BeO	1.40	
Na ₂ CO ₃	39.17	MnO	0.177	
Ta ₂ O ₅	35.53	TiO ₂	0.114	
NaCl	24.69	Co	0.0682	
Ni	22.24	Pd	0.0556	
Al	22.24	Cr	0.0274	
Pb	22.20	Nb ₂ O ₅	0.0012	
ZnO	13.80	Eu ₂ O ₃	0.0010	
Bi	11.70			
		Total	1,032.44	

Table 8.8 Solids Combustion Outputs, Gas and Fume

MATERIAL OUT @ 1,100°C				
Gas	kg	kg mole	Vol, m ³ (STP)	Vol %
N _{2(g)}	1,497.35	53.45	1,197.31	74.00634
CO _{2(g)}	422.00	9.59	214.79	13.27628
CO _(g)	245.00	8.75	195.93	12.11053
Zn _(g)	11.10	0.170	3.8	0.23488
Pb _(g)	22.10	0.107	2.39	0.147727
GeO _(g)	3.61	0.0407	0.913	0.056433
Bi _(g)	7.86	0.0376	0.842	0.052044
In ₂ O _(g)	3.06	0.0125	0.279	0.017245
Bi _{2(g)}	3.77	0.00902	0.202	0.012486
NaBr _(g)	2.58	0.02550	0.552	0.034119
NaCl _(g)	0.720	0.0123	0.726	0.044874
SnO _(g)	0.434	0.00322	0.0722	0.004463
In _(g)	0.104	0.000906	0.0203	0.001255
NaF _(g)	0.0231	0.000550	0.0123	0.00076
Pb _{2(g)}	0.0476	0.000115	0.00257	0.000159
Ga ₂ O _(g)	0.0146	9.39E-05	0.00210	0.00013
Bi _{3(g)}	0.0467	7.45E-05	0.00167	0.000103
PbO _(g)	0.0100	4.48E-05	0.00100	6.18E-05
Sn _(g)	0.00288	2.43E-05	0.000544	3.36E-05
Na _(g)	0.000552	2.40E-05	0.000538	3.33E-05
Cu _(g)	0.000901	1.42E-05	0.000318	1.97E-05
Cl _(g)	0.000236	6.66E-06	0.000149	9.21E-06
Bi _{4(g)}	0.00499	5.97E-06	0.000134	8.28E-06
Ga _(g)	4.81E-05	6.90E-07	1.55E-05	9.58E-07
Total	2,219.84	72.21	7,449.49	m ³ @ 1,100°C

It is with the combustion and melting of the solid material where the complex non-organic chemistry that exists within e-waste becomes of prime concern. Having developed a solution to the dioxin/furan question, the remaining gas handling issue becomes the metal and metal oxides present in the gas stream.

The remaining data for the heat and mass balance for the slag and metal phases is shown on Table 8.9.

Table 8.9 Solids Combustion Outputs, Slag and Metal

MATERIAL OUT @ 1,100°C					
Solids (Slag)	kg	Wt. %	Solids (Slag)	kg	Wt. %
SiO ₂	166.82	32.22	NaCl	23.50	4.54
FeO	114.00	22.02	Ga ₂ O ₃	3.22	0.62
NaBr	47.50	9.17	BeO	1.40	0.27
NaF	44.30	8.56	MnO	0.177	0.03
Al ₂ O ₃	42.00	8.11	TiO ₂	0.114	0.02
Na ₂ CO ₃	39.20	7.57	Cr ₂ O ₃	0.040	0.01
Ta ₂ O ₅	35.53	7.97			
			Total	515.80	
Solids (Metal)	kg	Wt. %	Solids (Metal)	kg	Wt. %
Cu	222.00	74.88	Ru	2.97	1.00
Sn	44.20	14.91	Au	1.48	0.50
Ni	22.20	7.49	Co	0.0682	0.02
Ag	3.50	1.18	Pd	0.0556	0.02
			Total	296.60	
Heat Balance -632,381 kcal (-734.8 kW-hr)					

The gas stream leaving solids combustion/melting still contains a large amount of heat value in the form of CO_(g). This stream is then combined with the offgas from the rotary kiln for final combustion/energy recovery (Tables 8.10 and 8.11).

Table 8.10. Gas Combustion Inputs, Energy Recovery

MATERIAL IN @ 25°C				
Combustion Air	kg	kg mole	Vol, m ³ (STP)	Vol %
O _{2(g)}	491.93	15.37	344.36	20.99%
N _{2(g)}	1,620.10	57.83	1,295.46	79.01%
MATERIAL IN @ 1000°C				
Fuel	kg	kg mole	Vol, m ³ (STP)	Vol %
N _{2(g)}	1,498.58	53.50	1198.4	61.33
CO _{2(g)}	453.39	10.30	230.72	11.81
CO _(g)	272.20	9.72	217.73	11.14
H _{2(g)}	17.30	8.58	192.19	9.84
H ₂ O _(g)	43.27	2.40	53.76	2.75
CH _{4(g)}	36.50	2.28	51.07	2.61
Zn _(g)	11.11	0.170	3.81	0.19
Pb _(g)	22.10	0.107	2.40	0.12
GeO _(g)	3.61	0.0408	0.914	0.047
Bi _(g)	7.86	0.0376	0.842	0.043
NaBr _(g)	2.58	0.0255	0.571	0.029
NaCl _(g)	0.720	0.0123	0.276	0.014
Hg _(g)	4.08	0.0203	0.455	0.023
Se _{2(g)}	2.93	0.0186	0.417	0.021
In ₂ O _(g)	3.06	0.0125	0.280	0.014
Bi _{2(g)}	3.78	0.00903	0.202	0.010
NaF _(g)	0.0231	0.000550	0.0123	0.0006
Total	2,386.30	87.23	9,122.10	m ³ @ 1,000°C

Inputs to energy recovery from the gas stream leaving the rotary kiln combined with the gas stream leaving the solids combustion/melting operation employ a standard 20.99% O_{2(g)} air stream at 25°C. The fuel stream is calculated at 1,000°C, taking into consideration some cooling of the gases after leaving their respective operations and mixing before final combustion. A temperature of 1,100°C was used as output gas temperature, with the excess enthalpy determined at that temperature. Any reduction in gas temperature through energy recovery would only increase the value of this operation. Unit operation outputs are shown in Table 8.11.

Table 8.11 Gas Combustion Outputs, Energy Recovery

MATERIAL OUT @ 1,100°C				
Gas	kg	kg mole	Vol, m ³ (STP)	Vol %
N _{2(g)}	3,118.23	111.31	2,493.39	73.88
CO _{2(g)}	966.94	21.97	492.15	14.58
H ₂ O _(g)	280	15.54	348.15	10.32
O _{2(g)}	42.3	1.32	29.61	0.88
Zn _(g)	11.1	0.17	3.80	0.11
Pb _(g)	22.1	0.11	2.39	0.071
GeO _(g)	3.61	0.041	0.91	0.027
Bi _(g)	7.86	0.038	0.84	0.025
SeO _{2(g)}	4.09	0.037	0.83	0.024
NaF _(g)	1.13	0.027	0.60	0.018
NaBr _(g)	2.58	0.03	0.56	0.017
Hg _(g)	4.05	0.020	0.45	0.013
In ₂ O _(g)	3.06	0.012	0.28	0.0083
NaCl _(g)	0.72	0.01	0.28	0.0082
Bi ₂ (g)	3.77	0.0090	0.20	0.0060
NO _(g)	0.24	0.0080	0.18	0.0053
As ₄ O _{6(g)}	2.19	0.0055	0.12	0.0037
SnO _(g)	0.434	0.0032	0.072	0.0021
NaF _(g)	0.0231	0.00055	0.012	0.00037
Total	4,494.44	150.66	15,543.04	m ³ @ 1,100°C
Solids				
	kg			
ZnO	0.0137			
In ₂ O ₃	8.15E-05			
Total	0.0138			
Heat Balance	-707,093 kcal	(-821.6 kW-hr)		

The streams leaving the gas combustion process would then be treated for dust collection and subsequent materials handling.

Overall, thermodynamic evaluation of the system shows that there is ample energy content within the material from the polymers fraction to facilitate processing. If pure oxygen were employed during the combustion/melting of the solid residue, the energy produced might be more than could be properly handled. A simple crushing via a roll crusher followed by screening

would allow for the removal of a carbon rich fraction that could be employed as a supplemental fuel source in a controlled manner. The distribution of sodium salts and other constituents may also be better controlled through conventional mineral processing techniques applied to portions on the kiln solids. This is an area of work that should/will be explored in future research.

A summary of the heat and mass balance combined with the flowsheet surrounding the proposed unit operation is shown in Figure 8.12. Total inputs to the system are comprised of: e-waste (1 tonne/hr), NaHCO_3 (186 kg/hr) and Air ($3,155 \text{ m}^3/\text{hr}$). Products from the flowsheet are comprised of an offgas, a slag, a metal phase and a potential net gain of 1,160.2 kW energy.

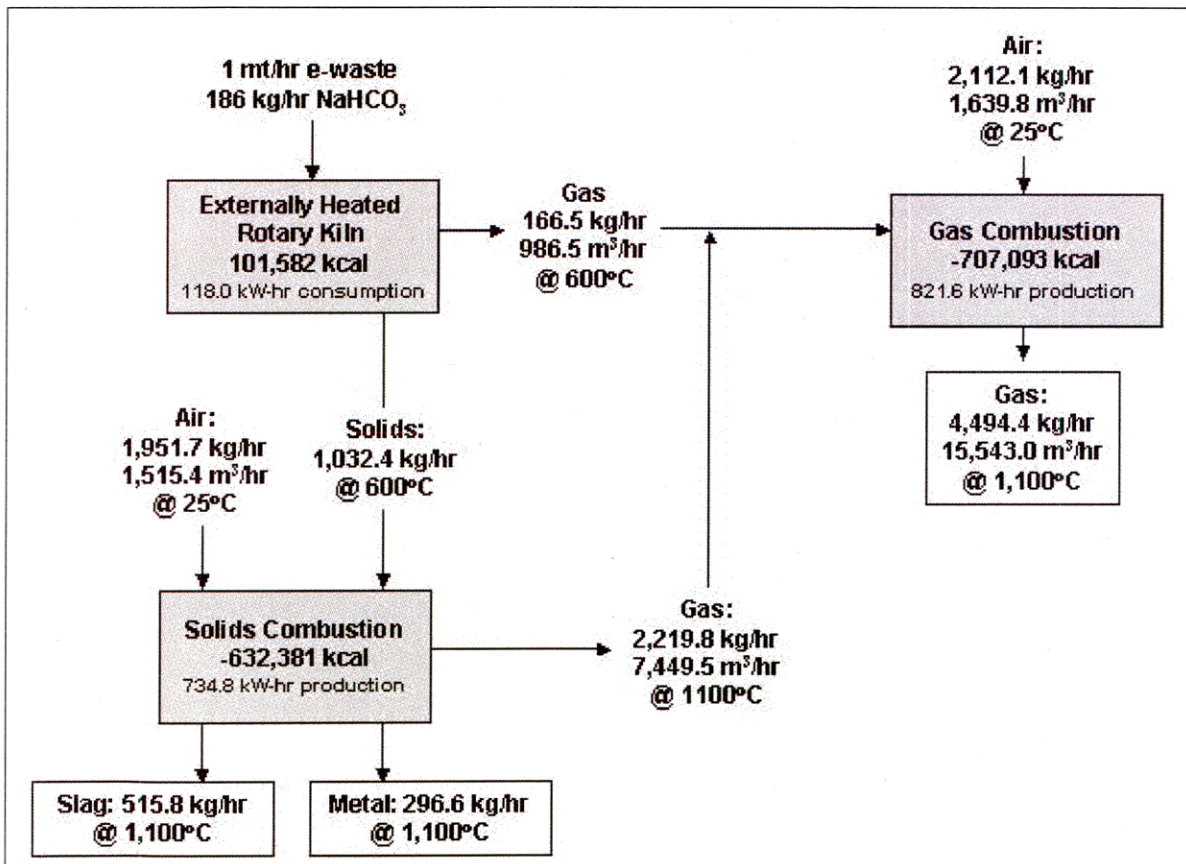


Figure 8.12 Heat and Mass Balance—Flowchart

Data in Table 8.9 show the primary constituents of the slag phase to be: SiO₂, FeO, Al₂O₃, Na₂CO₃ and sodium salts. In a molten environment, it is estimated that the remaining Na₂CO₃ will decompose to an oxide. If the sodium salts and Ta₂O₅ are, for the moment ignored, the slag composition can be expressed as Table 8.12.

Table 8.12 Primary Slag Constituents

Solids (Slag)	kg	Wt. %	kg mole
SiO ₂	166.82	48.25	2.78
FeO	114.00	32.97	1.59
Al ₂ O ₃	42.00	12.15	0.412
Na ₂ O	22.92	6.63	0.370

This composition can be recast via the components SiO₂, FeO and NaAlSiO₄ as shown in Table 8.13. The composition can be located on the phase diagram shown in Figure 8.13 This ternary diagram shows a large field of fayalite with a liquidus surface from 980°C to 1,200°C.

Table 8.13 Sodium Slag Composition

Solids (Slag)	kg	Wt. %	kg mole
SiO ₂	122.40	35.39	2.04
FeO	11.04	32.97	1.59
NaAlSiO ₄	109.40	31.63	0.770

As an initial evaluation of the slag produced based on the major constituents, this is encouraging. With a melting point of 1,872°C, Ta₂O₅ would most likely exist as particles in suspension in the slag, increasing the viscosity. The relative change in viscosity would be directly dependent on the actual concentration of Ta₂O₅ in the initial waste stream. The presence of NaF would have the opposite effect, reducing the viscosity of the slag. This too is dependent on the initial concentration of one compound (PTFE) but is easier to alter through flux additions. The control and final disposition of the remaining sodium salts would be controlled through flux additions and slag tempering.

Additional research will have to be conducted to explore the slag chemistry and behavior, but initial indications are encouraging. The existence of such compounds as Be₁₃Ca suggest that

beryllium could be controlled and made benign with the addition of CaO. Other metals present in the slag and metal phase may also benefit from slag chemistry manipulation.

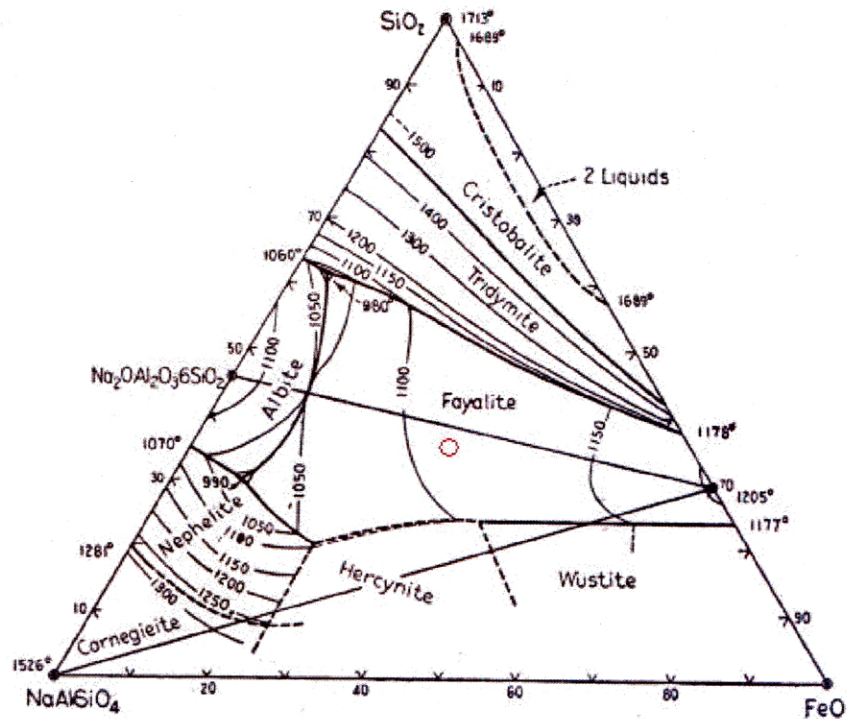


Figure 8.13 Sodium Slag Ternary Phase Diagram (Levin 1969)

The metal alloy produced is primarily a Cu, Sn and Ni—97.28% of the metal phase. These three metals taken together have the composition: Cu (76.95%)-Sn (15.36%)-Ni (7.69%) and are shown on the phase diagram in Figure 8.14. As indicated in that diagram, the alloy would have a melting temperature less than that of pure copper. Additional processing of the alloy for the removal of tin and nickel could follow a number of paths—hydro or pyrometallurgical. Of the remaining minor elements, Ag (1.18%) and Au (0.50%) tend to depress the melting temperature of the primary metal (Cu). The remaining elements, Ru (1.00%), Co (0.02%) and Pd/Pt (0.02%) tend to increase the melting temperature of the primary metal (Cu). With such small amounts, the effect of increasing and decreasing the melting point from the values seen in Figure 8.14 are estimated to be minimal.

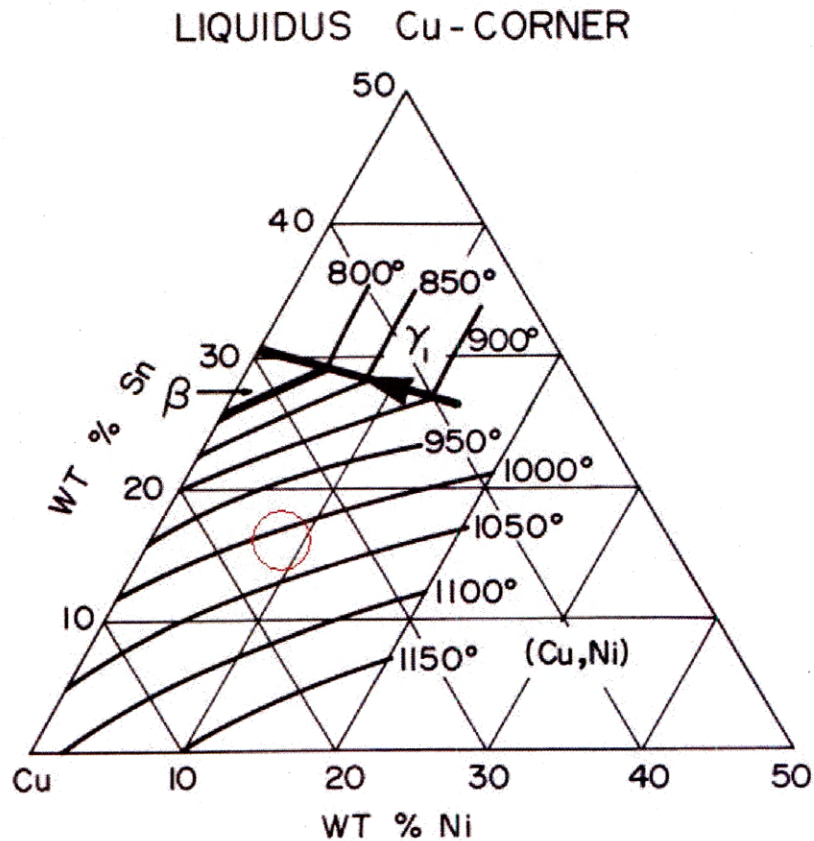


Figure 8.14 Cu-Ni-Sn Ternary Phase Diagram (Chang, 1979)

8.4 Process Summary

With the basis of understanding of the behavior of e-waste and its major components, the introduction of the relatively small processing operation to a conventional copper smelter as a supplemental system can be surmised. The process described would consist of a rotary kiln, co-generation facility (if one is not already on-site) and a furnace producing a Cu-Sn-Ni alloy possessing precious metals and a sodium slag. At a design capacity of 1 mt/hr, the process would produce: 2,432.10 mt/yr Cu, 38.33 mt/yr Ag, 16.24 mt/yr Au and 0.65 mt/yr Pt/Pd. Assigning an efficiency of 50% to energy recovery would allow the process to generate 660.2 kW

CHAPTER 9

CONCLUSIONS

In reviewing the components that comprise electronic waste one can see, from a processing point of view, a material that brings metal values to a process along with an inherent reductant. The carbon and hydrogen values contained in plastics can be harnessed, facilitating the recovery of resources. The complex material also brings with it areas of concern for large-scale processing. Concerns over the release of heavy metals that may be entrained in e-waste material are no different than those expressed in “conventional” scrap. Efficient dust handling systems employed in every pyrometallurgical operation have already shown their ability to deal with such materials when in a stable form. Metals as halides tend to have greater activity and mobility, causing greater concern for industrial operations that deal with such compounds. Dioxin/furan production/release associated with the processing of halogen and hydrocarbon-containing waste is an issue that is affecting many industries that deal with such materials. The work conducted here has demonstrated a process that has shown an ability to sequester halides in the form of sodium salts away from the gas/vapor phases where dioxins/furans are generated. The sodium addition, based on thermodynamic evaluation, reduce or functionally eliminate the formation of other mobile halides, such as AlCl_3 . The addition of sodium carbonate has also demonstrated an ability to increase the decomposition of polymers, producing a higher fuel value gas stream, adding to the value and self-sustainability of the process. Overall, this processes allows for the liberation of a metal-rich stream from an organic encapsulated waste material while recovering the energy potential of the organics themselves in the form of $\text{CH}_{4(g)}$, $\text{H}_{2(g)}$ and carbon. Specific accomplishments are:

- 92.2% +/- 6.8% containment of chlorine from PVC-rich material with the application of 1.5X stoichiometric NaHCO_3

- 74.5% +/- 13.6% containment of chlorine from PVC-poor material with the application of 1.5X stoichiometric NaHCO₃
- Increased production of combustible gases (CH_{4(g)}, H_{2(g)}, etc.) from e-waste samples with the addition of NaHCO₃. The energy produced with NaHCO₃ is 282% of the value produced without NaHCO₃ when measured by calorific value of combustion.
- Reduction of dioxin/furan production of 67.5% from e-waste samples with the addition of NaHCO₃.

While this research and process development was approached from the point of view of developing technology for application to the copper industry, this technology has application in a number of areas. Potential markets include (in addition to electronic waste) municipal waste incineration, automobile shredder residue and any material containing organic compounds and halides.

Additionally, with emissions accounting and local or in-plant air quality issues always of concern, the control of Cl_{2(g)}, F_{2(g)} and Br_{2(g)} as well as their respective acids and metal complexes through sequestration as sodium salts has innumerable benefits. Gaseous emissions are something that can be measured and evaluated on a daily basis. Employee health effects and the possibility of future litigation over exposure to toxic gases are something that cannot be immediately accounted for. Any reduction in halide and associated compound emissions will benefit a process and the company operating it.

CHAPTER 10

SUGGESTIONS FOR FURTHER WORK

With such a complex material, the elimination of the organic fraction without the generation of carcinogens is only a first step. In outlining a complete process for the efficient processing of this type of post-consumer material, there are many areas for process design and optimization, covering multiple areas of engineering. Initially, areas where further work should be conducted are:

1. Trona. Samples of trona ore should be obtained and evaluated against reagent NaHCO_3 to determine dosing levels for this industrial reagent.
2. Equipment. Alternate laboratory rotary kiln designs should be explored, optimizing gas/vapor phase retention time and in-situ gas/solid contact while allowing for extended duration, continuous feed operation and continuous solids discharge.
3. Mineral Processing/beneficiation. With the liberation of the many metal and ceramic components and the generation of large amounts of carbon through organic decomposition, the development of a mineral processing circuit to produce multiple value-added streams could be beneficial. A combination of crushing (roll crusher), screening and/or elutriation could produce a copper-silica majority fraction, aluminum-tin-Au-Ag (electrical contacts) fraction and a carbon (with sodium-halide salts) fraction. Chemical analysis of these fractions could dictate additional processing.
4. Kiln Oxidation Potential. Based on the lack of an effect in changes of the sequestering ability of the NaHCO_3 with changes in atmosphere, an investigation of

oxygen addition to the kiln for in-situ energy production should be evaluated. Care must be taken with regard to possible effects on carcinogen production and overall full-scale equipment sizing with increased gas flows.

5. Slag Chemistry. The proposed slag composition is based on the initial chemical make-up of a general e-waste stream. While the slag system shown possesses a large range of low-temperature compositions allowing for fluctuations in feed material without complication, the partitioning of metals will have to be explored in this system. Final slag composition will also dictate disposal/product options for the glass produced.
6. Refractory. Evaluation of acceptable refractory material will need to be conducted. While it is expected that the rotary kiln itself will not need refractory lining, operating at a relatively low temperature, refractory for the melt furnace will need to withstand high sodium levels without adverse reactions or the production of problematic materials for disposal.

REFERENCES

- American Metal Market (AMM), 2006, <http://www.amm.com>, last accessed 03/06/06.
- Ausmelt Ltd., 2005, <http://www.ausmelt.com.au/waste.htm>, last accessed 11/15/05.
- Busselle, L.D.; Moore, T.A.; Shoemaker, J.M. and Allred, R.E., 1999, "Separation processes and economic evaluation of tertiary recycling of electronic scrap," Proceedings of the 1999 IEEE International Symposium on Electronics and the Environment, IEEE, pp. 192-197.
- Computer Industry Almanac (C.I.A.), 2006, <http://www.gdsourcing.com/works/Almanac.htm>, last accessed 03/08/06.
- Chang, Y. Austin, 1979, Phase diagrams and thermodynamic properties of ternary copper-metal systems. The International Copper Research Association, p. 608.
- Conrad, Randal, 2000, "Background Document on Recycling Waste from Computers," Aug. 10, 2000, Randall Conrad and Associates, Ltd.
- EPA, 1991, Applications Analysis Report, Horsehead Resource Development Company, Inc. (HRD), Flame Reactor Technology, Risk Reduction Engineering Laboratory (RREL), Office of Research and Development (ORD), U.S. Environmental Protection Agency (EPA), Cincinnati, OH 45268, Contract No. 68-C0-0047, November 4, 1991.
- Felix, Noel and Chris Van Reit, 1994, "Recycling of Electronic Scrap at UM's Hoboken Smelter," Precious Metals 1994, TMS, pp. 159-169.

- Goodrich, Melissa, 1999, "Electronics recycling —Making electronic recycling connections," *Recycling Today*, v.37, no.9, September, 1999 pp.64–89.
- Goosen, David, "Electronics Recycling at Teck Cominco's Trail Operation," Presentation given at Recycling Metals from Industrial Waste Short Course, Colorado School of Mines, Golden, Colorado, June 20-23, 2005.
- Herrmann, C., P. Eyerer and J. Gediga, 2002, "Economic and ecological material index for end of life and design of electronic products," Proceedings of the 2002 IEEE International Symposium on Electronics and the Environment, IEEE, pp. 11-16.
- Hoffman, James E., 1992, "Recovering Precious Metals from Electronic Scrap," *JOM*, July 1992, pp. 43-48.
- Imperato, Dr. E.G. and M.A. Pashelinsky, 1988, "Pyrometallurgical Processing of Precious Metals Scrap in an Electric Arc Furnace," Precious Metals 1988, TMS, pp. 159-177.
- Kruesi, Paul R. 2004, "Method to recapture energy from organic waste," U.S. Patent Application No. 20040253166.
- Lehner, Theo, 1998, "Integrated Recycling of non-ferrous metals at Boliden Ltd. Ronnskar Smelter," Proceedings of the 1998 IEEE International Symposium on Electronics and the Environment, IEEE, pp. 42-47.
- Levin, Ernest M., Carl R. Robbins and Howard F. McMurdie, 1969, Phase diagrams for ceramists. American Ceramic Society, United States, National Bureau of Standards, p. 284.
- Mark, Frank E. and Theo Lehner, 2000, "Plastics Recovery from Waste Electrical & Electronic Equipment in Non-Ferrous Metal Processes," Association of Plastics Manufacturers in Europe (APME), 2000.

- Patos, Harilaos S., 1982, "A Mass Spectrometric Study of Gaseous Species Related to the Carbochlorination of Aluminum-Bearing Ores, M.S. Dissertation, Colorado School of Mines, Golden, Colorado, Thesis No. T-2652.
- Perry, Robert H., Perry's Chemical Engineers' Handbook (7th Edition) 1997, McGraw-Hill pp. 2-57 – 2-60.
- Phillips, Albert J., 1962, "The World's Most Complex Metallurgy (Copper, Lead and Zinc)," Transactions of The Metallurgical Society of AIME, August 1962, pp. 657-668.
- Reid, Robert, 1999, "High tech, low grade recycling" *Scrap*, v.56, no.3, May, p.76 –80.
- Schoukens A.F.S., Denton G.M., & Jones R.T., 1995, "Pilot-plant production of Prime Western grade zinc from lead blast-furnace slag using the Enviroplas process", Third International Symposium on Recycling of Metal and Engineered Materials, TMS Fall Extraction and Processing Meeting, Point Clear, Alabama, 12-16 November 1995, pp. 857-868.
- Thomas, Cindy, 2005, "Virtual Gold Mine: Canadian Company Digs into Resource Recovery" *Waste Management World*, May-June, 2005, pp. 42–46.
- Setchfield, John H., 1987, "Electronic Scrap Treatment at Engelhard," Precious Metals 1987, TMS, pp. 147-153.
- Sum, E.Y.L., 1991, "The Recovery of Metals from Electronic Scrap" *JOM*, April 1991, pp. 53-61.
- Teck Cominco Ltd, 2004, <http://www.teckcominco.com/articles/operations/tr-tech-broch.pdf>, last accessed 11/15/05.

U.S. Environmental Protection Agency (EPA), 2000, WasteWise Update, October 2000, EPA/530-N-00-007.

U.S. Environmental Protection Agency (EPA), 2001, Municipal Solid Waste in The United States: 2000 Facts and Figures, EPA/530-R-01-014, July 2001.

Wu, Benjamin H., Assistant Secretary for Technology Policy, U.S. Department of Commerce, Testimony before the House Committee on Energy and Commerce Subcommittee on Environment and Hazardous Materials, July 20, 2005.

Yarnes, Scott R., 1995, "Pyrometallurgical Processing of Electronic Scrap," Sabin Metal Corp, Precious Metals 1995, TMS, pp. 167-173.